



1979

Quantitative Measures of Subjective Contours

Gregory John Ozog
Loyola University Chicago

Recommended Citation

Ozog, Gregory John, "Quantitative Measures of Subjective Contours" (1979). *Dissertations*. Paper 1869.
http://ecommons.luc.edu/luc_diss/1869

This Dissertation is brought to you for free and open access by the Theses and Dissertations at Loyola eCommons. It has been accepted for inclusion in Dissertations by an authorized administrator of Loyola eCommons. For more information, please contact ecommons@luc.edu.



This work is licensed under a [Creative Commons Attribution-Noncommercial-No Derivative Works 3.0 License](https://creativecommons.org/licenses/by-nc-nd/3.0/).
Copyright © 1979 Gregory John Ozog

QUANTITATIVE MEASURES OF SUBJECTIVE CONTOURS

by

Gregory Ozog

A Dissertation Submitted to the Faculty of the Graduate
School of Loyola University of Chicago in Partial
Fulfillment of the Requirements for the
Degree of Doctor of Philosophy

July

1979

ACKNOWLEDGMENTS

I would like to thank the members of my committee; Dr. Mark Mayzner, Dr. William Yost, and Dr. Richard Bowen. I especially wish to thank Dr. Mayzner for serving as chairman of the committee, for the use of his equipment to conduct these experiments, and for his support.

I would also like to thank Dr. Ira Appelman for his programming help with the PDP/8E and Ken Kirsch, Mark Goodfriend, and Arthur Krumrey for making computer time available to me at Northwestern University.

The filter changer was constructed especially for experiments 1 and 2. It would not have been built without the two critical insights and much skill of my father.

I would like to thank Barbara Grabowski who has been a constant source of support, encouragement, programming help, suggestions, and resources both physical and emotional. She found Ken Kirsch and Mark Goodfriend for me and also typed some of the manuscripts.

Thanks to Erika, Ann, Mark, and Tom for spooling those miles of paper tape.

Dr. Naomi Weisstein was responsible for germinating my interest in vision.

My thanks to my friend, Ron Szoc, who has co-mis-

erated with me during our long graduate careers.

Finally, as with any significant event in one's life, this comes as a climax to a long process. Without my family I would surely never have endured. To my parents, aunt and uncle, brother and cousin in gratitude and love I dedicate this effort.

VITA

The author, Gregory John Ozog, is the son of John Edward Ozog and Erika Antonia (Berger) Ozog. He was born August 15, 1948 in Chicago, Illinois.

His elementary education was obtained at Our Lady of Mount Carmel Grade School, and his secondary education at Quigley North Preparatorial Seminary, where he graduated in 1966.

He graduated from Niles College of Loyola University in 1970 with a Bachelor of Science in psychology. He entered the graduate school at Loyola in psychology and was awarded a departmental assistantship. In June, 1974 he received a Master of Arts in psychology.

He has co-authored: Differential Adaptation to Gratings Blocked by Cubes and Gratings Blocked by Hexagons: A Test of the Neural Symbolic Activity Hypothesis in 1972 and A Comparison and Elaboration of Two Models of Metacontrast in 1975.

TABLE OF CONTENTS

	Page
ACKNOWLEDGMENTS	ii
LIFE	iv
LIST OF TABLES	v
LIST OF FIGURES	vi
CONTENTS OF APPENDICES	viii
INTRODUCTION	1
REVIEW OF SUBJECTIVE CONTOUR LITERATURE	4
Subjective Contour vs. Real Contour	4
Hypotheses Explaining Subjective Contour	5
EXPERIMENT 1	21
Introduction	21
Method	21
Subjects	21
Design	21
Apparatus and stimuli	22
Procedure	23
EXPERIMENT 2	26
Introduction	26
Method	26
Subjects	26
Results of Experiment 1 and Experiment 2	26
Discussion of Experiment 1 and Experiment 2	30
EXPERIMENT 3	36
Introduction	36
Rationale for choosing the masks	38
Selecting a Frequency Mask	41
Finding the frequency spectra of masks and test contours	42
Computing the discrete Fourier Transform	48
Computing the similarity between masks and test contours	56

TABLE OF CONTENTS (cont'd)

	Page
Method	61
Subjects	61
Design	61
Apparatus and stimuli	62
Procedure	63
Results	65
Mask data	66
Context data	69
Discussion of Experiment 3	74
Mask effects	74
Context effects	80
Context specific mask effects	84
GENERAL SUMMARY	93
REFERENCES	94
APPENDIX A	100
APPENDIX B	103
APPENDIX C	122

LIST OF TABLES

Table		Page
1.	Visual Angle for Displays Used by Dumais & Bradley	18
2.	Similarity Values for Mask Candidates and Test Contour 1	58
3.	Similarity Values for Mask Candidates and Test Contour 2	59
4.	Similarity Values for Mask Candidates and Test Contour 3	60
5.	Length and Separation of lines for Contexts 1 through 9	72
6.	Luminance and Mean Percent Correct for Each Mask in Experiment 3	75
7.	Response Contingency Tables for Subjects	78
8.	Response Contingency Tables for Masks	79
9.	Mean Percent Correct and Number of Illuminated Points for Each Context	81
10.	Differences in Dynamic Range Among Contexts	89
11.	Differences in Mean Percent Correct Between Strong and Weak Contours	90

LIST OF FIGURES

Figure	Page
1. Examples of Subjective Contours	2
2. Simultaneous Brightness Contrast and Subjective Contours	7
3. Comparison of Classical Brightness Contrast Displays and Subjective Contours	8
4. Neural Units and Lateral Inhibition in Subjective Contour Effects	9
5. Figures Which Do Not Support Simultaneous Brightness Contrast as an Explanation for Subjective Contours	11
6. Examples of the Perceptual Organization Hypothesis	13
7. A Subjective Line	16
8. Displays Used in Experiment 1	24
9. Mean Magnitude of Subjective Lines as a Function of Size	27
10. Mean Magnitude of Subjective Lines as a Function of Filter Density	29
11. Mean Magnitude Plotted Separately for Each Size	31
12. Log-Log Plot of Mean Magnitude as a Function of Size	34
13. Display Type Used in Experiment 3	37
14. Obtaining One-dimensional Image Profiles . .	43
15. A White Square	45
16. Image Profile of a White Square	46
17. Image Profile of a Sine Wave	50
18. Transform of a Sine Wave (Magnitude Plot) . .	51

LIST OF FIGURES (cont'd)

Figure	Page
19. Inverse Transform of a Sine Wave	52
20. Image Profile of an Impulse	53
21. Transform of an Impulse	54
22. Inverse Transform of an Impulse	55
23. Contexts 1 through 9 for Experiment 3	64
24. Mean Percent Correct for Each Mask	67
25. Mean Percent Correct for Each ISI	68
26. Mean Percent Correct for Each Mask Plotted Separately as a Function of ISI	70
27. Mean Percent Correct for Each Context	71
28a. Mean Percent Correct for Each Context for the Blank Mask	85
28b. Mean Percent Correct for Each Context for the Luminance Mask	86
28c. Mean Percent Correct for Each Context for the Pattern Mask	87
28d. Mean Percent Correct for Each Context for the Frequency Mask	88
29. Mean Percent Correct for Each Mask as a Func- tion of ISI for Weak, Strong, and No Context Conditions	91

CONTENTS FOR APPENDICES

	Page
APPENDIX A Photographs of the Filter Changer . .	100
APPENDIX B Program Listings for the Trans-	
form Programs	103
1. Main Program	104
2. FFTM	111
3. HIDE	116
APPENDIX C Similarity Program Listing	122

INTRODUCTION

Contour is defined as the border separating non-homogenous regions in the visual field. The stimulus conditions giving rise to such contours are usually abrupt differences in luminance, hue, or saturation between adjacent regions in the stimulus display. However, as early as 1904, Schumann (1904) reported observations of what he termed "subjective contours" where contour was perceived in the absence of an abrupt change in the gradient of illumination. He presented illusory contours, such as those in Figure 1a, which extend over objectively homogenous regions of the visual display. In the central region of Figure 1a, observers report seeing a lighter square bounded on the left and right sides by faint contours extending between the top and bottom segments of the black bordering region. These illusory contours are sometimes rather weak and unstable, especially when the figure subtends a large visual angle or when the point of fixation lies along the contour. They are also influenced by the organization of the figure and by contrast.

Kanizsa (1955, 1974) has presented a number of configurations in which stable and salient subjective contours are seen by most observers (see Figures 1b-1d). For example, in Figure 1b, contours corresponding to the "sides" of a triangle can be seen extending between the black induc-

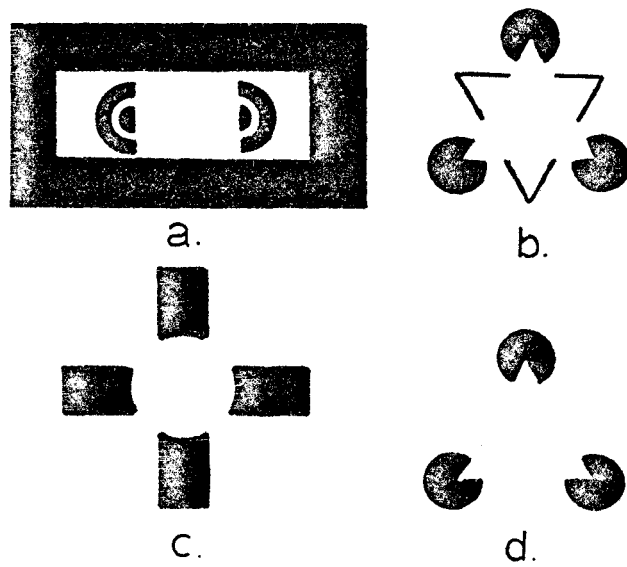


Figure 1. Examples of Subjective Contours

ing elements. The subjective figure appears phenomenally complete, brighter or more intense than its background, displaced into the foreground, and delineated by subjective edges.

Since these original presentations, there have been a number of qualitative and quantitative descriptions of subjective contours. These reports have focused on two issues: (1) establishing the reality of subjective contours by comparing their effects to those of real contours under various psychophysical tests; and, (2) finding explanations for the phenomena based on various hypothetical physiological and cognitive mechanisms. The research exploring these two areas is summarized below.

REVIEW OF SUBJECTIVE CONTOUR LITERATURE

Subjective Contour vs. Real Contour

Smith & Over (1977) have shown that orientation-selective masking occurs between subjective contours as well as between real contours. Real contours can be masked by subjective contours, and vice versa, and the tilt illusion (apparent expansion of the angle formed by intersecting lines) can be induced with subjective as well as with real contours. They attribute the perception of real and subjective contour to fundamentally similar processes.

In another comparison of real vs. subjective contour, Weisstein, Maguire, & Berbaum (1977) report motion after-effects" obtained within regions of the visual field that had not been stimulated by moving contours". "Phantom stripes" are seen moving through this region. They were induced by real vertical stripes moving above and below that region. These "phantom stripes" produced motion after-effects equivalent to real stripes.

As noted earlier, most subjective contours are accompanied by an apparent brightness difference within the area bounded by the contour. Coren & Theodor (1977) attempted to measure this apparent brightness effect by measuring the increment threshold on either side of the contour. Their data indicate a small change in increment threshold in the

direction expected from the apparent brightness of the figure. Thus, all the evidence thus far indicates that subjective contours behave like their real counterparts. These findings form the basis for the experiments reported here. If subjective contours are producing measurable effects these effects should vary with the strength of the contour. This was one of the hypotheses tested here.

Hypotheses Proposed to Explain Subjective Contour

Brigner & Gallagher (1974) have suggested that the perceptibility of subjective contours varies systematically with the magnitude of simultaneous brightness contrast. The black inducing elements in Figure 1 produce brightness induction in the central white regions of the displays. They suggest that in producing subjective contours two properties of simultaneous brightness contrast are involved: (1) the converging edges forming a corner increase the magnitude of simultaneous contrast and therefore, the magnitude of the contrast varies inversely with the angle size; (2) the magnitude of simultaneous brightness contrast increases as the area of an inducing field increases. Viewed in this context, Figure 1c elicits subjective contours because (a) the corner elements have inducing fields (black circular areas) which increase the magnitude of brightness contrast; (b) the magnitude of brightness contrast will be greatest within the corner elements, i.e., within the relatively small angle formed by the converging edges where a sector of the circle

has been removed. Those differences in brightness contrast produce the apparent brightness differences. By juxtaposing the areas of comparable apparent brightness, the perception of a subjective contour is evoked. Figure 2 does not produce subjective contours because of the relatively small inducing area, even though Figure 2 produces the figure of a triangle by closure. They had subjects rank displays which varied in the size of the inducing area and others where the angle between the edges in the inducing circle was varied and found support for a simultaneous brightness contrast model for subjective contours.

Frisby & Clatworthy (1975) extended the brightness contrast explanation to some new figures. They pointed out the similarities between classical brightness contrast displays and the Kanizsa-type figures (see Figure 3). They suggest that a neural unit described by Rodieck & Stone (1965), with a receptive field whose "on area was flanked on just one side by an elongated off zone" (see Figure 4e), mediates via lateral inhibition, the effects shown. It is their view that through lateral inhibition brightness contrast operates to produce illusory brightness gradients which are used together with physically present brightness gradients to generate perceptions. Thus, if we look at the patterns in Figure 4a and Figure 4c we see subjective contours which are due to the interaction of line endings with neural units of the type in Figure 4e. Figures 4b and 4d

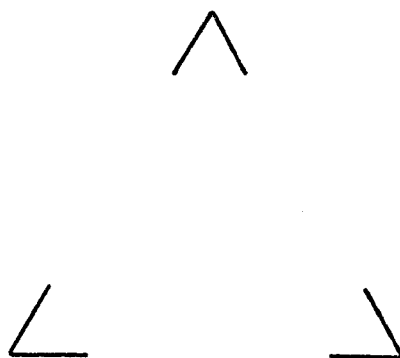


Figure 2. Simultaneous Brightness Contrast in Subjective Contours

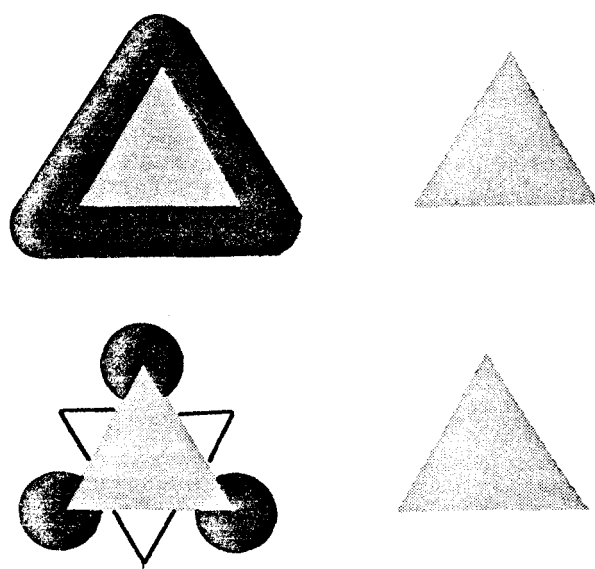


Figure 3. Comparison of Classical Brightness Contrast Displays and Subjective Contours.

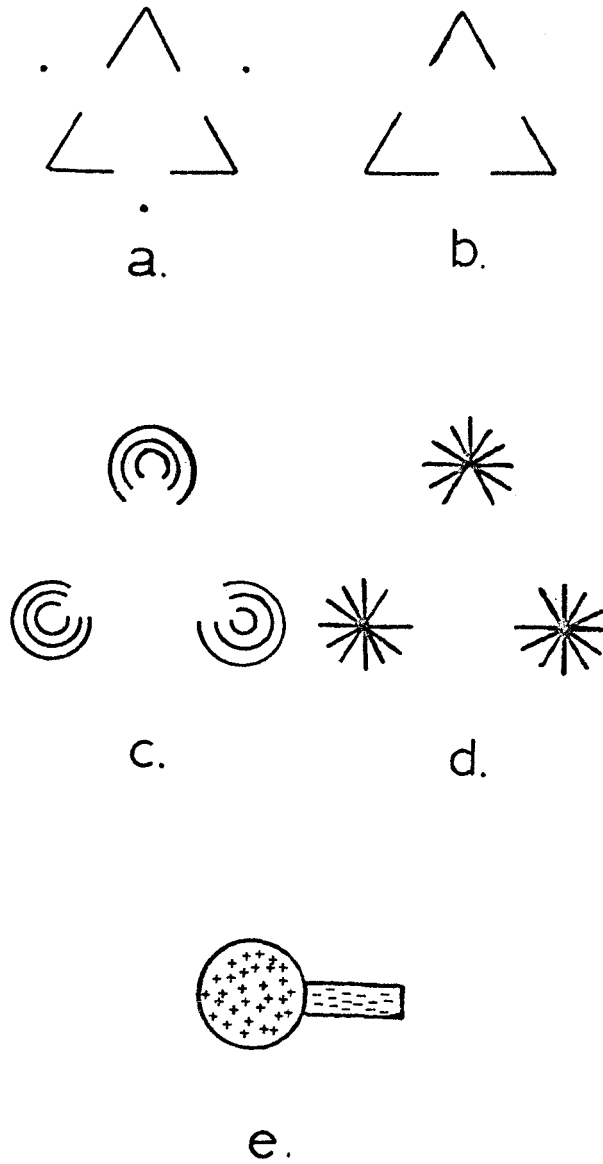


Figure 4. Neural Units and Lateral Inhibition in Subjective Contour Effects

do not produce brightness differences; in Figure 4b because there is brightness induction only at the ends of the lines; in Figure 4d because the brightness induction is distributed to the entire surface, background as well as area within the triangle.

While the fact that the subjective contours differ in brightness from the background in the direction which might be predicted by a peripheral inhibitory interaction, there are a number of counterexamples which are not accommodated by a simple brightness contrast explanation. Bradley & Dumais (1975) point out that a brightness contrast explanation cannot account for the homogenous appearance of the subjective boundaries. Coren & Theodor (1975) present a set of figures which seem to rule out the likelihood that subjective contours are caused by simple action of simultaneous brightness contrast. Figure 5 is redrawn from Coren & Theodor (1975). Notice that a white rectangular bar is seen interposed in front of the word STOP. The white of the bar is considerably brighter than the white of the background, and it is bounded by apparent contours which extend over the intermediate areas. It is interesting to compare the white of the bar in this array with the white in the upper portion of the letter P. In the letter, the white area is completely surrounded by black, which should provide the optimal configuration for brightness contrast. However, the apparent brightness of the subjectively bounded

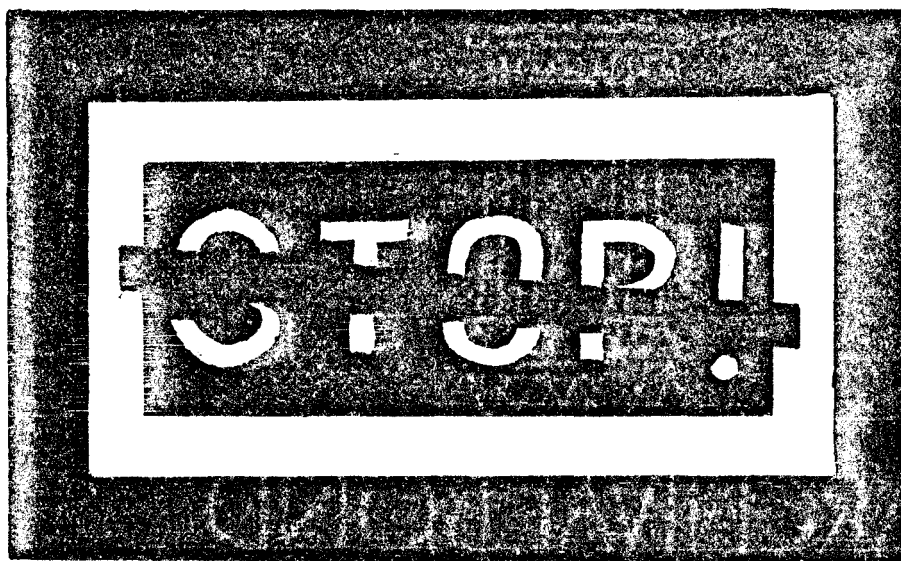
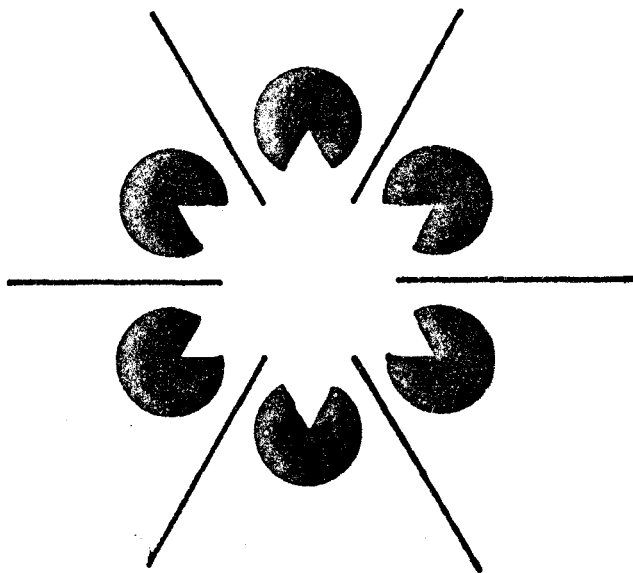


Figure 5. Figures Which Do Not Support Simultaneous Brightness Contrast as an Explanation for Subjective Contours.

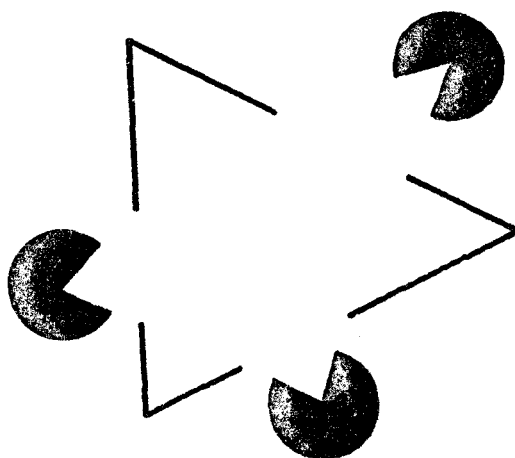
overlying bar is considerably greater than that of this enclosed region, despite the fact that it is only bounded in an interrupted fashion by black inducing fields. When we look at the negative of this configuration (see Figure 5b), we again find that the actual percept is at variance with the prediction based on simultaneous brightness contrast. Here, the inner region of the letter P is completely surrounded by the white inducing field and should be seen as darker than the subjectively interposed rectangle.

These inadequacies have led Coren & Theodor to ascribe the perception of subjective contours to organizational factors which utilize implicit depth cues in the configuration. This explanation can be considered as belonging to a more cognitive interpretation first put forth by Gregory (1972). He suggests that an illusory object is "postulated" as a perceptual hypothesis by the visual system to account for the black sectors and the breaks in figures that produce subjective contours. This position is supported by configurations like those in Figure 6. In Figure 6a either a six-pointed star or two superimposed triangles (with one inverted) may be seen. The perceived location of the illusory contours depends on the prevailing perceptual organization.

Coren (1972) and Gregory & Harris (1974) have elaborated the cognitive explanation. They have shown that perception of subjective contours is related to apparent depth



a.



b.

Figure 6. Examples of the Perceptual Organization Hypothesis.

cues in the figure. Coren (1972) states that the presence of forms or planes at various depths produces the perception of subjective contours. The only prerequisite is that the cues be strong enough so that the configuration is seen as tridimensional rather than bidimensional.

Harris & Gregory (1973) and Gregory & Harris (1974), in two different experiments, find support for the interposition hypothesis. They presented subjects with a binocular display which when fused formed a standard subjective contour (see Figure 1b). They then varied the disparity of the left and right images such that it would be consistent with an interposed object or opposite to it. They found that both the subject's phenomenal reports of the strength of the subjective contour and judgments of its depth were consistent with an interposed foreground object when the disparity cues were consistent. But, there was rivalry and reversal of the contour when the cues were not consistent with a foreground object.

The cognitive explanation, however, cannot predict which object hypothesis, of the many possible, will be selected in a given instance, nor has the theory attempted to explain the brightness differences that are so frequently found. In addition, the creation of three-dimensional planes out of a two-dimensional array of elements is not a new phenomenon. Hochberg & Brooks (1960) have shown that when a complex two-dimensional figure is presented to observers,

they very frequently "simplify it" by interpreting it as a three-dimensional figure. The main difference with subjective contours seen in depth is that in these figures the subject not only renders the percept into three-dimensionality, but also supplies the missing edges to make the stimulus apparently complete. Most recently Marr (1976) and Ware & Kennedy (1977) have reported illusory lines (see Figure 7). These configurations present an additional difficulty for the cognitive-depth explanation since it is not as clear how one can account for these types of subjective contours with an interposed object or implicit depth cues.

It is perhaps surprising that with the numerous theories attempting to explain subjective contours that there is only one quantitative or parametric study by Dumais & Bradley (1976) investigating the type of subjective contour shown in Figure 1 and none investigating the subjective line. Dumais & Bradley, using configurations like Figure 1d, had subjects give magnitude estimates of the strength of subjective contours as compared to real contours varying the retinal size and illumination of the display. Retinal size was found to be a powerful determinant of apparent contour strength, regardless of whether changes in this variable are achieved by varying figure size, viewing distance, or both.

Since an infinite number of figure size/viewing distance combinations can generate the same visual angle, Bradley & Dumais varied physical size and distance independently.

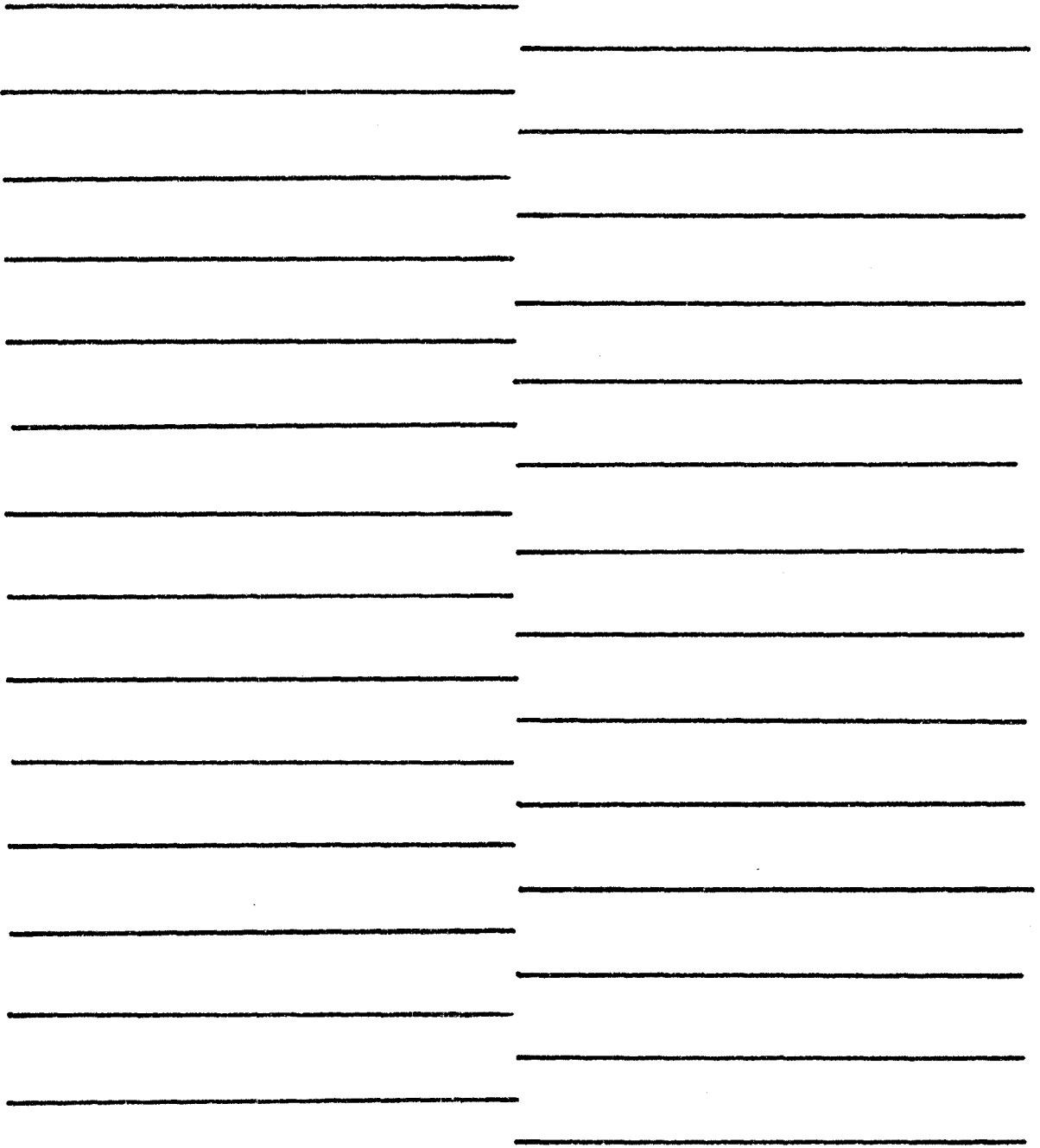


Figure 7. A Subjective Line.

They presented subjective triangles of three different sizes (10.16, 20.32, and 40.64 cm) at viewing distances of (121.92, 243.84, and 487.68 cm). These combinations resulted in visual angles shown in Table 1.

In order to maintain proportion between the inducing elements and the subjective contour, they also varied the radii of the inducing circles from 1.9 cm. to 7.62 cm. to correspond to the length of the sides of the subjective contour. Each size and distance combination was viewed at five illuminance levels (.10, 1.49, 2.21, 2.65, and 2.89 log lx). These conditions were presented in a 3 x 3 x 5 mixed factorial design with viewing distance as the only between-groups factor. Subjects gave magnitude estimates of the contours produced by the various combinations of conditions by comparing the displays to real contours with an angular size of 18.43° and illuminated at .62 log lx.

They found that the magnitude of the subjective contours varied inversely with the log of the illumination and inversely with the log of the retinal size of the displays. The finding that apparent contour strength varied with the inverse log of the incident illumination is of considerable theoretical import since it is opposite to the prediction made by the simultaneous brightness model.

Given the sparse quantitative data on subjective contours and subjective lines several experiments were conducted to further explore these phenomena. The first experiment

Table 1
 Visual Angle for Displays
 Used by Dumais and Bradley

Figure Size	Viewing Distance		
	4'	8'	16'
4"	4.77 ^o	2.39 ^o	1.19 ^o
8"	9.53 ^o	4.77 ^o	2.39 ^o
16"	18.92 ^o	9.53 ^o	4.77 ^o

was designed to replicate Dumais & Bradley (1976) using stimulus conditions which produce subjective lines to determine: (1) if these stimuli followed the same psychophysical functions as the contours they studied, (2) to determine if the strength of the contours varied systematically as a function of size and luminance.

A second experiment used the same stimuli as experiment 1 but at different orientations. A number of researchers have reported different response sensitivities as a function of the orientation of the stimuli (Blakemore & Nachmias, 1971; Campbell & Kulikowski, 1966; Blakemore & Campbell, 1969). In addition, Weisstein et al. (1977) report differences in the strength of the "phantom motion" after-effect as a function of the orientation of the display. They found that horizontal occlusion without interruption of moving grating patterns gives rise to moving phantoms while vertical interruption or horizontal occlusion without interruption (having the grating move only above or only below an empty region) does not. Kitterle (1973) has shown that brightness contrast is stronger for vertical and horizontal than for oblique stimuli. These findings suggest that there may be orientational asymmetries in the subjective contour phenomenon. The second experiment extended the investigation of subjective lines to horizontal and oblique lines, as well as vertical lines to determine if subjective lines show similar sensitivities.

The third experiment used the results of the first two experiments to construct stimuli that varied in the strength of subjective contour they produced. These stimuli were presented in a masking paradigm. Some masking effects have been reported with subjective contours. Smith & Over (1977) have shown that orientation-selective masking occurs between phenomenal edges (subjective contours) as well as between real edges. In addition, they reported that real contours can be masked by subjective contours and vice versa. Weisstein et al. (1974) using a masking paradigm report that when subjects view stationary illusory gratings for a prolonged time, the apparent contrast of subsequently presented gratings decrease. Experiment 3 extended these findings by systematically varying parameters of the mask and target to determine: (1) if the detectability of a target varied as a function of the strength of the subjective contour in the display, (2) one of several masks (luminance, pattern, and spatial frequency) would interfere with the contour effects. Quantitative measures of the perceived strength of the subjective contours as a function of differences in the inducing patterns and the masking stimuli were reported.

EXPERIMENT 1

Introduction

In experiment 1 subjects rated the strength of horizontal subjective lines formed by vertical inducing lines of various sizes and intensities. The size of the display was varied by varying the length and spacing of the inducing lines. The luminance of the displays was varied by having subjects view the displays through one of four neutral density filters.

Method

Subjects. Six students acted as observers. It was required that the observers have 20/20 vision, or vision corrected to 20/20 as tested with a Snellen eye chart. They received course credit for their participation.

Design. A 4 x 4 repeated measures design with replications was used with four figure sizes (2.39° , 4.76° , 9.53° , and 13.99°) and four filter values (0.0, 0.3, 0.8, and 1.1 N. D.). Since retinal size, rather than physical size or viewing distance, has been shown to effect the strength of subjective contours, viewing distance and size were not varied independently. The ratio of figure size to viewing distance was kept close to values used by Dumais & Bradley, so that the visual angle subtended by the figures overlapped the values used in their experiment. The viewing distance was 26.5 in. (67.31 cm).

The dependent measure was the subject's magnitude estimate of the "strength or saliance" of the subjective contour.

In the Dumais & Bradley experiment viewing distance was a between-subjects factor. Here there were no between-subjects variables. There were 16 stimulus combinations. Each subject gave 10 responses per condition for a total of 160 responses. In addition, each subject received one practice trial at each combination of luminance and size to provide the subject with some experience at using magnitude estimation as a means of assessing the perceived strength of subjective contours. The order of presentation was completely randomized.

Apparatus and Stimuli. The stimuli were presented on the face of a display CRT driven by a PDP 8/E computer.

Figure size was varied by changing the spacing of the lines that produce the subjective contour. The number of inducing lines was held constant at sixteen for all displays. This was analogous to Dumais & Bradley varying the radius and separation of the inducing elements to produce different size figures. For each of the size conditions the separation between the lines was varied so that the length of the contour would be either 2.49° , 4.76° , 9.53° , or 13.99° . The length of the inducing lines was approximately $.56^\circ$ for the smallest figure, and was increased proportionately with the figure size giving lengths of $.56^\circ$, 1.12° , 2.28° , and 3.27° .

The inducing lines were vertical, thus producing horizontal subjective contours. Figure 8 shows the four figure sizes drawn to scale.

The displays used were opposite in contrast from those used by Dumais & Bradley; that is, the figures were bright lines on a black background. The intensity of the display dots was set as high as good image quality would allow, about .1 ft. lam. as measured by an SEI Ilford model photometer. The luminance of the stimuli was varied by inserting neutral density filters in the subject's line of sight. This was accomplished with a specially constructed apparatus which rotated one of the four filters into the subject's line of sight. The apparatus was remotely operated so that the experimenter was able to change filters from the control room. A photograph of the apparatus is included in Appendix A.

Since the luminance of each display varies as a function of the number of points displayed, and the larger figures had more points, the intensity of the display dots was equated by displaying null points for the smaller figures.

The standard was a real edge formed by two adjacent rectangles, one darker than the other. It was at a constant angular size of 5° and assigned a modulus of 10 in magnitude.

Procedure. The experimenter briefly explained the subjective contour phenomenon and the magnitude estimation technique emphasizing the need to preserve a ratio scale in

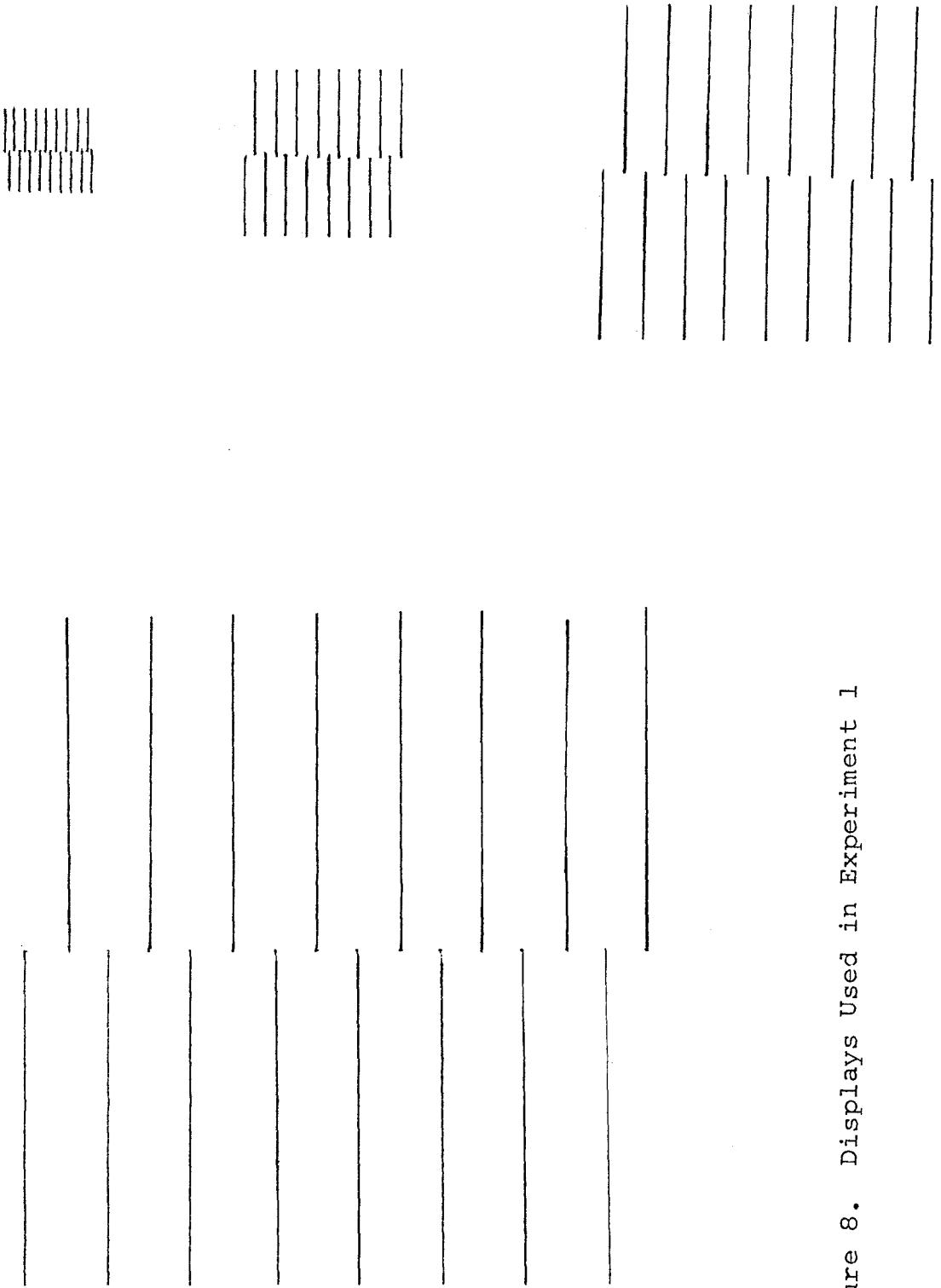


Figure 8. Displays Used in Experiment 1

the judgments. The observer was told that his/her task was to compare the apparent strength of the clearly perceptible real contour, of modulus 10, as standard, to the "strength or salience" of the subjective contours. A practice trial was given at each of the treatment combinations. A trial consisted of the following sequence: a $\frac{1}{2}$ -second presentation of a fixation point, followed immediately by a $\frac{1}{2}$ -second presentation of the subjective contour, followed by a pause. At this time the magnitude estimate was verbally reported.

EXPERIMENT 2

Introduction

The second experiment extended the investigation of subjective lines to vertical and oblique, as well as horizontal lines. The same size and luminance conditions as experiment 1 were used and subjects rated the strength of the contours formed at different orientations.

Method

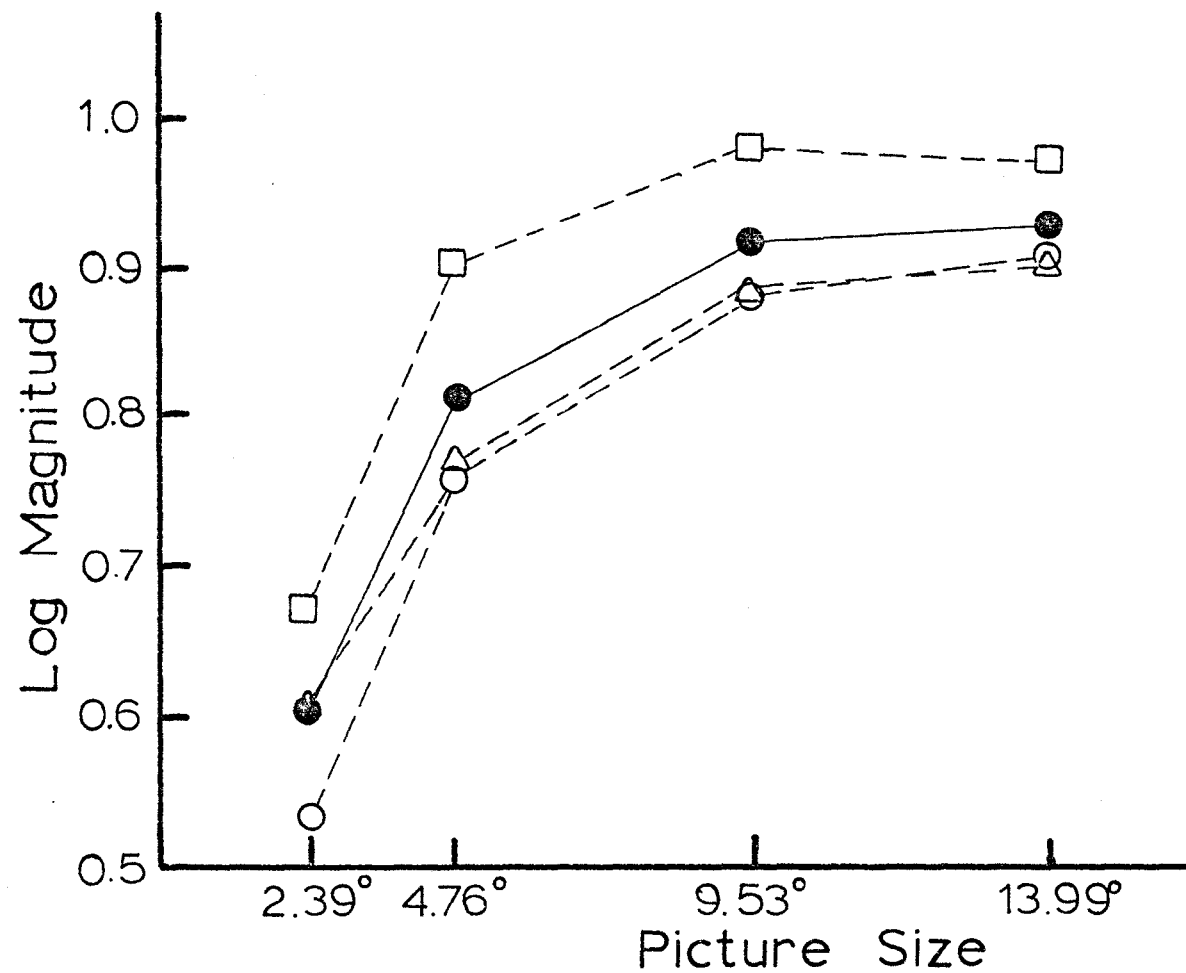
The methodology and procedure were the same as in experiment 1, except that there were two sets of stimuli, one with horizontal inducing stimuli and vertical subjective lines, and another with inducing stimuli oriented at 135° and subjective lines at 45° . In all other respects the experiments were identical.

Subjects. The subjects were the same six students who participated in the first experiment. They participated in the second experiment after they had completed the first one.

Results of Experiment 1 and Experiment 2

Figure 9 shows the mean of the log of the magnitude estimates as a function of the size of the display on a linear scale. There are four lines plotted on the graph: three dashed lines, one for each orientation, and a solid line which is the mean of the three orientations. The graph sug-

Figure 9. Mean Magnitude of Subjective Lines as a Function of Size.
○---○ Horizontal; □---□ Diagonal; △---△ Vertical; ●---● Composite.

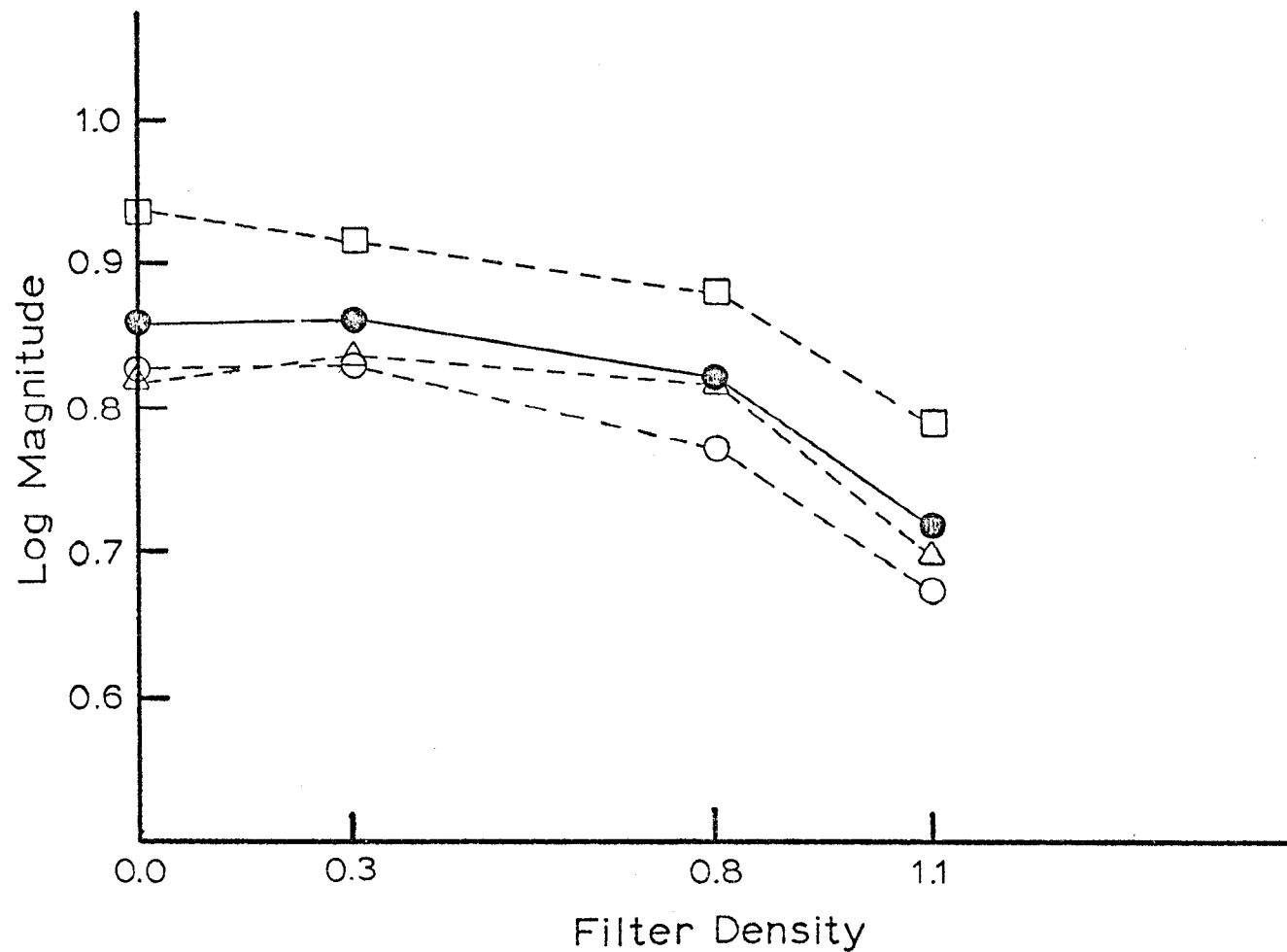


gests that the magnitude of the subjective lines was least for the smallest figures and increased as the figure size increased. This effect was statistically significant, $F(9, 45) = 22.0491$, $p < .00001$. The graph also shows that the magnitude estimates asymptoted at 9.53° . Duncan's Range tests among the means bear out this impression, indicating that the means for 2.39° , 4.76° , and 9.53° differ from each other at the $p < .05$ level but 9.53° does not differ from 13.99° at the $p < .05$ level for all orientations.

Figure 10 shows the mean perceived magnitude of the subjective lines plotted this time as a function of the filter density. The scale on the vertical axis is log magnitude and the scale on the horizontal axis is filter density. Again, there are four lines plotted on the graph: three dashed lines, one for each orientation, and a solid line for the mean of the orientations. The graph shows that magnitude estimates were greatest for the lower density filters and decreased as the density became greater. This effect was statistically significant, $F(3, 15) = 4.3885$, $p < .02$.

Looking at both Figure 9 and Figure 10 we see that for all densities and all sizes the vertical and horizontal orientations seem to cluster while the diagonal condition is always greater. This difference resulted in a significant main effect for orientation, $F(2, 10) = 5.1388$, $p < .02$. Further tests on the means of the horizontal, vertical, and diagonal conditions for each density and size show that in

Figure 10. Mean Magnitude of Subjective Lines as a Function of Filter Density.
○---○ Horizontal; □---□ Diagonal; △---△ Vertical; ●---● Composite.



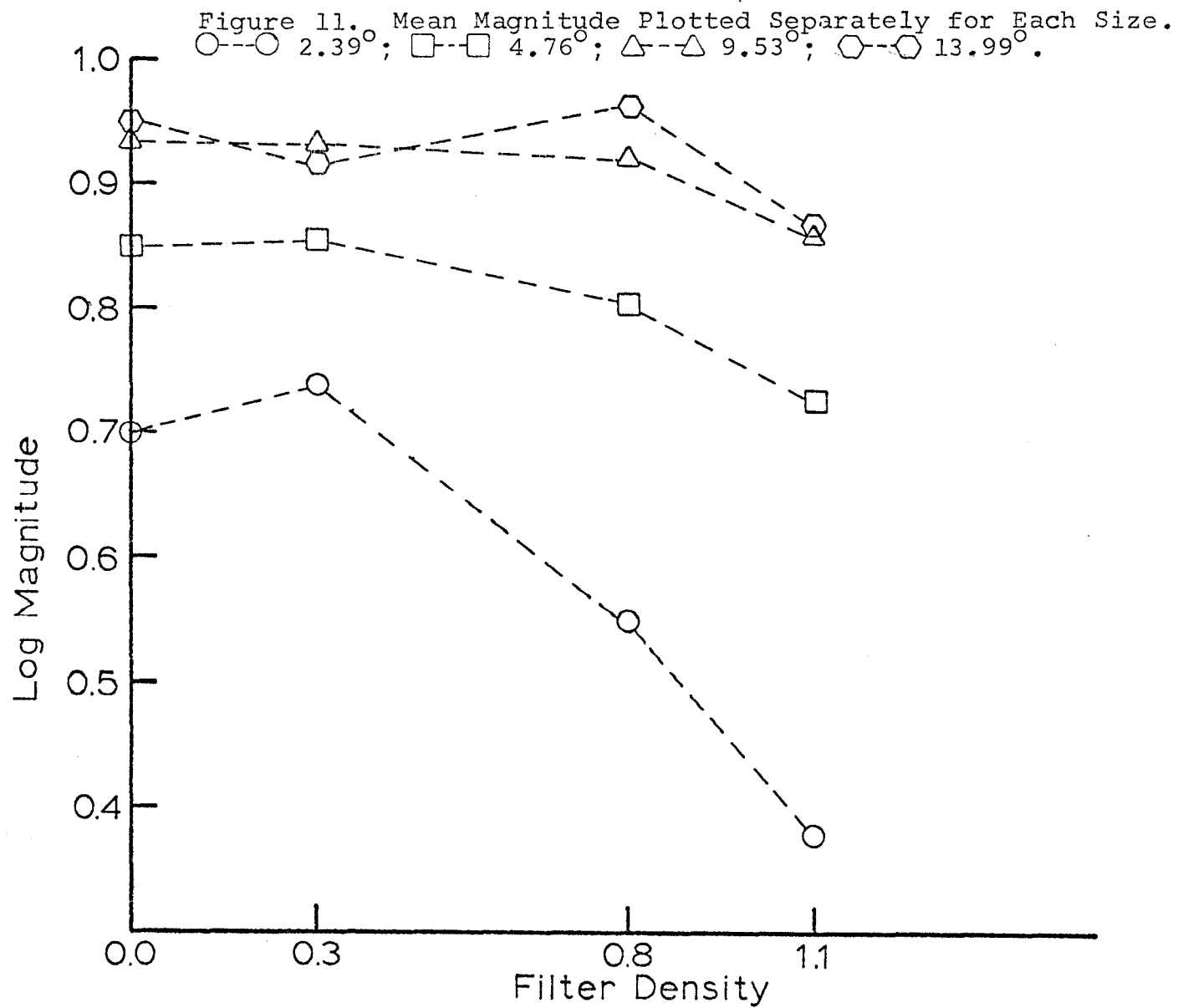
all cases the horizontal and vertical means are not significantly different at the $p < .05$ level while the diagonal mean is significantly different from both the horizontal and vertical means at $p < .05$.

To summarize the results thus far, the main effects for orientation, size, and filter density were significant. The data have indicated, then, that the perceived magnitude of subjective lines increases with increases in both the size and luminance of the contour inducing display. Increasing the size of the display beyond approximately 9° visual angle does not increase the strength of the subjective line. In addition, there was no significant difference between the perceived strength of horizontal and vertical contours, but the diagonal contours were consistently more salient.

The analysis of variance indicated a significant interaction between size and filter density. Figure 11 shows the interaction from one perspective by plotting each size separately. There are four lines plotted on the graph, one for each size display. The vertical axis is log magnitude estimate and the horizontal axis is filter density. The larger displays (9.53° and 13.99°) were not greatly influenced by changes in filter density. However, as the displays got smaller the effect of filter density increased.

Discussion of Experiment 1 and Experiment 2

There were a number of differences between these data and the data reported by Dumais & Bradley (1976). They



reported that the perceived strength of subjective figures varied inversely with changes in the luminance and retinal size of the contour inducing displays, that is the contours became more salient as the luminance or size of the display was reduced. These experiments showed the opposite effect. The perceived strength of the contours increased with increased luminance and it also increased as the size of the display increased.

Perceived magnitude was a monotonically increasing function of luminance (see Figure 10). The reverse effect of display luminance may be due to the reversal in contrast between these displays and those used by Dumais & Bradley. They presented black inducing elements on a bright background, while the displays in these experiments were composed of white inducing elements on a black background. Thus, changes in luminance in the Dumais & Bradley experiment meant changes in the background luminance, while in these experiments the background remained constant (black) and the luminance of the inducing elements changed. This meant that the adaptation level differed also.

The Dumais & Bradley displays were front-lighted patterns drawn on paper. It is possible that as the illuminance was increased, more detail in the texture of the homogeneous area became visible. This may have reduced the strength of the effect by reducing the homogeneity of the background by adding real texture to the region in which the

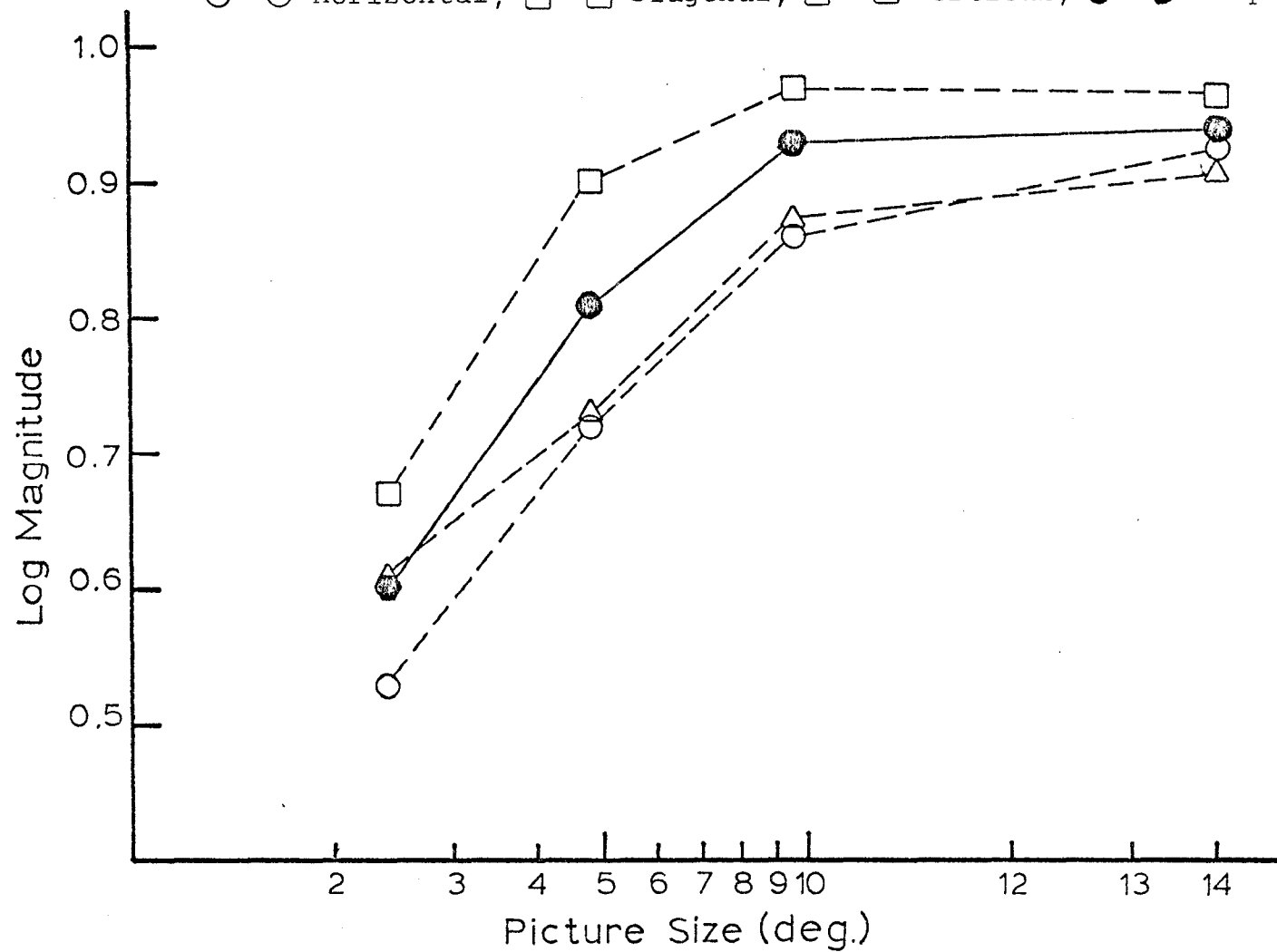
the contour would be formed. It is not known what effects non-homogeneities in the background have on the strength of contours.

To test these hypotheses as well as the alternative hypothesis that there are different functions for different types of subjective contours additional data is needed.

Magnitude estimates were also a monotonically increasing function of size. The data are plotted on log-log coordinates in Figure 12. Except for the last point, 13.99° , the ratings vary approximately linearly with the logarithm of size, especially the horizontal and vertical data. Ratings at 13.99° are not significantly different from ratings at 9.76° and this probably reflects an asymptote for the stimulus configuration used here. The different direction of the size effects may be due to the fact that subjective lines are shortened in the smaller displays. The illusion created by the subjective lines is that there is a crack or overlap in the display. The shorter displays did not fill the entire screen and as a result the large homogenous region beyond each end of the subjective contour might reduce the illusion of a crack or overlap. As the displays get larger this area was reduced and the contour became more salient. The size effect may be consistent with other hypotheses about subjective contours (see Discussion following experiment 3).

Finally, the diagonal contours were more salient than

Figure 12. Log-Log Plot of Mean Magnitude as a Function of Size.
 ○---○ Horizontal; □---□ Diagonal; △---△ Vertical; ●---● Composite.

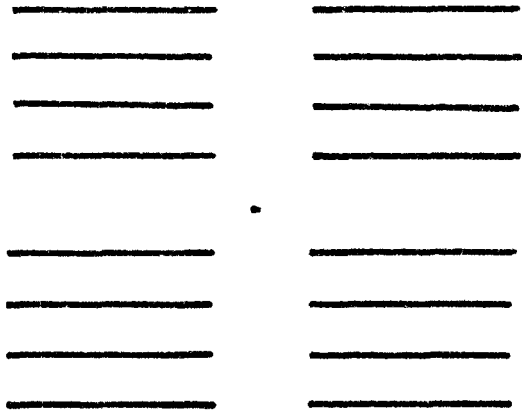


either vertical or horizontal contours. This finding was interesting since the literature generally reports a reduction in sensitivity to oblique stimuli. It is not clear why the diagonal stimuli produced stronger contours. The orientation effect does suggest that the effects are not due to peripheral mechanisms, since receptive fields in the periphery are usually circular.

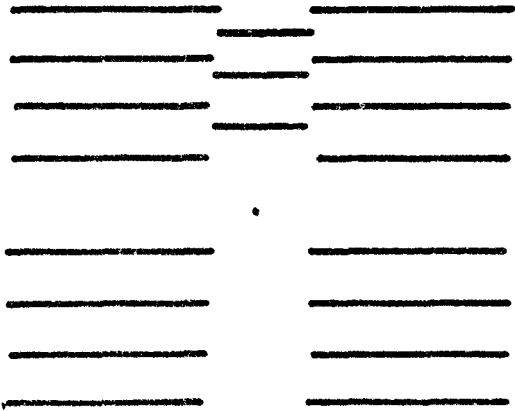
EXPERIMENT 3

Introduction

The third experiment used the findings of the earlier experiments about the strength of subjective lines to test whether or not subjective contours would produce other measurable effects. It is clear that the characteristics of the inducing stimuli strongly influence the formation of subjective contours. Thus, several features of the inducing stimuli were varied to explore in more detail the relationship between the strength of the subjective contour and the detection of the target. If subjective contour does have "real" effects as some research has indicated, then these effects should co-vary with the strength of the contour. Experiments 1 and 2 showed that the strength of the contours did vary with the size of the display. To test whether or not the detectability of a target would vary with changes in the strength of contours, a set of displays was constructed in which a target was an integral part of a subjective figure. The strength of the subjective contours was varied by changing the lengths and separations of the inducing lines. A target formed a subjective line with the inducing lines and the area in which the target appeared was in a subjectively darker area due to the effects of the inducing lines. An example of the display is shown in Figure 13.



a.



b.

Figure 13. Display Type Used in Experiment 3.

If we look at the inducing lines alone, (see Figure 13) they produce a subjectively brighter inner bar. The target was presented in this area. If we look at the target plus context we see that the target produced a subjective line with the inducing lines. This was true for all the context/target combinations. The displays used in the experiment had opposite contrast to those shown in Figure 13. This did not effect the subjective line but did result in a subjectively darker inner bar rather than a brighter bar. The subjective effects were judged by the experimenter.

In addition these displays were presented in a forward masking paradigm. Four masks (a blank, a luminance mask, a pattern mask, and a frequency mask) tested the effects of luminance, feature detectors, and spatial frequency analyzers on the formation of subjective contours. The time course of the formation of these effects was also investigated by varying the ISI between the mask and the test contour.

Rationale for Choosing the Masks

The term visual masking refers to events which occur when two or more stimuli are presented close to each other in time and space and for relatively short durations. The threshold of one of the stimuli (the target) is raised, or, if the target presentation is suprathreshold, its appearance is changed by the presence of another stimulus (the mask). We make the hypothesis that these perceptual effects

are correlated with changes in neural activity within the visual pathway. Populations of single units vary in their spatial and temporal properties (Barlow, 1953; Rodieck & Stone, 1965; Bishop, 1971). Once a neuron begins to fire, it fires in a characteristic way. Given a certain stimulus pattern presented for a certain duration, some number of neurons sensitive to that type of pattern will go through characteristic changes in their frequency of firing, or in their ability to fire. We hypothesize that these changes have perceptual effects. Threshold or, if the stimulus presentation is above threshold, apparent clarity, contrast, or brightness, depending on the nature of the stimulus, is assumed to be proportional in some manner, to this neural activity. Presentation of a target in visual masking allows a measure of these variations in neural activity.

There is a large amount of psychophysical evidence supporting the feature detection model of pattern recognition. The visual system has been shown to respond independently to different orientations (Blakemore & Nachmias, 1971), widths (Pantle & Sekuler, 1968), lengths (Nakayama & Roberts, 1972), directions of motion (Pantle & Sekuler, 1969), and non-local features based on a decomposition of the pattern into its spatial frequency components. For example, threshold for a subsequent grating is raised after viewing an adaptation grating of similar width and orientation (Pantle & Sekuler, 1968; Weisstein & Bisaha, 1972). On the other

hand, the perception of gratings whose stripes are much wider or narrower than the adaptation grating generally remains unaffected, as does the perception of gratings of sufficiently different orientation.

Some of these findings are supported by physiological data. Hubel & Weisel (1968) have discovered cortical cells that are selectively sensitive to a number of features including orientation, length, and width. The frequency of firing of single units, therefore, might serve to signal the presence of various properties. While there is no clear evidence for spatial frequency units in the visual system, there are some indications from the data of Bishop (1971) and Glezer, Ivanoff, & Tscherbach (1973) that the receptive fields of certain units in the visual system of cats and monkeys may consist of as many as five, seven or even thirteen alternating excitatory and inhibitory areas. Such units might form the basis for a reasonably precise Fourier analysis.

Based on these findings two masks were constructed, a pattern mask which shared local features such as line length, orientation, and width with the test contour, and a spatial frequency mask which shared spatial frequency components with the test contour. These masks were constructed so that as much as possible the spatial frequency mask did not share local features with the test contour and the pattern mask mask did not share spatial frequency compo-

nents. Two additional masks were used to control for luminance effects, a blank field and a luminance patch.

Selecting a Frequency Mask

A number of researchers (Pantle & Sekuler, 1968; Weisstein & Bisaha, 1972; Blakemore & Campbell, 1968) have suggested that the visual system analyzes patterns by decomposing the image into its spatial frequency components. The set of these frequency components, which is unique for each image, is the frequency spectrum of that image. The function which describes these frequency components is called the spectral density function. The purpose of the frequency mask was to test for interactions between the spatial frequency components of the mask and the test contour and thereby to quantify the amount of involvement, if any, of spatial frequency analyzers in the formation of subjective lines. In order to maximize the potential interaction, the mask should have a frequency spectrum similar to that of the test contour. This similarity must be in the frequency domain only since similarity in the image domain would confound the results. The first step, then, in selecting a frequency mask was to find the spectral density function of the test contour. Then, find the spectra of a number of possible masks and, finally, compare these spectra, selecting the mask with the greatest overlap in the frequency domain yet having little overlap in the image domain as the best candidate.

Finding the Frequency Spectra of Masks and Test Contours

The spectral density function, $F(\omega)$, can be gotten by taking the Fourier transform of the image function $f(t)$. The relationship between $f(t)$ and $F(\omega)$ is given by

$$F(\omega) = \int f(t) e^{-j\omega t} dt. \quad (1)$$

This equation is known as the continuous direct Fourier transform of $f(t)$.

In order to use the computational algorithms available to compute a discrete approximation to the spectral density function we must specify the image function, $f(t)$. What we have are drawings of the images to be used in the experiment. What is needed is a function describing those drawings to which the transform can be applied, that is, we must find an $f(t)$ for each image.

The method of obtaining this function is best illustrated in an example. Consider the following image, a bright bar on a dark background as shown in Figure 14. Alongside the image in Figure 14 is a profile of the intensity distribution in the image. This profile is gotten by moving from left to right across the image and at each point recording the intensity at that point. In this image, all the left to right slices would yield the same profile, as will be shown later this will not always be true. The profile we have generated in this manner represents the intensity distribution in the image. This profile can be rewrit-

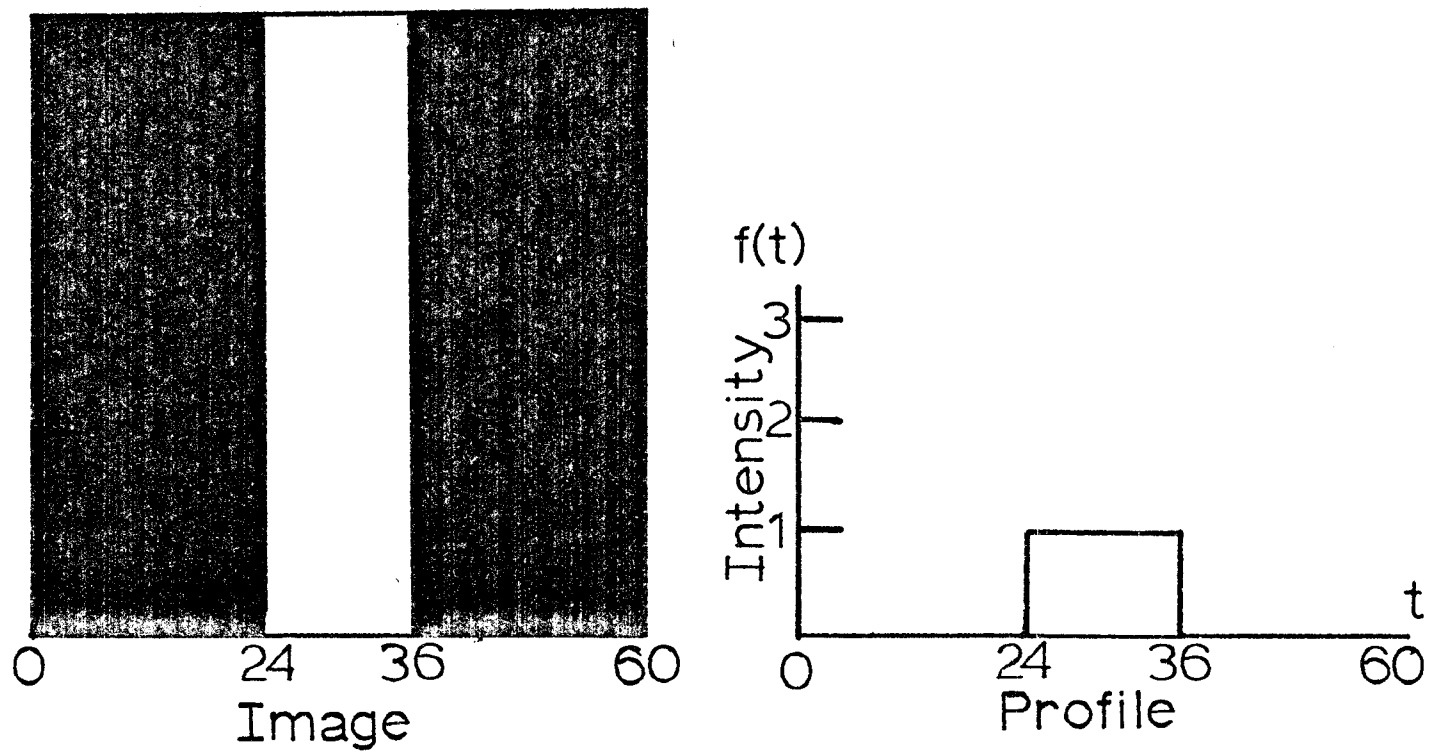


Figure 14. Obtaining One-dimensional Image Profiles.

ten as follows

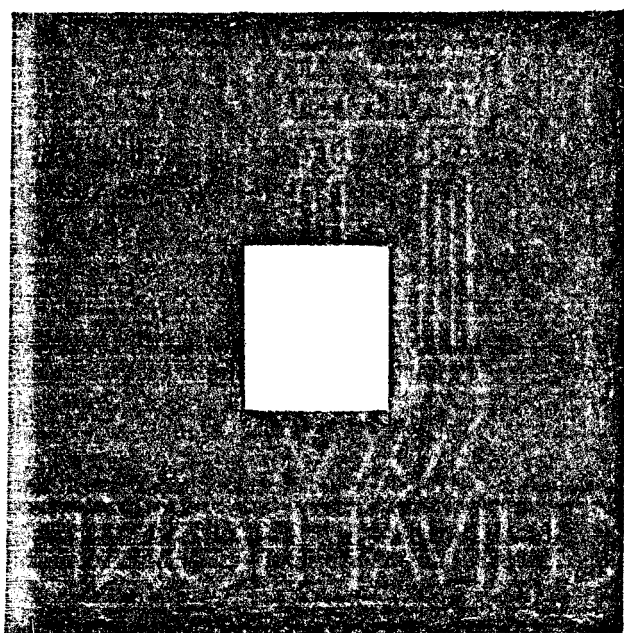
$$f(t) = \begin{cases} 0 & \text{for } t < 24 \\ 1 & 24 \leq t \leq 36 \\ 0 & t > 36 \end{cases} \quad (2)$$

That is, the intensity is zero for all points to the left of 24 and to right of 36 in the image. Between these points the intensity is 1. In general, this function can be written

$$f_D(t) = f_I(t) \delta(t) \quad (3)$$

where $f_D(t)$ is the discrete image function, $f_I(t)$ is the continuous image function, and $\delta(t)$ is the sampling function. The sampling function is a series of unit impulses. The separation between impulses determines the sampling rate. The function $f_D(t)$ obtained in this way can be used to obtain the Fourier transform.

As noted above the profile for most images is not the same for each left to right slice that can be made. Consider the image profile (see Figure 16) of a solid square (see Figure 15). We notice that all the slices from left to right that pass through the square have the same profile. However, those that pass either above or below are different. We, therefore, cannot represent the image with a single profile but must use a number of them. In Figure 16 there are 16 slices taken in equal increments moving up the image. These profiles are plotted together in 3-d to give a compo-



Image

Figure 15. A White Square.

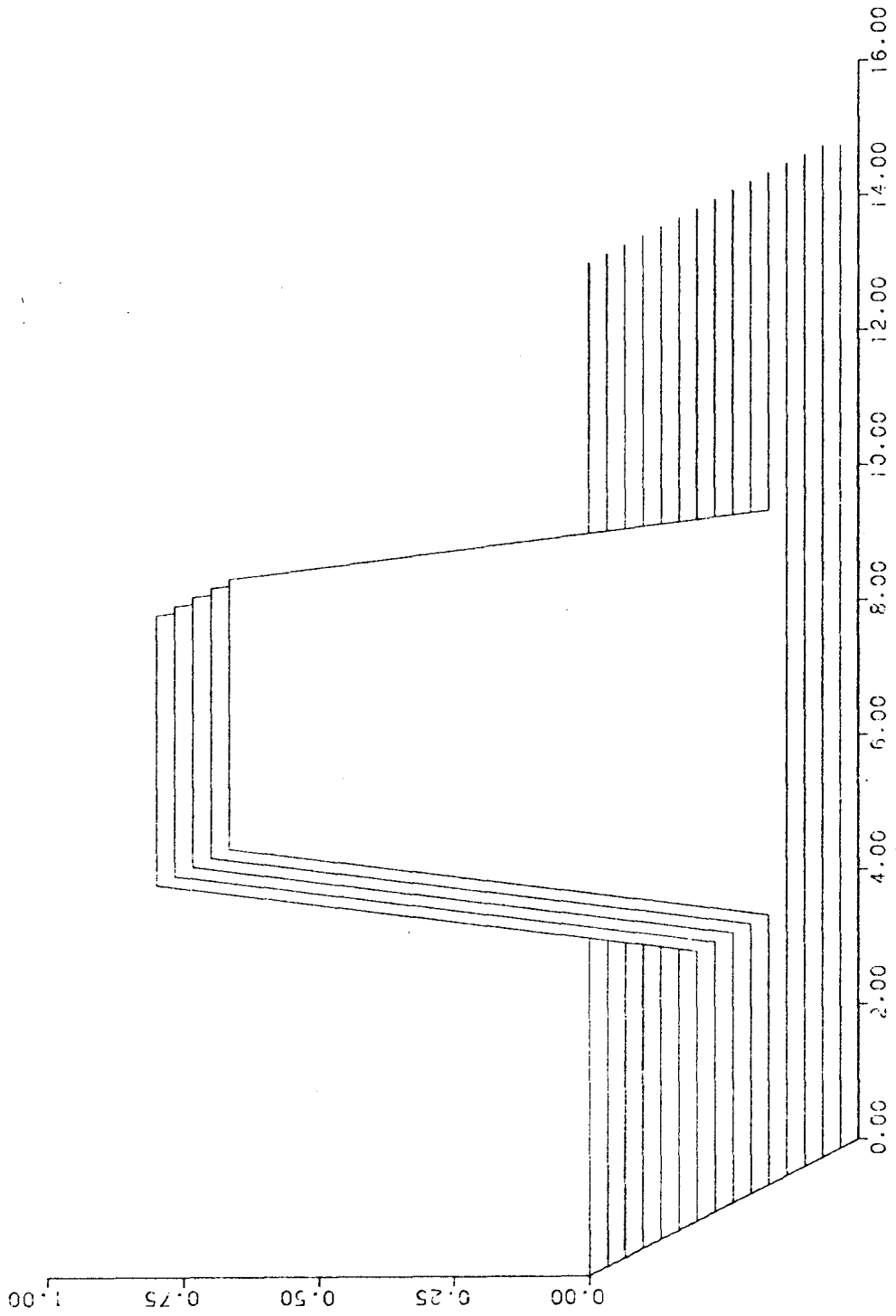


Figure 16. Image Profile of a White Square.

site for the image. Each mask and test contour analyzed was quantized in this way. The number of slices, in the example 16, was chosen arbitrarily, as was the number of points sampled in each slice. The greater the number of samples the finer the resolution and the greater the information preserved from the image function. For all the later analyses 64 profiles were taken and each profile was sampled at 64 points. By the uniform sampling theorem, a bandlimited signal is uniquely determined if it is sampled at regular intervals less than $\frac{1}{2}f_m$ apart. The sampling rate used resolved frequencies as high as 32 cycles/degree.

The fact that all the slices are not the same in a given image added an extra dimension of complexity. Where in the first case we could compute a 1-dimensional transform, we now must compute a 2-dimensional transform. Equation 1 can be rewritten

$$F(u,v) = \iint f_D(x,y) e^{-j2\pi (ux+vy)} dx dy. \quad (4)$$

and equation 3 as

$$f_D(x,y) = f_I(x,y) \delta_{x,y}(x,y). \quad (5)$$

Here the x's and y's replace the single variable t in the image functions and u and v replace ω in the transform.

We can now compute an approximation to the spectral density function, equation 4, by sampling the image function $f_I(x,y)$ to produce a discrete image function $f_D(x,y)$ and

then applying a 2-dimensional discrete Fourier transform to $f_D(x,y)$. The discrete transform is given by

$$F(u,v) = \frac{1}{N} \sum_{x=0}^{N-1} \sum_{y=0}^{N-1} f_D(x,y) e^{-j2\pi \frac{(ux+vy)}{N}} \quad (6)$$

for $u,v = 0, 1, 2, 3, \dots, N-1$.

Computing the Discrete Fourier Transform

Computing the transforms involved several steps.

Since the computations are tedious and for the resolution desired very numerous, special computer programs were written to compute the discrete image functions and the transforms. These programs are listed in Appendix B. A program product available from IBM called FFTM was used to compute the transforms. FFTM performs finite multidimensional direct and inverse transformations for complex arrays whose dimensions are powers of two using an algorithm developed by Cooley & Tukey (1965). The test contours and potential masks were run through these programs and the spectral density functions for each were computed. Each image function and its transform was plotted on a Calcomp drum plotter. While it seemed a large task to implement the plotting routine (Hide--see Appendix B for a source listing) it seemed to be the only way to verify the accuracy of the computations. For example, the graphical representations of a number of simple transforms are well known and were compared to results obtained here for verification. Similarly, the image profiles were plotted and inspected for accuracy.

Because of the nature of the transform, in order to display one full period, it is necessary to move the origin of the transform to the point $u,v = N/2$ (Gonzalez & Wirtz, 1977). This was accomplished by multiplying $f_D(x,y)$ by $(-1)^{xy}$. This operation required another step in the process and another short program.

Also, since the spectral density function is usually a complex function consisting of a real and imaginary part, the magnitude of the function is what is normally plotted. The magnitude is given by

$$F(u,v) = \left[R^2(u,v) + I^2(u,v) \right]^{\frac{1}{2}}. \quad (7)$$

Extra program code was written to compute the magnitude of the function to be plotted whenever it was the spectral density function.

The output for some simple test functions is shown in Figures 17 through 19. They show a sine wave, its transform, and the inverse transform, respectively. Figures 20 through 22 show the same sequence for an impulse function. These tests conform very well with expected results.

The set of potential masks was limited to simple figures that could be easily generated on the PDP/8E CRT. The display capabilities of the CRT are limited to about 1000 points and these points can only be displayed as horizontal, vertical, and 45° diagonal vectors. This constrained the choice of a frequency mask.

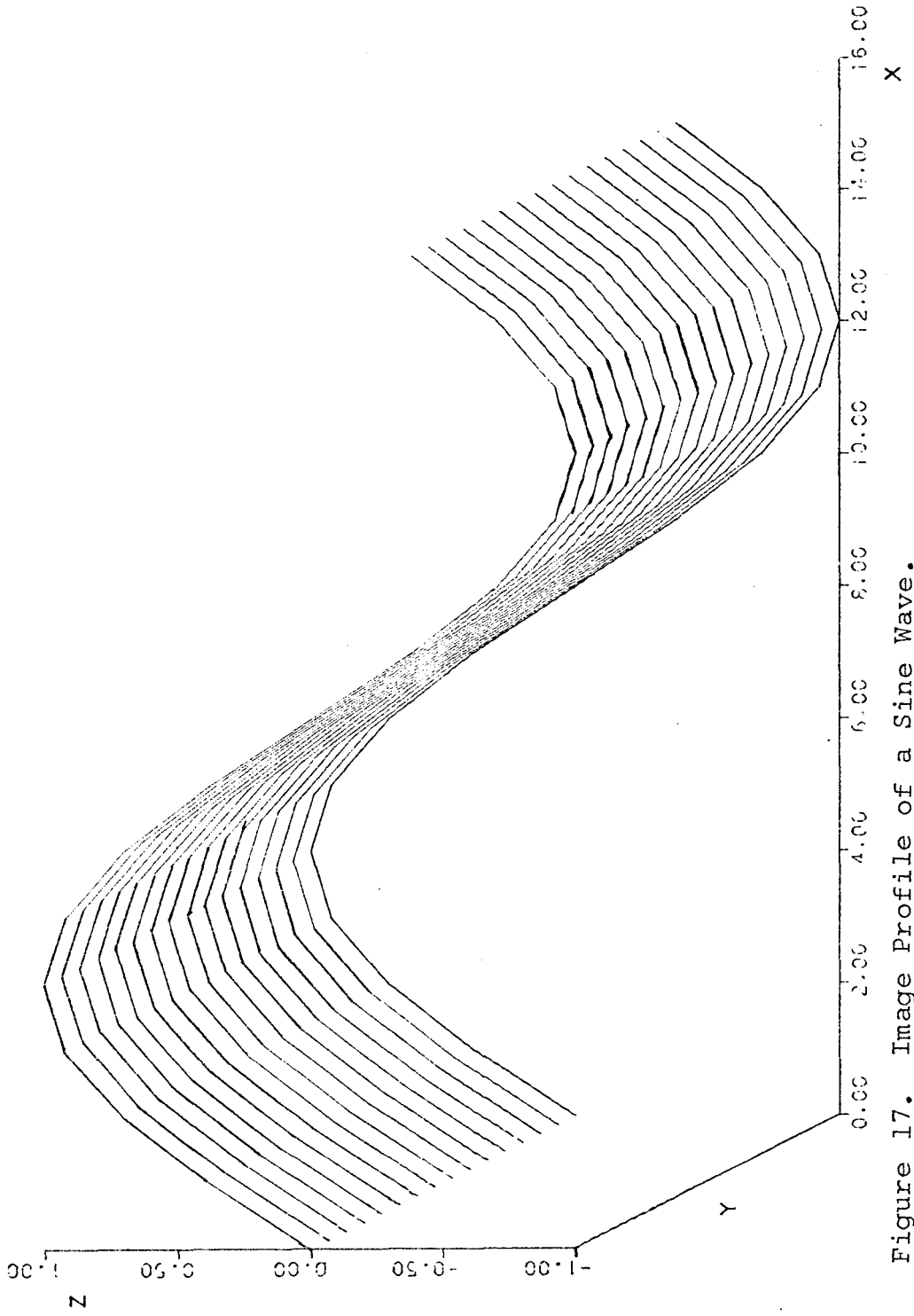


Figure 17. Image Profile of a Sine Wave.

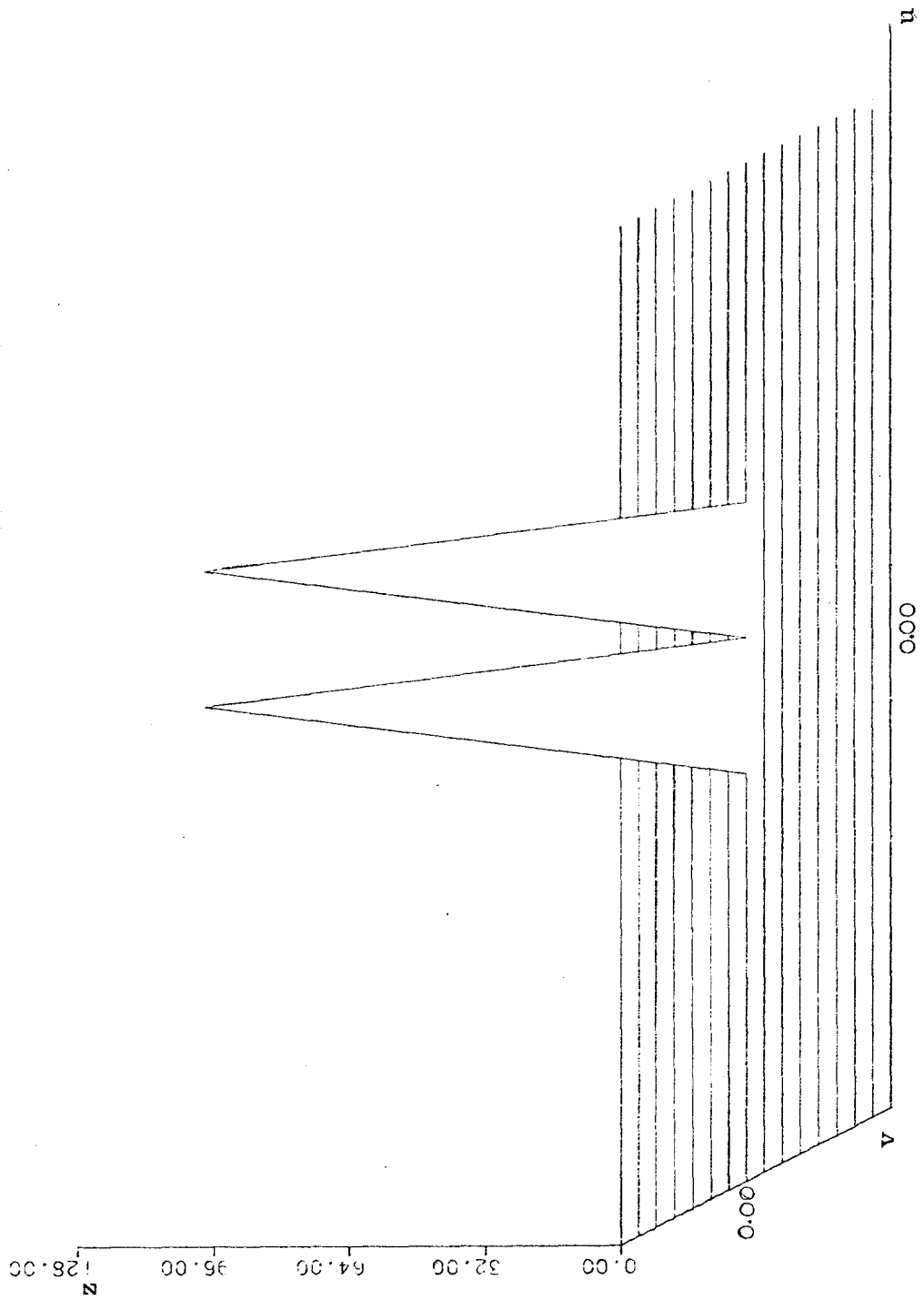


Figure 18. Transform of a Sine Wave (Magnitude Plot).

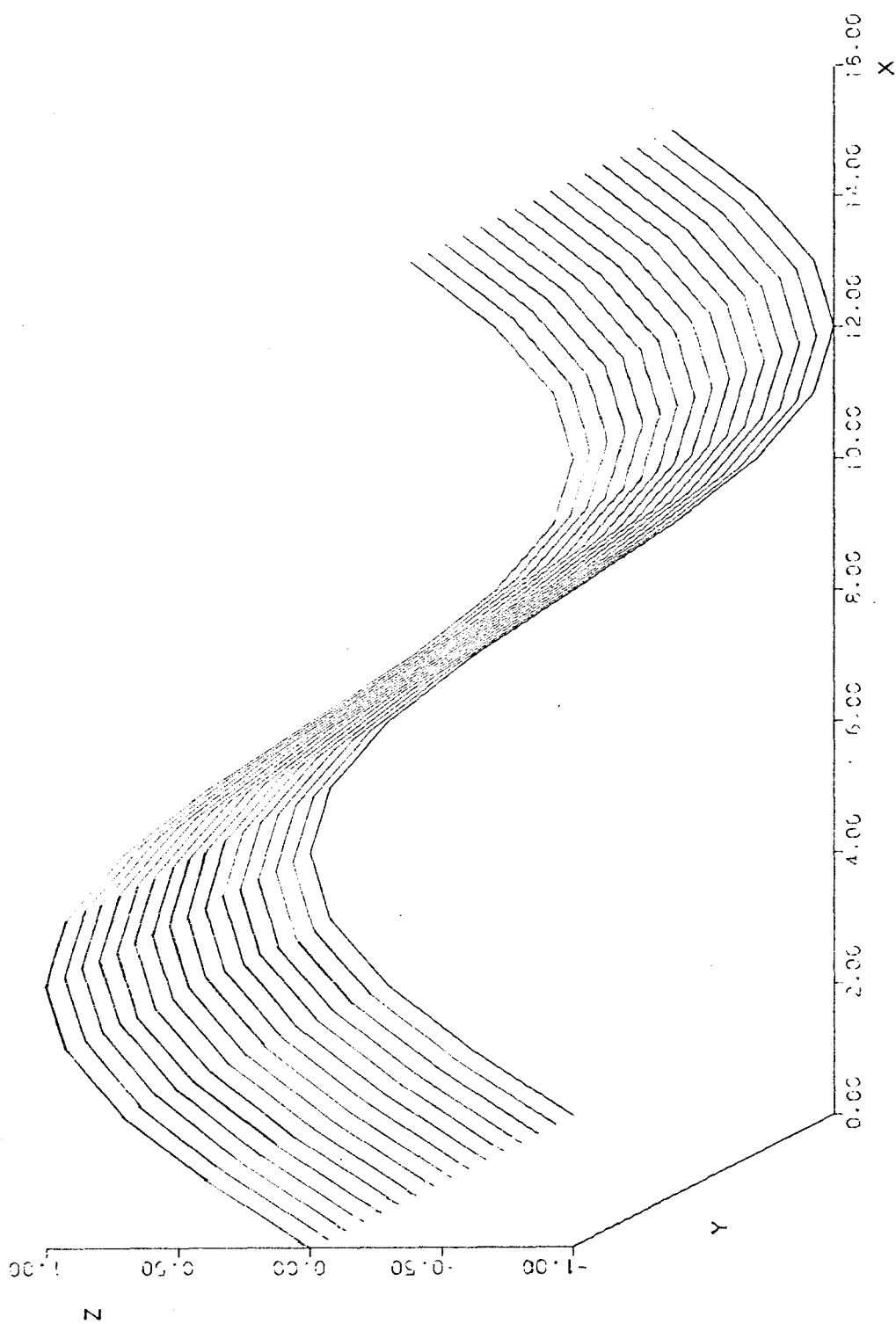


Figure 19. Inverse Transform of a Sine Wave

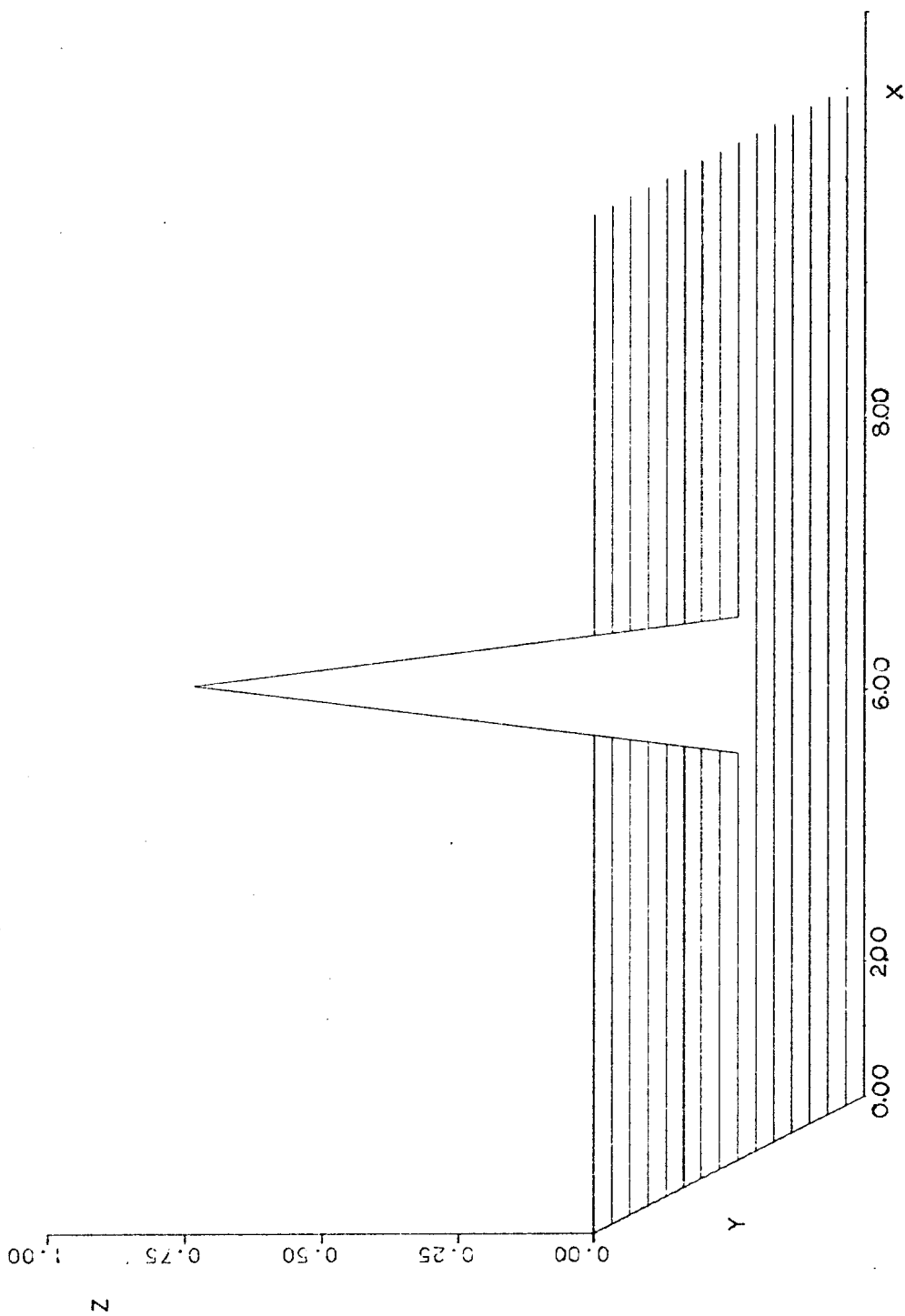


Figure 20. Image Profile of an Impulse.

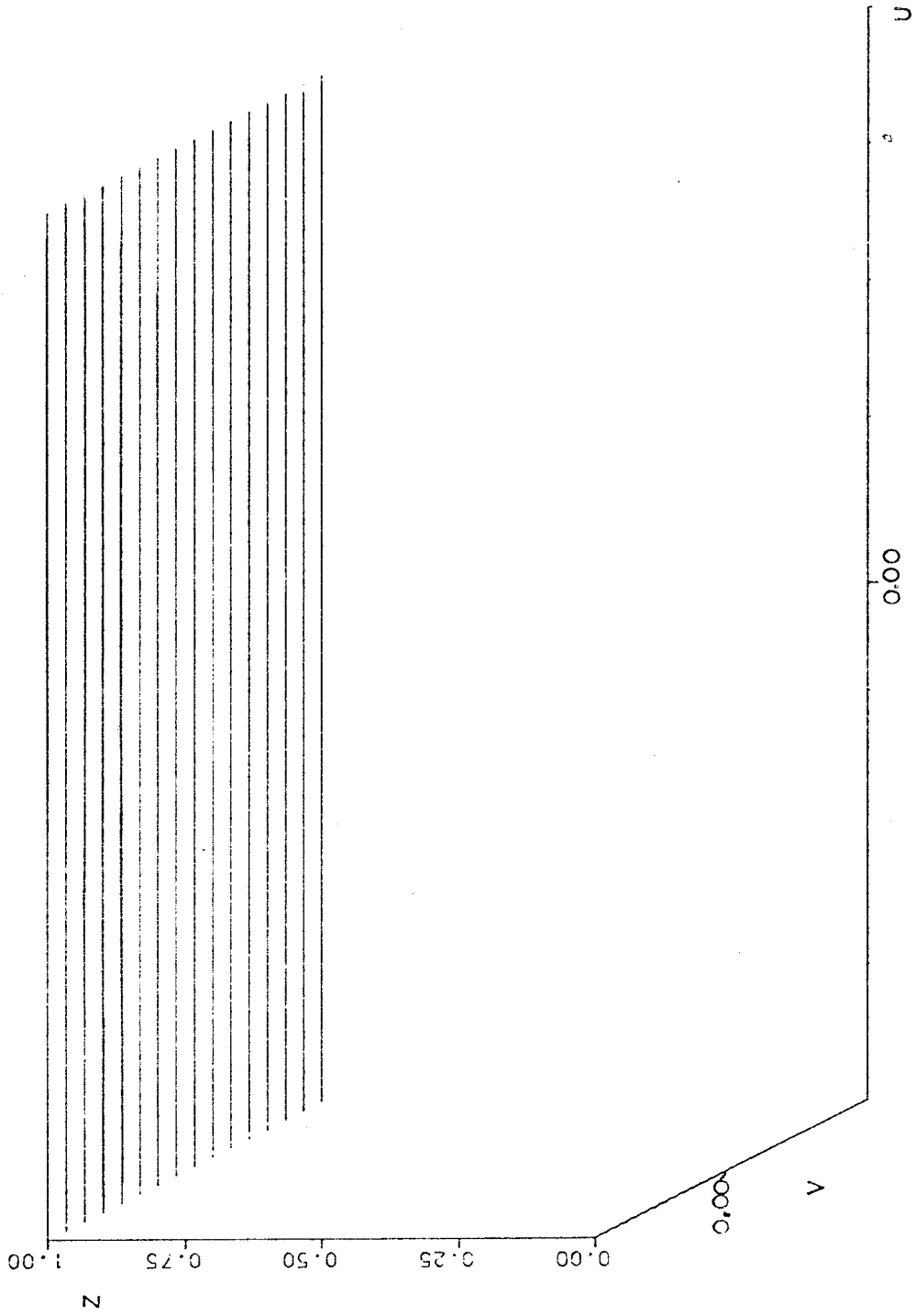


Figure 21. Transform of an Impulse.

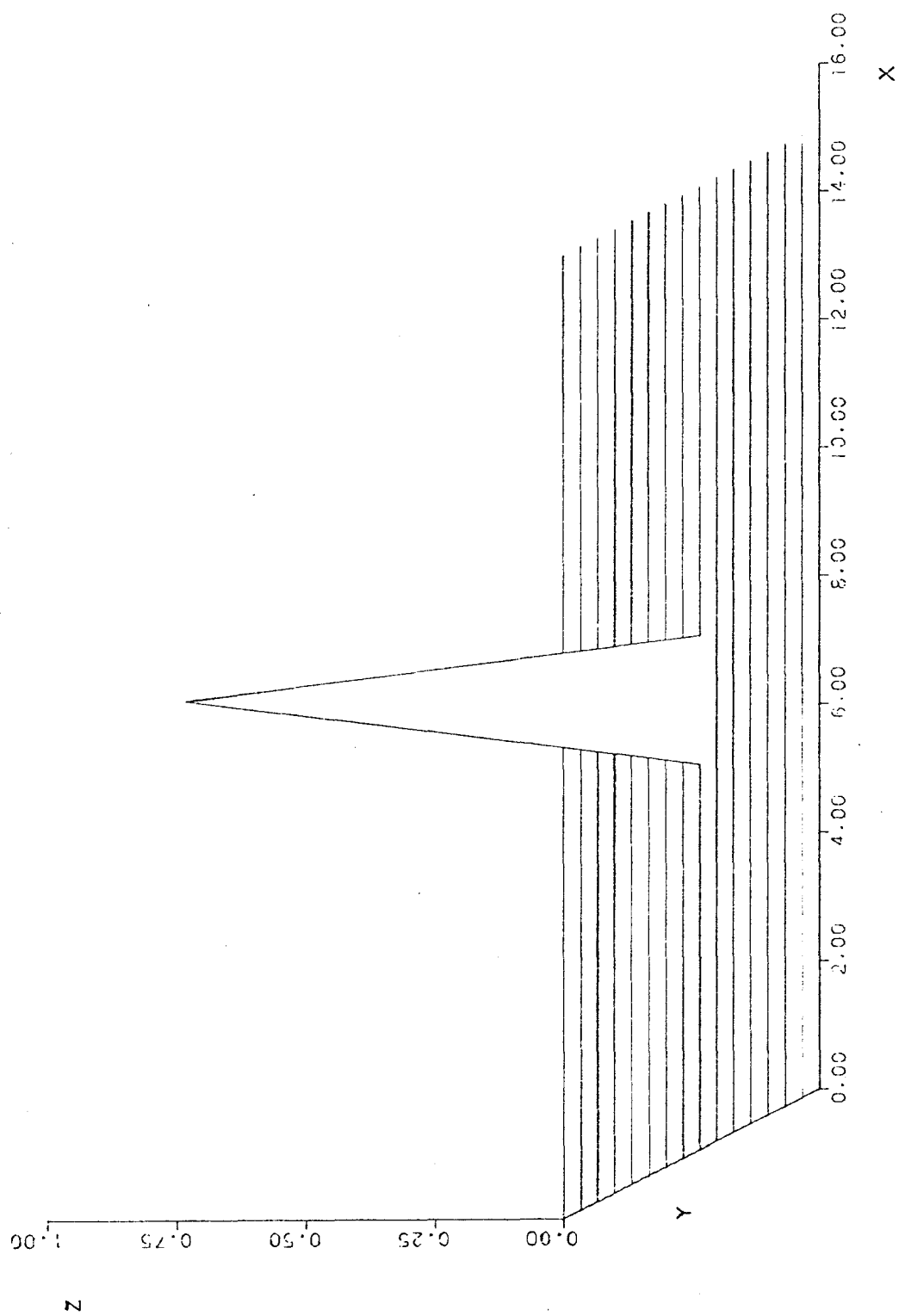


Figure 22. Inverse Transform of an Impluse.

Computing the Similarity Between Masks and Test Contours

Once a set of transforms was available, another program was written (see Appendix C) to compute a measure of similarity between the test contours and the masks. The optimal frequency mask was chosen by comparing the spectra of the various candidates with the spectra of the inducing pattern/target combinations. This was done as follows:

- a) the 2-dimensional transform of each stimulus was taken.
- b) each frequency spectrum was normalized by dividing through by the largest amplitude, thus setting the maximum to 1.
- c) a measure of similarity between the frequency spectra of each stimulus was obtained by sampling points at set intervals of frequency. Then the ratio of the two functions at each of these sampling points was taken.
- d) the ratios were summed. The frequency mask with the greatest total was selected.

Sums close to the number of points indicate high similarity, sums close to zero indicate low similarity, as do sums much greater than the number of points. However, if the ratio is the ratio of the mask to the target, sums greater than the number of points indicate that the mask has much greater energy than the target. This latter condition, while showing low similarity, is not a sufficient reason for eliminating

a mask. This measure does not indicate whether the high amplitude in the target was coincident with high amplitude in the mask or whether the large sum was due to high amplitude in the mask spectrum coinciding with low amplitude in the test contour. As a result, two other measures of similarity were made.

One measure used a least squares approach in which the sum of the squared differences between mask and test contour was computed. The criteria for selection for this measure was the mask with the smallest sum.

Another measure summed those instances when the mask had greater amplitude than the target at a given frequency separately from those instances when the mask had less amplitude than the target. For this measure the criteria for selection was a minimum "less than" sum and a maximum "greater than" sum. The measures of similarity are shown in Tables 2 through 4. Based on these measures, the small box was chosen as the best frequency mask.

Once the frequency mask had been chosen based on similarity in the frequency domain, the same comparisons were made in the image domain, to assure that the frequency mask was not similar to the contexts in this respect. The box scored best on these measures also.

In addition, the frequency spectrum of the pattern mask was compared to the contexts to assure that its spectrum was sufficiently different. As is shown in Tables 2, 3, and

Table 2
Similarity Values for Mask Candidates
and Test Contour 1

Mask	Similarity ^a			
	1	2	3 Less /Greater	
Box (Size 16)	4052.9	21.9	93.2	30.9
Box (Size 24)	2130.4	18.1	102.7	10.2
Rectangle (Size 8 x 16)	8524.8	29.5	77.5	67.3
Rectangle (Size 8 x 24)	6018.0	22.5	82.5	41.6
Square (Size 16)	24213.4	48.3	42.2	195.7
Circle (Size 8)	52773.9	52.7	29.7	318.4
2 Dots (Size 16)	4165.8	23.0	103.6	24.4
2 Dots (Size 2)	51950.1	94.5	46.3	319.2
Dot (Size 8)	9744.0	22.5	75.4	47.4
Dot (Size 12)	5476.9	18.7	91.1	18.8
Dot (Size 16)	3602.2	18.3	100.6	9.4
Circle (Size 16)	54548.5	45.6	35.0	298.6
4 Boxes (Size 8)	6447.2	21.8	85.6	40.9
Dot (Size 2)	75374.8	186.7	25.0	530.7
Dot (Size 4)	25219.0	52.5	45.5	175.8
Dot (Size 24)	1955.3	18.5	110.8	2.4
Dot (Size 32)	1350.3	19.2	115.4	1.1
Circle (Size 2)	107836.6	241.3	19.8	751.0
Square (Size 3)	135434.0	430.0	5.7	1004.6
Box (Size 2)	188285.8	902.7	5.5	1534.5
Pattern Mask	45017.7	30.1	42.0	215.7

^a Similarity measure 1 is the sum of the normalized ratio of the mask to the test contour. Measure 2 is the sum of the squared differences between the mask and the test contour. Measure 3 is separate sums for those cases where the mask is less than the test contour and those where it is greater than the test contour.

Table 3
Similarity Values for Mask Candidates
and Test Contour 2

Mask	Similarity			
	1	2	3 Less /Greater	
Box (Size 2)	2136.5	32.6	159.7	20.4
Box (Size 24)	1132.1	31.8	175.1	5.6
Rectangle (Size 8 x 16)	4678.7	37.8	139.7	52.6
Rectangle (Size 8 x 24)	3278.4	33.3	148.1	30.2
Square (Size 16)	13844.9	50.8	89.9	166.4
Circle (Size 8)	32415.6	48.3	58.1	270.0
2 Dots (Size 16)	2700.3	35.5	171.6	15.4
2 Dots (Size 2)	29111.1	89.7	85.0	281.1
Dot (Size 8)	5888.0	32.0	137.4	32.4
Dot (Size 12)	3280.3	31.3	159.8	10.5
Dot (size 16)	2080.9	32.6	172.8	4.6
Circle (Size 16)	33328.1	46.6	69.4	256.1
4 Boxes (Size 8)	2969.0	31.9	149.8	28.1
Dot (Size 2)	42904.0	170.9	50.2	479.0
Dot (Size 4)	15012.0	53.6	90.2	143.5
Dot (Size 24)	1081.9	34.0	186.2	0.7
Dot (Size 32)	789.6	35.2	191.5	0.2
Circle (Size 2)	65220.2	217.8	35.3	689.6
Square (Size 3)	77058.3	391.4	13.9	935.9
Box (Size 2)	118260.0	841.1	11.7	1463.7
Pattern Mask	27127.3	34.3	81.3	178.1

Table 4
Similarity Values for Mask Candidates
and Test Contour 3

Mask	Similarity			
	1	2	3	Less /Greater
Box (Size 16)	5434.7	16.9	66.2	34.6
Box (Size 24)	2904.8	13.2	74.3	12.5
Rectangle (Size 8 x 16)	12295.8	25.4	52.7	73.3
Rectangle (Size 8 x 24)	8676.1	19.2	57.7	47.5
Square (Size 16)	36637.5	47.8	23.0	207.3
Circle (Size 8)	83659.3	54.5	19.6	339.0
2 Dots (size 16)	6794.1	15.9	74.7	26.2
2 Dots (Size 2)	74144.9	96.3	32.3	335.9
Dot (Size 8)	14849.4	18.5	52.1	54.8
Dot (Size 12)	8049.6	13.8	64.2	22.6
Dot (Size 16)	5405.9	13.0	72.0	11.5
Circle (Size 16)	82205.1	45.7	22.3	316.6
4 Boxes (Size 8)	8889.2	17.2	59.9	45.9
Dot (Size 2)	109138.7	193.1	16.1	552.6
Dot (Size 4)	38332.7	52.6	30.2	191.3
Dot (Size 24)	2812.2	12.6	30.2	191.3
Dot (Size 32)	1994.0	12.9	84.4	0.9
Circle (Size 2)	163423.9	250.5	13.4	775.3
Square (Size 3)	203471.9	445.9	3.4	1033.1
Box (Size 2)	306047.2	928.4	3.1	1562.8
Pattern Mask	67370.4	28.5	27.5	232.0

4 the pattern mask scored moderate to low on these measures of similarity. The spectrum of the luminance mask was not compared to test its similarity. However, since it consisted of a large array of dots its spectrum should be a broadband low amplitude modulated Bessel function.

Method

Subjects. Four students acted as observers. They were tested for 20/20 visual acuity with a Snellen eye chart. For their participation they received a combination of course credit and \$3.50/hour.

Design. A 4 x 12 x 4 repeated measures design with replications was used with 4 masks (blank, luminance, pattern, and frequency), 12 inducing patterns (3 lengths x 3 spacings, broken lines, closed figure, and blank), and 4 ISI's (0, 35, 70, 105).

The response measure was a forced-choice discrimination of the position of the target. There were two positions, top and bottom. Each target position was matched with each mask and inducing pattern. The order of presentation was randomized. Each subject received the 288 treatment combinations 10 times for a total of 2880 responses per subject.

The blank field mask was run separately from the others since it consisted of only the context plus target preceded by a 4-second presentation of the fixation point. It was paired with each of the 12 contexts and 2 targets.

Each subject received 10 replications of these 24 treatment combinations, each randomized, for an additional 240 observations per subject.

Apparatus and Stimuli. All the stimuli were prepared as described for experiment 1 and presented using the PDP/8E.

Masks) The blank mask consisted of a 4-second presentation of the fixation point followed by the context plus target.

The luminance mask consisted of a $3^{\circ} \times 7^{\circ}$ patch of points. The spaces between points were clearly visible due to hardware limitations which prevent display of more than about 1000 points. The distribution of points was homogeneous. There was a fixation dot at the center of the field.

The pattern mask consisted of a $3^{\circ} \times 7^{\circ}$ random assortment of 24 line segments of random lengths at vertical, horizontal, and 45° orientations. It had a fixation dot at its center.

The frequency mask was a small $.48^{\circ} \times .56^{\circ}$ box at the center of the field.

Inducing Patterns) The inducing patterns consisted of two groups of line segments located above and below a central fixation dot. Each group contained two sets of four parallel line segments. The targets appeared in the space between sets of parallel lines. Each context contained one separation and one length of line. Three separations and lengths were used ($30'$, $50'$, $1^{\circ}10'$). Making all combina-

tions of these values yielded nine different inducing patterns (C1 through C9). These are shown in Figure 23.

Inducing pattern 10 through 12 (C10 through C12) were controls.

Inducing pattern 10 consisted of pattern C5 with the line segments made into dashed lanes.

Inducing pattern 11 consisted of pattern C5 with the line segments foreshortened and joined in pairs at their end points.

Inducing pattern 12 consisted of the target alone.

Targets) The targets consisted of three horizontal line segments 40' long and 40' apart. The targets appeared either above or below the fixation point in the space between the context inducing lines.

The masks and contexts were approximately equal in total energy, except for the frequency mask which had slightly less energy than the others. The target to mask energy ratio for the frequency mask was about 1:1.82. Individual points in the displays were illuminated at $-.75 \log \text{ ft. lam.}$ except for the frequency mask which was at $.1 \log \text{ ft. lam.}$ Eventhough the points composing the frequency mask were brighter, there were more points illuminated in the other masks. This resulted in lower total luminance for the frequency mask.

Procedure. The experimenter briefly explained the subjective contour phenomenon and the forced-choice task.

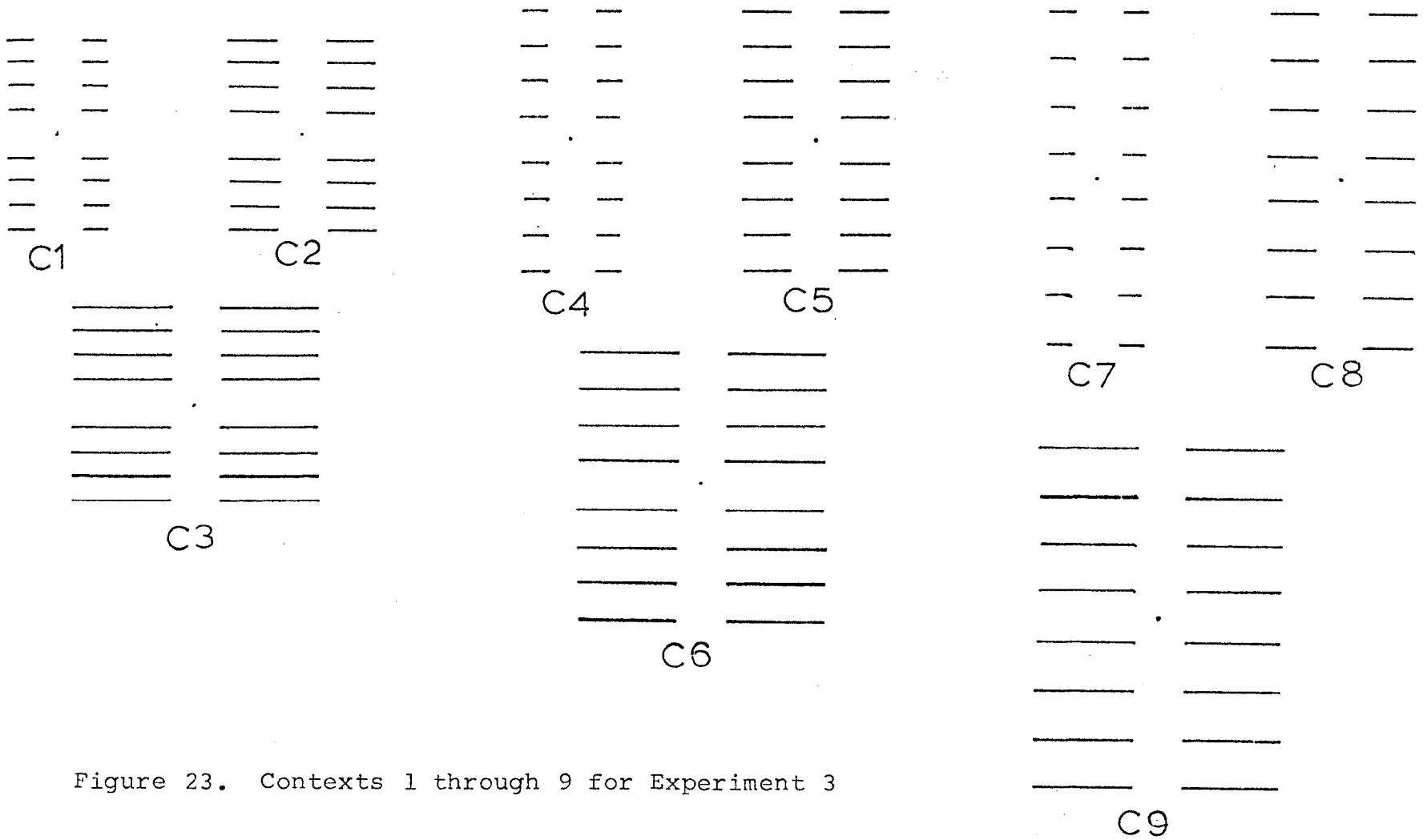


Figure 23. Contexts 1 through 9 for Experiment 3

The observer was told that his/her task was to indicate which target, top or bottom, was presented on a given trial. A practice trial was given for each of the treatment combinations. A trial consisted of 4 seconds adaptation to the masking pattern followed after the appropriate ISI by the context pattern plus target. The observers were instructed to fixate on the fixation point at the center of the field during the stimulus presentation. The duration of the inducing pattern plus target display was varied during the practice session to achieve approximately 75% correct. These durations varied between 26 and 40 msec. across subjects.

Results

An analysis of variance and other statistical tests were performed on the raw data and on transformed data [arcsin transformation, Kirk, 1963]. The transformation was performed to correct for non-normality in the percent correct distribution and thus meet a required assumption of the analysis of variance. Significant effects were the same for both tests. The results reported here use the results of the tests on the raw data so that they can be interpreted in units of percent correct rather than transformed units. Overall, the manipulations resulted in lowered accuracy for detection of the target. These results can be grouped into effects due to the masks and effects due to the contexts. First, the results due to the masks are presented, then those due to the contexts.

Mask Data. Figure 24 shows the mean percent correct on the vertical axis for each of the four masks. Each point, except the blank mask data point, is a summation across all 4 subjects, 4 ISI's, 12 contexts, 2 targets, and 10 replications giving a total of 3840 observations per data point. The blank mask condition did not have different ISI's so that it is based on 960 observations. The error bars indicate the 95% confidence interval for each data point. The graph suggests that detection of the target was easiest following the blank mask, about equal for the luminance mask and frequency mask, and most difficult for the pattern mask. A one-way analysis of variance, using all four masks, showed a significant difference among masks, $F(3, 1224) = 6.608$, $p < .0002$. Duncan's Range tests among the mask means indicate that the blank mask is significantly higher than the other masks, the frequency mask is not significantly different from the luminance mask, and the pattern mask is significantly lower than the others at $p < .05$.

The mask effects were accompanied by a significant main effect for ISI, $F(3, 6) = 6.1854$, $p < .02$. Figure 25 shows the mean percent correct for each of the four ISI's (0, 35, 70, 105). Percent correct is plotted on the vertical axis and ISI is plotted on the horizontal axis. Each data point is based on 2880 observations. The graph indicates that accuracy improved as ISI increased. However, comparisons among the means indicate that ISI 35, 70, and

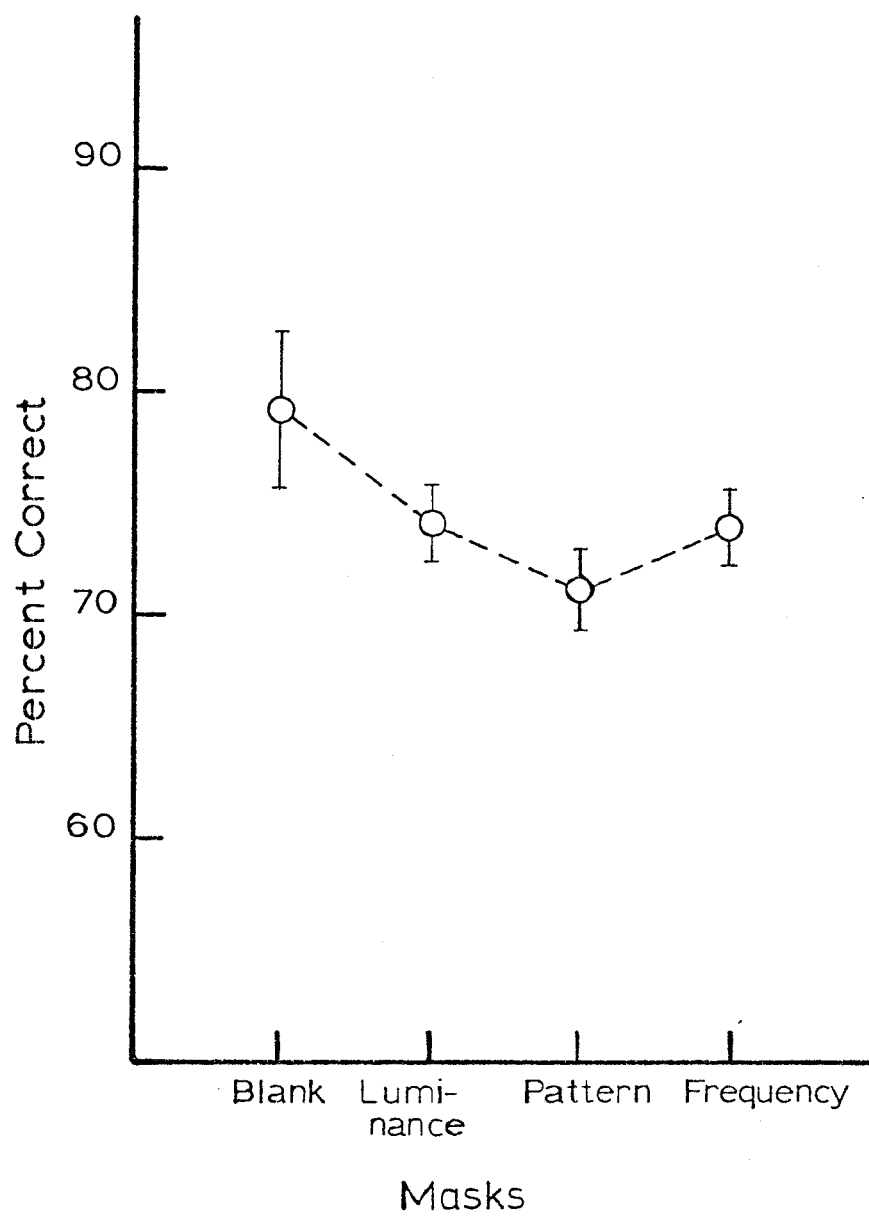


Figure 24. Mean Percent Correct for Each Mask.

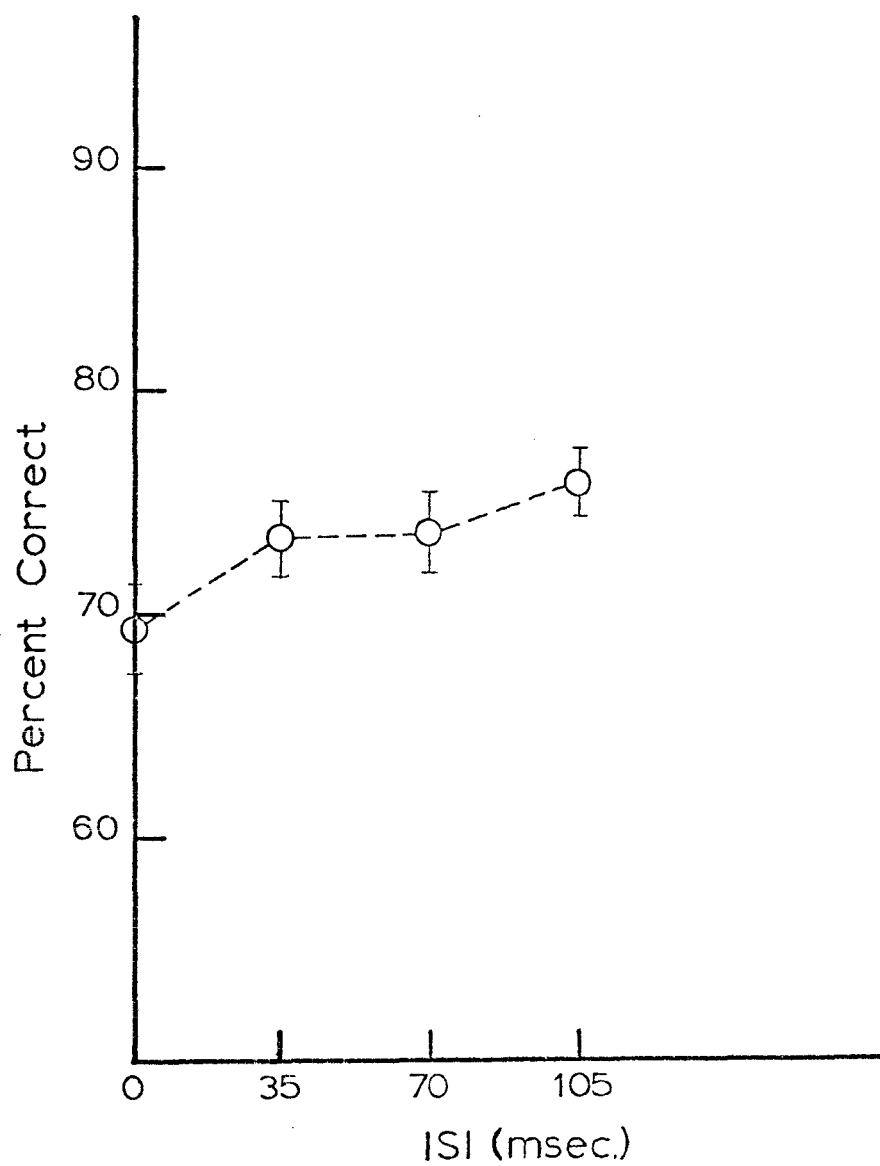


Figure 25. Mean Percent for Each ISI.

105 were not significantly different at $p < .05$.

While the mask x ISI interaction was not significant, a plot of the ISI function for each mask, shown in Figure 26, reveals a very clear pattern. Each mask is plotted separately. Each data point is based on 960 observations. The functions for the luminance mask and the frequency mask were nearly superimposed and also showed a dip at 70 msec. The ISI function for the pattern mask, on the other hand, was monotonic increasing.

The masking results above were based on analyses which included all the subjects. Analysis of individual subjects revealed that three of the four subjects showed significant masking effects while one did not.

Context Data. The second main influence on the accuracy of subjects' performance was due to the contexts adjacent to the targets. Figure 27 shows the mean percent correct for each of the 12 contexts. Each data point is based on 960 observations. The error bars indicate the 95% confidence intervals for each point. The graph shows that percent correct varied widely as a function of context and the analysis of variance confirms the significance of this effect, $F(11, 22) = 7.7702$, $p < .00003$.

Contexts C1 through C9 represent all combinations of three separations and three lengths of inducing lines. The combinations are shown in Table 5.

Figure 27 shows that for each separation, as the

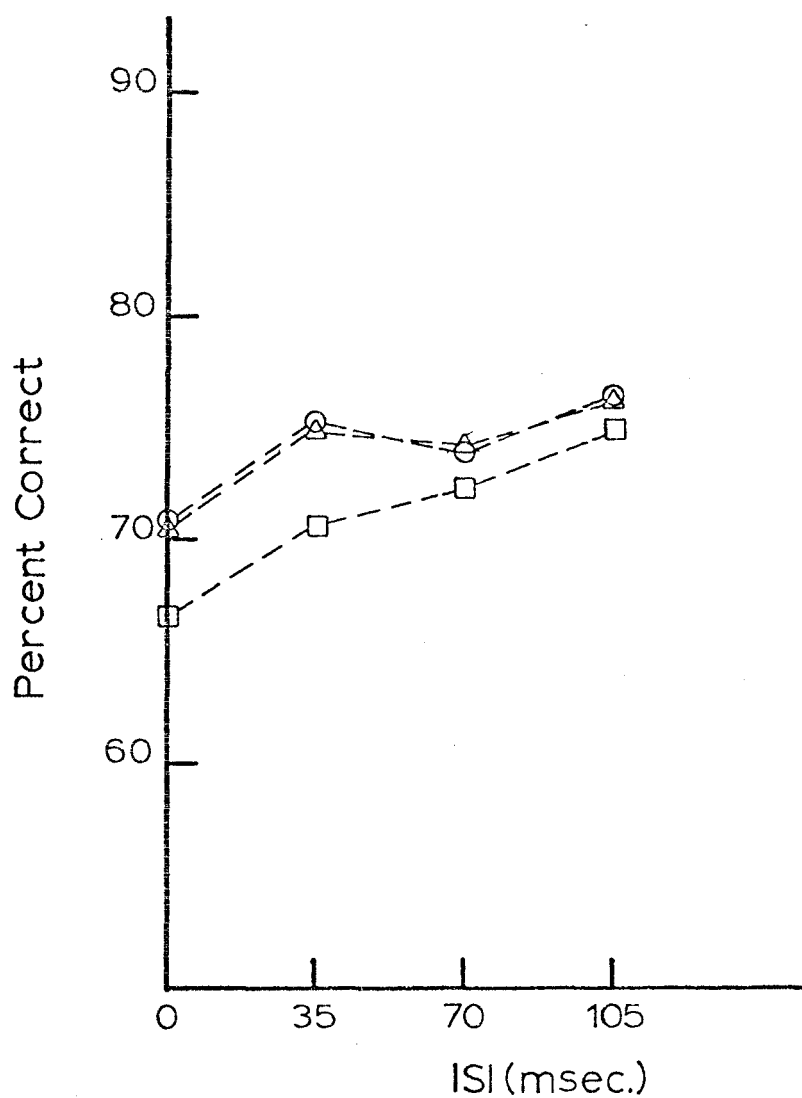


Figure 26. Mean Percent Correct for Each Mask Plotted Separately as a Function of ISI. \circ -- \circ Luminance Mask; \square -- \square Pattern Mask; \triangle -- \triangle Frequency Mask.

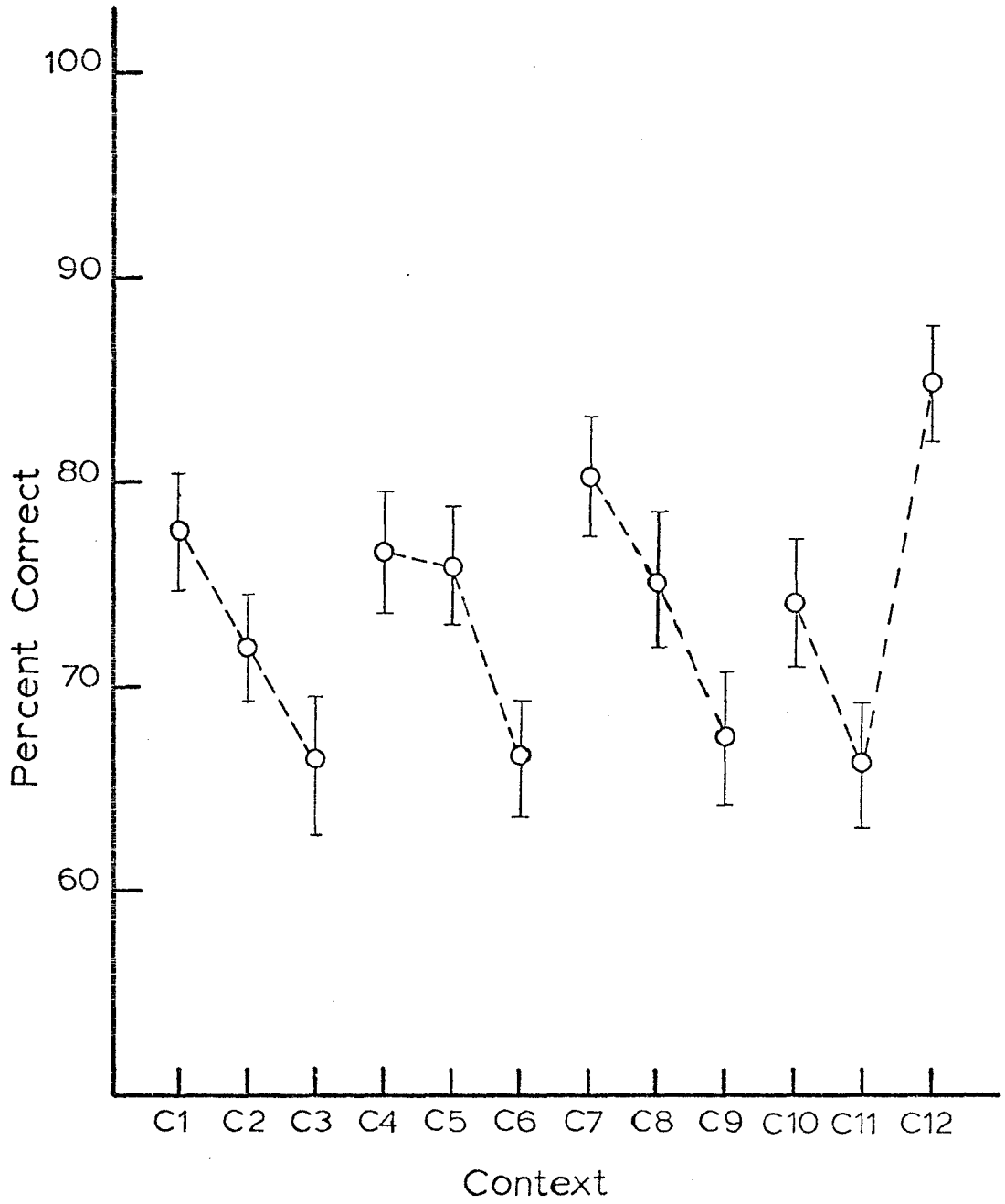


Figure 27. Mean Percent Correct for Each Context.

Table 5
 Length and Separation of Lines
 for Contexts 1 through 9

Separation	Length	Context
30'	30'	C1
	50'	C2
	1°10'	C3
50'	30'	C4
	50'	C5
	1°10'	C6
1°10'	30'	C7
	50'	C8
	1°10'	C9

length of the inducing lines increases accuracy decreases. For example, for separation 1, i.e. C1 through C3, C1 produces greater accuracy than C2, and C2 produces greater accuracy than C3. Comparisons among means indicate that except for C4 and C5 all contexts within each separation differ significantly at the $p < .05$ level. Thus, with the exception of C4 and C5, for all separations increasing the length of the inducing lines decreased accuracy.

Further comparisons showed that for no length of inducing line did changing the separation influence accuracy. For example, differences among C1, C4, and C7 were not significant at $p < .05$. This was true for all lengths. Thus, changes in separation of inducing lines, for a given length, had no effect on accuracy.

Contexts C10, C11, and C12 were controls. C10 was not significantly different from the length 2 contexts (C2, C5, C8) or from C1 and C4. Performance for C10 was significantly better than performance on all length 3 contexts (C3, C6, C9) at $p < .05$.

C11 produced the worst accuracy, but this was not statistically worse than any length 3 context at $p < .05$. It was less than all length 2 and length 1 contexts, however.

C12 was the target alone. This condition produced the best performance. It was greater than any context at $p < .05$.

Discussion of Experiment 3

Several significant effects have been demonstrated, some due to effects of the masks, some due to the effects of the contexts. First, the effects of the masks will be considered, than the effects due to the contexts to determine what conclusions can be drawn about subjective contours.

Mask Effects. Before concluding that the masking effects were due to particular characteristics of the various masks we should consider the alternative hypotheses that the masking effects may have been due to luminance masking, spatial inhibition, or response bias.

The masks differed in total luminance. These differences were quantified in the following way. The luminance of a patch of non-overlapping points was measured on the CRT at the intensity used in the experiment. This measurement was taken as a measure of the luminance of an individual point, and was multiplied by the number of points displayed in each mask to obtain a total luminance for each display. Since the intensity of a point varies inversely with the number of points displayed simultaneously, a number of luminance patches were used. The total luminance for each mask computed in this way is shown in Table 6. The masks are listed in the table in descending order of luminance. If the masking effects were due to luminance we should expect percent correct to be in increasing order. However, the frequency mask produced about as much masking as the lumi-

Table 6
Luminance and Mean Percent Correct
for Each Mask in Experiment 3

Mask	Energy ^a	Points	Mean Percent Correct
Luminance	97.70	977	74.219
Pattern	96.92	800	71.198 ^b
Frequency	53.22	150	74.063
Blank	0.00	0	79.375 ^b

^a Energy = luminance of individual point x number of points.

^b Significantly different at $p < .05$.

nance mask, but had only about half the total luminance. The pattern mask, which had about the same luminance as the luminance mask produced significantly more masking. Therefore, these data do not support luminance as an explanation of the mask effects.

A number of factors combine to suggest that the masking effects are not due to simple center-surround interaction like that described by Barlow (1953) or Westheimer (1965). Both the luminance mask and the pattern mask have about the same total energy and this energy is about equally distributed across the target area and the area adjacent to the target. Yet, these masks produce different amounts of masking. The frequency mask has all its energy concentrated at about 0.8° from the nearest edge of the target and about 1.93° from the farthest edge. Simple center-surround interactions generally involve a center excitatory area of about $10'$ surrounded by a $20' - 40'$ inhibitory area (Teller, Matter, & Phillips, 1970). Thus, the frequency mask was outside the area of inhibition, especially if we consider the entire spatial extent of the target. Finally, Barlow, Fitzhugh, & Kuffler (1957) indicate that at low luminances, surrounds of receptive fields of retinal ganglion cells disappear and, consequently, lateral inhibitory interactions. The low mean spatial luminance of these displays suggest that these interactions were minimal. Spatial inhibition, then, cannot account for the masking results.

Table 7 shows the response totals for each subject and Table 8 shows the totals for each mask. There was no apparent bias for any subject or for any mask. No subject showed a tendency to choose one alternative, top or bottom, more consistently. Similarly, there was no bias of this kind for any of the masks. The results cannot be attributed to different response strategies for the different masks.

If we look at Figure 25 we see that the pattern mask produced monotonic, almost linear masking as a function of ISI, while the frequency mask and the luminance mask showed first a decrease in masking from 0 to 35 msec., then a slight increase in masking at 70 msec. The functions for the luminance mask and the pattern mask can at best be interpreted as trends since the dip at 70 msec. was not great enough to reach significance. This lack of significance may be due in part to the narrow dynamic range of the masking effect overall which was about 8.2% for no mask to pattern mask, 10% for the pattern mask at 0 ISI to luminance mask at 105 msec. ISI, and 12.7% for the pattern mask at 0 ISI to no mask. This along with the fact that the no mask performance was around 80% correct suggests that the task was difficult with or without the masks. Perhaps, the dynamic range could be increased by (a) decreasing target to mask energy ratios, (b) changing the target to make it more detectable, i.e. making lines thicker or brighter, (c) finding more effective masks. An increased dynamic range might more

Table 7
Response Contingency Tables for Subjects

Subject Presentation	Response		Total
	Top	Bottom	
#1			
Top	988	452	1440
Bottom	511	929	1440
Total	1499	1381	2880
#2			
Top	978	462	1440
Bottom	452	988	1440
Total	1430	1450	2880
#3			
Top	1258	182	1440
Bottom	393	1047	1440
Total	1651	1229	2880
#4			
Top	1164	276	1440
Bottom	364	1076	1440
Total	1528	1352	2880

Table 8
Response Contingency Tables for Masks

Mask	Presentation	Response		Total
		Top	Bottom	
Blank				
	Top	395	85	480
	Bottom	113	367	480
	Total	518	452	960
Luminance				
	Top	1477	443	1920
	Bottom	547	1373	1920
	Total	2024	1816	3840
Pattern				
	Top	1396	524	1920
	Bottom	582	1338	1920
	Total	1978	1862	3840
Frequency				
	Top	1515	405	1920
	Bottom	591	1329	1920
	Total	2106	1734	3840

effectively delineate the details of the masking functions.

The failure to obtain detailed masking functions does not prevent us from drawing the following two conclusions about the main masking effects. First, the pattern mask produced the greatest masking overall. Secondly, all three masks produced some masking when compared to the no mask condition. This latter fact suggests that more than one type of masking was taking place. In particular, the effects of the frequency mask were about equal to the luminance mask and this masking was due to two different mechanisms.

Context Effects. A second major, but not necessarily independent (see below), influence on the targets detectability was due to the surrounding context, i.e. the inducing lines which formed the subjective contour. As with the masks, luminance and spatial inhibition could provide alternative explanations for the results.

Table 9 shows the contexts ordered by their luminance. Each lighted point in the contexts had the same intensity so that their total luminance can be compared by comparing the number of lighted points. This is shown in column two of the table. If luminance were the prime factor in the context effects we would expect percent correct to decrease as luminance increased. However, percent correct for C11 was lower than C3, C6, and C9 with only about half the luminance. C11 differed greatly from C2, C5, and C8 even though it had about equal luminance. Similarly, the comparison be-

Table 9
Mean Percent Correct and Number of
Illuminated Points for Each Context

Context	Points	Mean Percent Correct
C12	0	85.00 ^a
C1, C4, C7	176	78.24 ^b
C11	288	66.15 ^a
C2, C5, C8	304	74.42 ^b
C10	416	74.13 ^a
C3, C6, C9	560	66.79 ^b

^a Based on 1040 observations

^b Based on 3120 observations

tween C10 and C2, C5, and C8 does not support a luminance hypothesis, especially considering the fact that the added luminance in C10 was near the target and presumably more effective. Luminance alone does not account for the differences among the contexts.

The contexts used here to produce the subjective contours can be considered as masks presented at 0 msec. SOA in a metacontrast paradigm. Since no other SOA's were investigated the context effects can not be compared to temporal metacontrast functions. The spatial extent of the contexts can be compared to spatial effects in metacontrast, however. In this regard there are a number of distinctions to be made between these stimuli and regular metacontrast displays. The apparent brightness reduction in metacontrast masking is largely dependent on edge interactions (Growney, 1976). Growney has shown that one obtains negligible amounts of metacontrast masking without sharp edges and that the specific type of edge in both the target and mask can change the amount of masking obtained. Sturr & Frumkes (1965) also present data supporting a border inhibition model of metacontrast spatial interactions. The stimuli used here, however, do not have real borders or edges so that these interactions should be minimal. In addition, as the spatial extent of the mask is increased, in metacontrast paradigms, beyond about 1.5° the masking effect diminishes (Sturr & Frumkes, 1965). So the reduction in accuracy here, which

increased as the length of the inducing lines was increased through about 4° , suggests mechanisms other than metacontrast are involved. Also, metacontrast effects are not usually obtained with forced-choice detection criteria (Breitmeyer & Ganz, 1975; Schiller & Smith, 1966).

The reduction in accuracy could also be attributed to center-surround interaction between the context and the target. As the inducing lines are extended they stimulate larger portions of the inhibitory surround thus raising the target threshold. Westheimer (1965) and Teller, Matter, & Phillips (1970) have shown that stimulation beyond about $45'$ causes a decrease in threshold (sensitization). For the displays here we would have expected a reduction in threshold if peripheral center-surround interactions were involved. This reduction was not found.

These experiments suggest that the context masking was due to a combination of subjective effects which produced measurable changes in the detectability of the target. The area between the sets of inducing lines, where the target was located, appears subjectively darker than the surrounding background. These data have shown that a target which appears in this subjective area is also affected. Moreover, by varying the strength of the subjective contour, it has been shown that as the contour becomes more salient the target becomes less detectable. This effect does not appear to be a function of the separation between the in-

ducing lines, but rather a function of their length. Experiment 1 showed that the salience of the subjective contours increased with increased size, but length and separation of the inducing lines were not varied independently. Experiment 3 has suggested that the size effect may have been due to lengthening of the inducing lines rather than increased separation between them.

Context Specific Mask Effects. The effect of the subjective contours, then, was to reduce the detectability of the target by creating a subjectively darker area which lowered the apparent brightness of the target as well. Interestingly, the ability of the inducing lines to reduce target detectability was not equal for all the masks. If we plot the context effects for each mask we see that the range of the context effect was lower for the frequency mask than for any other (see Figure 28a through 28d). The plots show that the range of the effect for C1 vs. C3, C4 vs. C6, and C7 vs. C9 was about the same for the luminance mask and the pattern mask, but least for the frequency mask. Table 10 shows the range of the effect computed as the difference between C12, the no context condition, and the strongest contour conditions. The table shows the smallest range of masking for the frequency mask. Similarly, the difference between the strong contour and the weak contour conditions for each separation of inducing lines shows that the frequency mask had an effect on context masking. Table 11 shows these

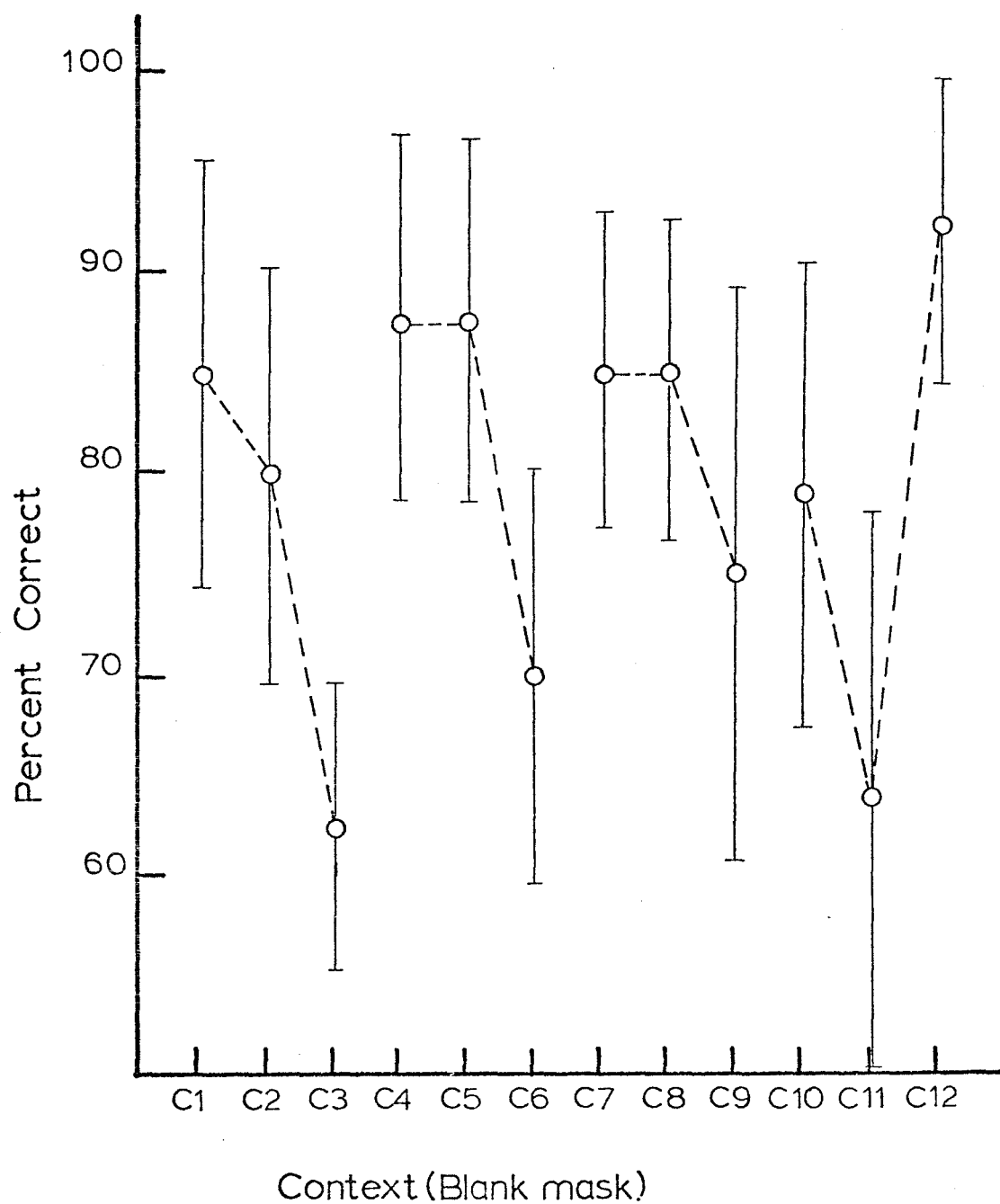


Figure 28a. Mean Percent Correct for Each Context for the Blank Mask.

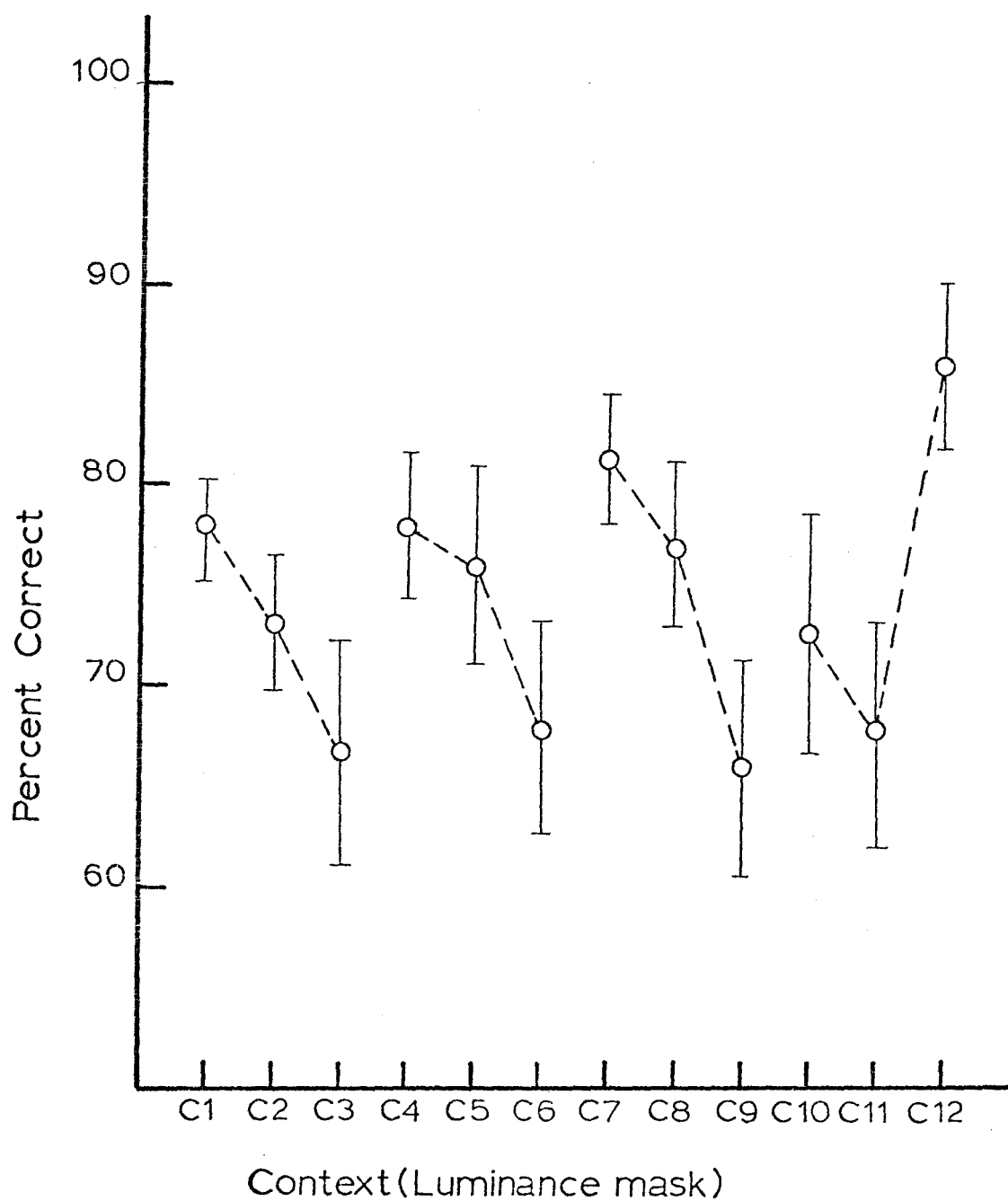


Figure 28b. Mean Percent Correct for Each Context for the Luminance Mask.

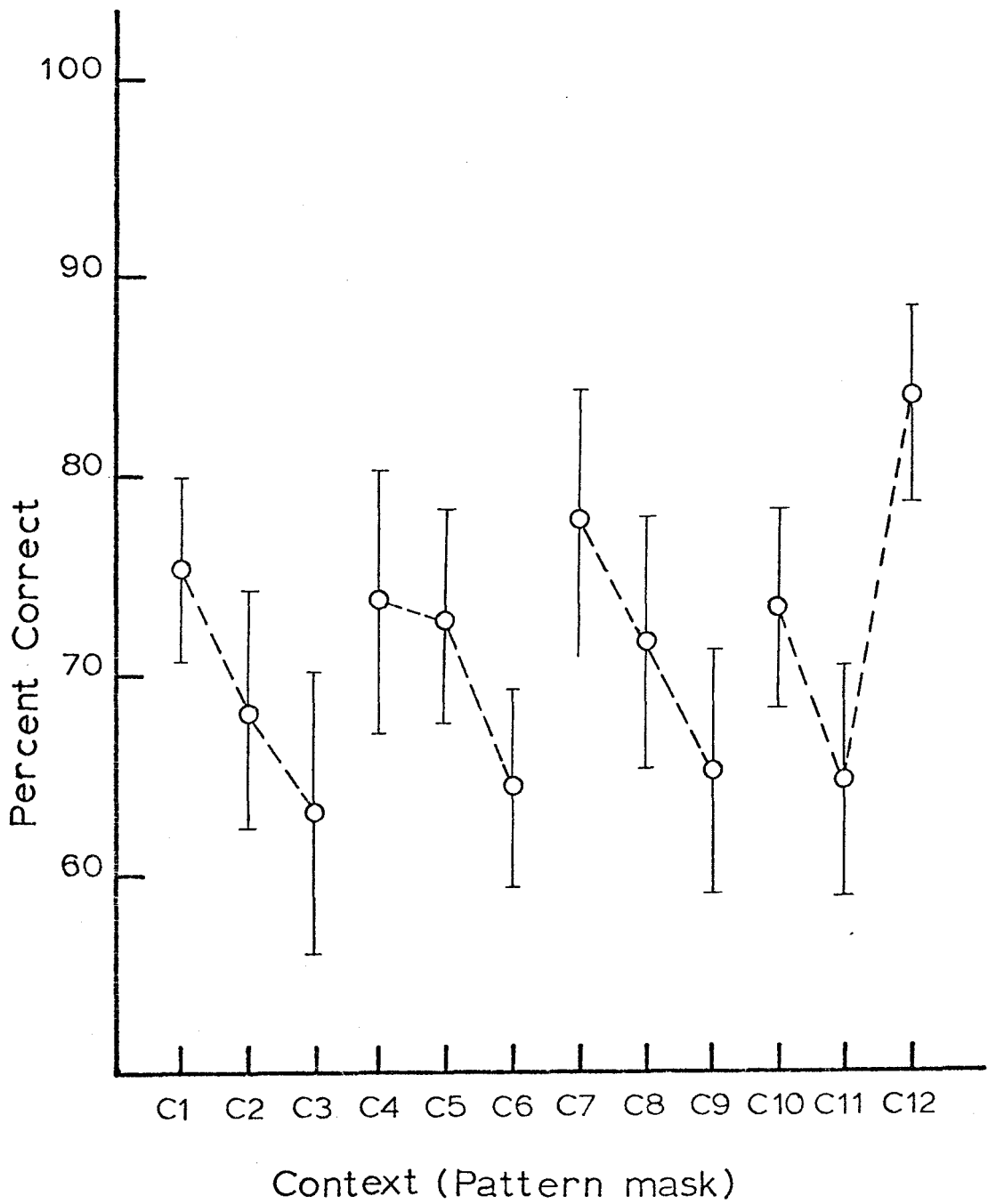


Figure 28c. Mean Percent Correct for Each Context for the Pattern Mask.

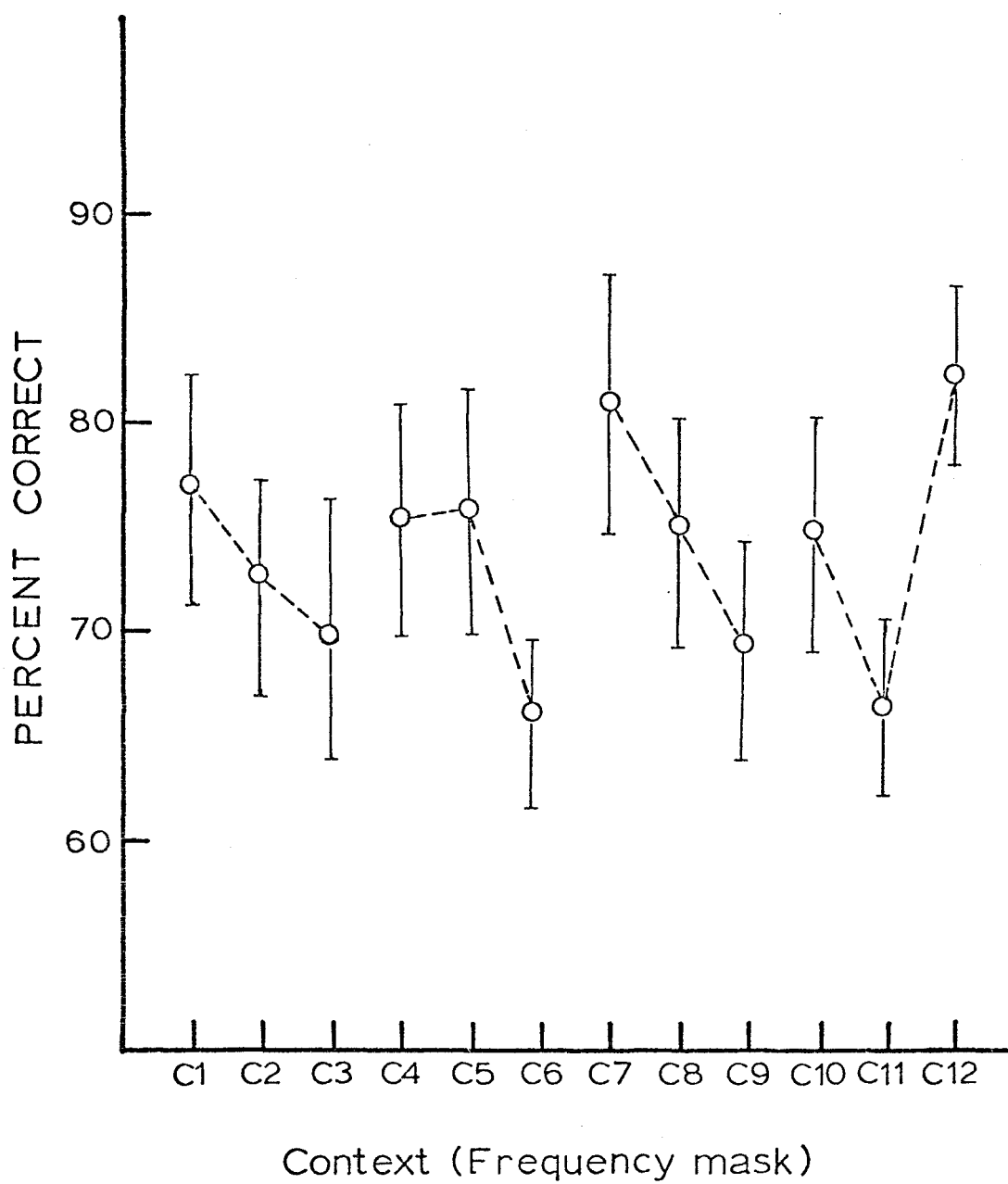


Figure 28d. Mean Percent Correct for Each Context for the Frequency Mask.

Table 10
Differences in Dynamic Range Among Contexts

Mask ^a	C12 (max)	C9 (min)	Range
Blank	92.50 ^b	62.50	30.00
Luminance	86.25	65.93	20.32
Pattern	84.06	63.12	20.94
Frequency	82.81	66 56	16.25

^a Percent correct for the blank mask based on 80 observations; for other masks 320 observations per context.

^b Percent Correct.

Table 11
Differences in Mean Percent Correct
Between Strong and Weak Contours

Mask ^a	Contexts			Mean Difference
	C3-C1	C6-C4	C9-C7	
Blank	22.50	17.50	10.00	16.66
Luminance	11.56	10.00	15.31	12.29
Pattern	12.50	9.37	12.50	11.45
Frequency	7.18	9.06	11.56	9.26

^a Percent correct for blank mask based on 80 observations for each context; for other masks 320 observations per context.

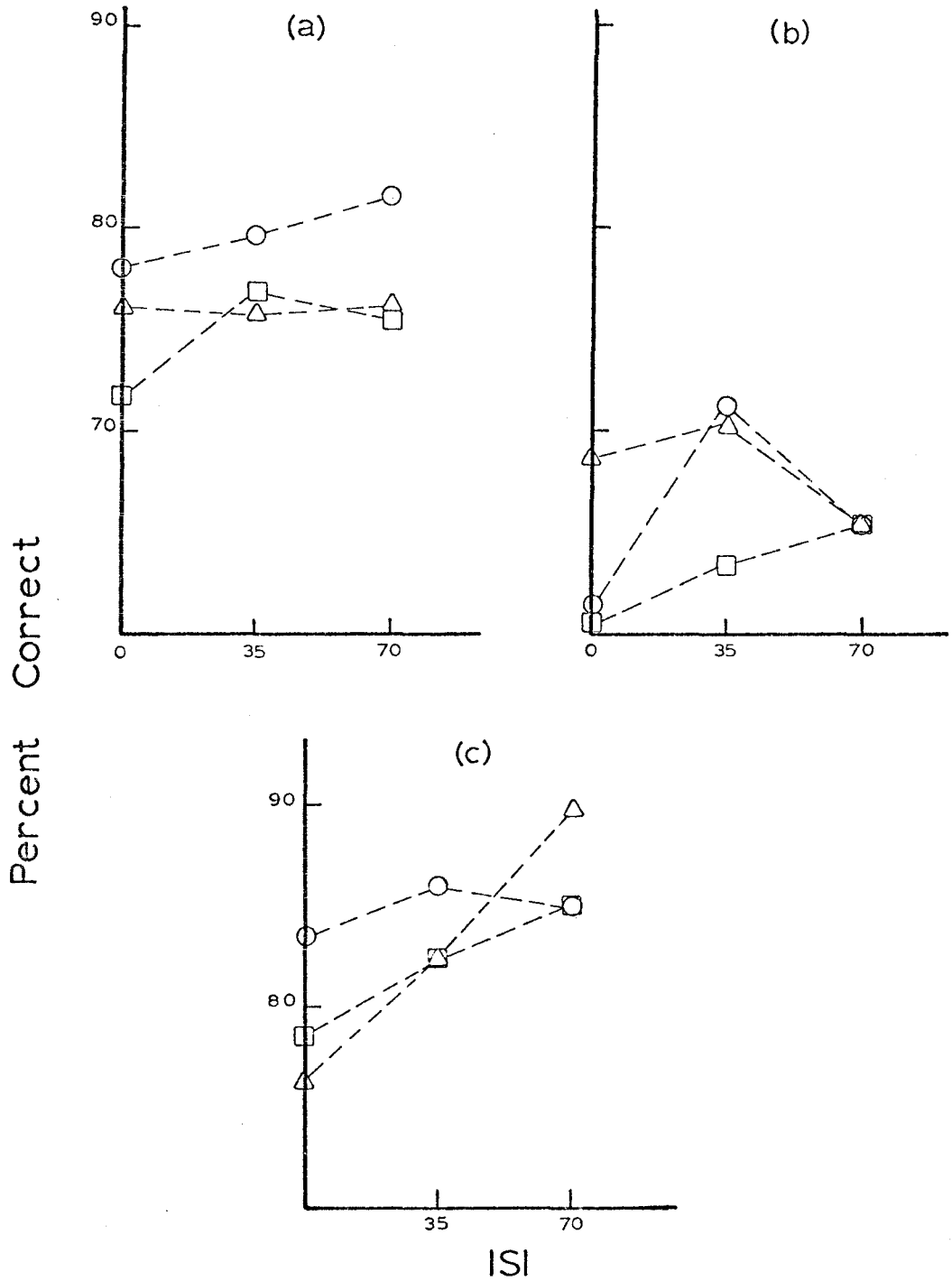


Figure 29. Mean Percent Correct for Each Mask as a Function of ISI for (a) Weak (b) Strong, and (c) No Context Conditions. ○—○ Luminance Mask; □—□ Pattern Mask; △—△ Frequency Mask.

differences. Figure 29 shows plots of percent correct for each mask as a function of ISI. Each data point is based on 960 observations. Figure 29a shows the average of the weak contour conditions for each mask. While there is some variation it does not appear to be mask specific. Figure 29b shows the strong contour conditions. The frequency mask shows much less context effect at 0 msec. ISI, the point of maximum masking, than the luminance or pattern mask. Figure 29c shows the mean percent correct for the no context condition (C12) and does not show the interaction between mask and target. This interaction seems to depend on the presence of a context. Thus, the frequency mask, while not producing the greatest masking, reduced the range of the context effect and had a larger effect on the strong contour conditions. This is especially interesting since the frequency mask contained about half the total luminance of the other masks. It suggests that frequency analyzers may be involved in the subjective contour forming process, at least for displays of this type.

Ginsberg (1975) has argued that subjective contours are not subjective at all, but that the spectrum of a contour producing display contains a substantial portion of the frequencies that would be present if a real contour were there. Tyler (1975) points to serious flaws in his methodology, however. These data support the hypothesis that frequency analyzers may be involved in subjective contour

formation. Further experiments using bandlimited masks and a broader array of contours could answer some interesting questions about the involvement of spatial frequency analyzers in this phenomenon. This could help illuminate how individual features and components of patterns are organized to produce holistic perceptions.

General Summary

A number of interesting facts have emerged concerning subjective contours. It has been shown that the salience of the contours varies with the retinal size of the image and also with its intensity. The ratings follow a monotonic increasing function of the log of the luminance and size of the display. In addition, the salience of the contours is orientation sensitive, being greatest for oblique orientations. The orientation effects suggested that the phenomenon is not peripheral in origin since peripheral receptive fields are generally circular. The size effects also implicate non-peripheral processing, perhaps at the level of the striate cortex where size tuned fields have been found in the monkey and cat. These contours had real effects, as measured in a forced-choice detection task, in which targets became more difficult to detect as the contours became stronger. Finally, spatial frequency analyzers may be involved in their formation since adaptation to a broadband mask reduced their masking effect.

References

- Barlow, H. A. Summation and inhibition in the frog's retina. Journal of Physiology, 1953, 119, 69-88.
- Barlow, H. B., Fitzhugh, R., & Kuffler, S. W. Change of organization in the receptive fields of the cat's retina during dark adaptation. Journal of Physiology, 1969, 203, 237-260.
- Bishop, P. O. Binocular interaction fields of single units in the cat striate cortex. Journal of Physiology, 1971, 216, 39-68.
- Blakemore, C. & Campbell, F. W. On the existence of neurons in the human visual system selectively sensitive to the orientation and size of retinal images. Journal of Physiology, 1969, 203, 237-260.
- Blakemore, C. & Nachmias, J. The orientation specificity of two visual aftereffects. Journal of Physiology, 1971, 213, 157-174.
- Bradley, D. R. & Dumais, S. T. Ambiguous cognitive contours. Nature, October 16, 1975, 257, 582-584.
- Brigner, W. L. & Gallagher, M.B. Subjective contour: Apparent depth of simultaneous brightness contrast? Perceptual and Motor Skills, 1974, 38, 1047-1053.
- Campbell, F. W. & Kulikowski, J. J. Orientational selectivity of the human visual system. Journal of Physiology

- logy, 1966, 187, 437-445.
- Cooley, J. W. & Tukey, J. W. An algorithm for the machine calculation of complex Fourier series. Mathematics of Computations, 1965, Vol. 19, 297-301.
- Coren, S. Subjective contours and apparent depth. Psychological Review, 1972, 79, 359-367.
- Coren, S. & Theodor, L. H. Subjective contour: The inadequacy of brightness as an explanation. Bulletin of the Psychonomic Society, 1975, 6(1), 87-89.
- Coren, S. & Theodor, L. H. Neural interactions and subjective contours. Perception, 1977, 6, 441-447.
- Dumais, S. T. & Bradley, D. R. The effects of illumination level and retinal size on the apparent strength of subjective contours. Perception and Psychophysics, 1976, 19(4), 338-345.
- Frisby, J. P. & Clatworthy, J. L. Illusory contours: Curious cases of simultaneous brightness contrast? Perception, 1975, 4(3), 349-358.
- Ginsberg, A. P. Is the illusory triangle physical or imaginary? Nature, Sept. 8, 1975, 257, 219-220.
- Glezer, V. D., Ivanoff, V. A. & Tscherbach, T. A. Investigation of complex and hypercomplex receptive fields of the visual cortex of the cat as spatial frequency filters. Vision Research, 1973, 13, 1875-1904.
- Gonzalez, R. C. & Wintz, P. Digital Image Processing.

Addison-Wesley, 1977.

Goodman, J. W. Introduction to Fourier Optics. McGraw-Hill, 1968.

Gregory, R. L. Cognitive contours. Nature, July 7, 1972, 238, 51-52.

Gregory, R. L. & Harris, J. P. Illusory contours and stereo depth. Perception and Psychophysics, 1974, 15(4), 411-416.

Growney, R. The function of contour in metacontrast. Vision Research, 1976, 16, 253-261.

Harris, J. P. & Gregory, R. L. Fusion and rivalry of illusory contours. Perception, 1973, 2, 235-247.

Hochberg, J. & Brooks, V. The psychophysics of form: Reversible perspective drawings of spatial objects. American Journal of Psychology, 1960, 73, 337-354.

IBM SSP/PLI manual

Kahneman, D. Method, findings and theory in studies of visual masking. Psychological Bulletin, 1968, 70, 404-425.

Kanizsa, G. Marzini quasi-perretivi in campi con stimolazione omogenea. Revista di Psicologia, 1955, 49, 7-30.

Kanizsa, G. Contours without gradients or cognitive contours? Italian Journal of Psychology, 1974, 1, 93-113.

- Kinsbourne, M. & Warrington, E. K. Further studies on the masking of brief visual stimuli by a random pattern. Quarterly Journal of Experimental Psychology, 1962, 14. 235-294.
- Kirk, R. E. Experimental Design: Procedures for the Behavioral Sciences. Brooks-Cole, 1968.
- Kitterle, F. L. The possible locus of lightness contrast. Perception and Psychophysics, 1973, 14, 585-589.
- Lathi, B. P. Signals, Systems, and Communication, John Wiley & Sons, 1965.
- Marr, D. Early processing of visual information. Philosophical Transactions of the Royal Society of London, Oct. 19, 1976, 275(942), 483-524.
- McFadden, D. Three computational versions of proportion correct for use in forced-choice experiments. Perception and Psychophysics, 1971, 9, 275-278.
- Nakayama, K. & Roberts, D. J. Line length detectors in the human visual system: evidence from selective adaptation. Vision Research, 1972, 12, 1709-1713.
- Pantle, A. & Sekuler, R. W. Size-detecting mechanisms in human vision. Science, 1968, 162, 1146-1148.
- Pantle, A. & Sekuler, R. W. Contrast response of human visual mechanisms sensitive to orientation and direction of motion. Vision Research, 1968, 9, 397-406.
- Rodieck R. W. & Stone, J. Analysis of receptive fields of cat retinal ganglion cells. Journal of Neurophysi-

- ology, 1965, 28, 833-849.
- Schiller, O. & Smith, M. C. Detection in metacontrast. Journal of Experimental Psychology, 1966, 71, 32-39.
- Schumann, F. Einige beobachtungen uber die zusammenfassung von gesichtseidrucken zu einheiten. Psychological Studies, 1904, 1, 1-32.
- Smith, A. T. & Over, R. Orientation masking and the tilt illusion with subjective contours. Perception, 1977, 441-447.
- Spinelli, D. N. & Pribram, K. H. Changes in visual recovery functions and unit activity produced by frontal and temporal cortex stimulation. Electroencephalography and Clinical Neurophysiology, 1967, 22, 143-149.
- Sturr, J. F. & Frumkes, T. E. Spatial factors in masking with black or white targets. Perception and Psychophysics, 1968, 4(5), 282-284.
- Teller, D. Y., Matter, C. F., & Phillips, W. D. Sensitization by annular surrounds: Spatial summation properties. Vision Research, 1970, 10, 549-561.
- Turvey, M. T. On peripheral and central processes in vision: Inferences from an information-processing analysis of masking with patterned stimuli. Psychological Review, 1973, 80, 1-52.
- Tyler, C. W. Is the illusory triangle physical or imaginary? Perception, 1977.
- Ware, C. & Kennedy, J. M. Illusory line linking solid rods.

Perception, 1977, 6, 601-602.

Weisstein, N. W-shaped and U-shaped functions obtained for monoptic and dichoptic disc-disc masking. Perception and Psychophysics, 1971, 9, 275-278.

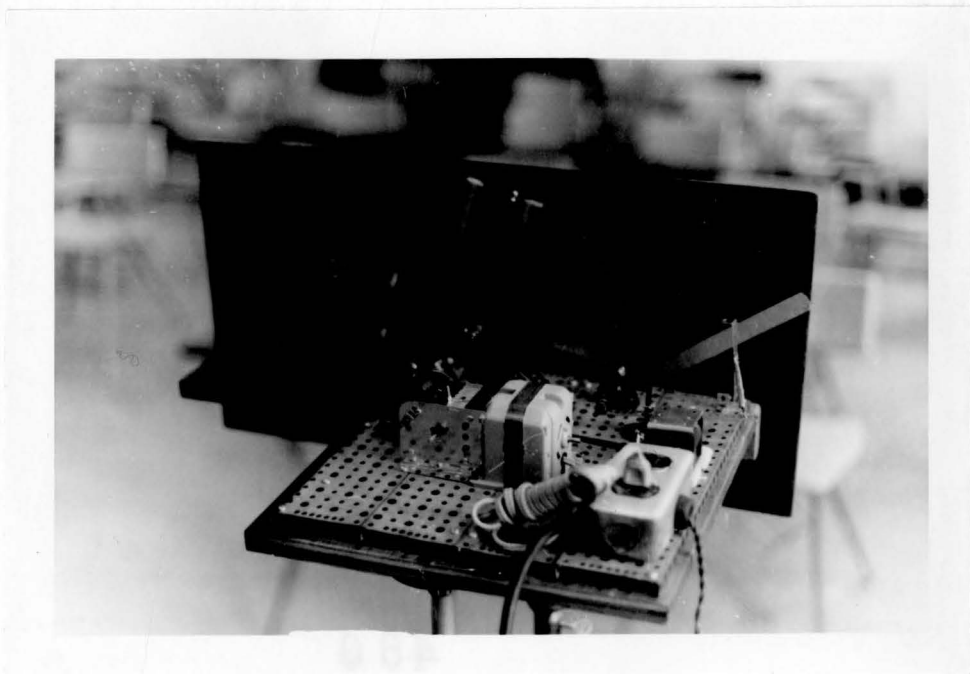
Weisstein, N & Bisaha, J. Gratings mask bars and bars mask gratings: Visual frequency response to aperiodic stimuli. Science, 1972, 176, 1047-1049.

Weisstein, N., Maguire, W., & Berbaum, K. A phantom-motion aftereffect. Science, Dec. 7, 1977, 955-958.

Weisstein, N., Ozog, G., & Szoc, R. A comparison and elaboration of two models of metacontrast. Psychological Review, 1975, 82(5), 325-343.

Westheimer, G. Spatial interaction in the human retina during scotopic vision. Journal of Physiology, 1965, 181, 881-894.

Appendix A



Filter Changer



Filter Changer

Appendix B

SOURCE LISTING

STMT LEV NT

```

1      0  FFT: PROC OPTIONS(MAIN) REORDER;
/******
/*  ARGUMENTS FOR FFTM
/*      Y(*) = ARRAY OF POINTS TO BE TRANSFORMED
/*      M(*) = ARRAY SPECIFYING THE NUMBER OF LEVELS FOR EACH
/*      NDIM = NUMBER OF DIMENSIONS OF DATA
/*      OPT = '0' DO FORWARD TRANSFORM
/*            '1' DO BACK TRANSFORM
/*      ERRUM = ERROR CODE DUMMY LEFT FROM FFT
/*  ARGUMENTS FOR PLTHID
/*      A(*,*,*) = ARRAY WHICH HOLDS THE POINTS TO BE PLOTTED
/*      XBOUND = SIZE OF THE X DIMENSION OF ARRAY A(POWER OF 2)
/*      YBOUND = SIZE OF THE Y DIMENSION OF ARRAY A(POWER OF 2)
/*      XLNTH = LENGTH IN INCHES OF THE X AXIS OF THE PLOT
/*      YLNTH = LENGTH IN INCHES OF THE Y AXIS OF THE PLOT
/*      XMIN = LOWEST X VALUE FOR THE X AXIS
/*      XMAX = HIGHEST X VALUE FOR THE X AXIS
/*      SCALE = -1. PLOT A(1,J,1)
/*                0. PLOT THE MAGNITUDE OF A
/*                1. PLOT THE MAGNITUDE OF A WITH EACH POINT
/*                   DIVIDED BY XBOUND*YBOUND
/*      TI = 20 ELEMENT ARRAY CONTAINING A TITLE FOR THE
/*            PLOT. IT IS OVERLAYED ON TITLE CHAR(80).
/*            SET TITLE EQUAL TO THE CHARACTER STRING YOU
/*            WANT ON THE PLOT.
/*  THINGS TO CHANGE WHEN THE SIZE OF A IS CHANGED.
/*      SIZE OF APLOT IN PLTHID
/*      SIZE OF OTHER ARRAYS IN PLTHID
/*      SIZE OF Y. SET EQUAL TO XBOUND*YBOUND*4
/*      VALUES IN M. MUST BE POWERS OF TWO. EQUAL SIZE OF A
/*      NDIM
/******
2      1  0  DCL FFTM EXT ENTRY((*) FLOAT BIN(21);
/*            (*) FIXED BIN(15);
/*            FIXED BIN(15);
/*            CHAR(1);
/*            CHAR(1));
/*  PLOTS EXT ENTRY(FIXED BIN(31);
/*            FIXED BIN(31);
/*            FIXED BIN(31)) OPTIONS (FORTRAN INTER);
/*  PLTHID EXT ENTRY((*,*,*) FLOAT DEC(6);
/*            FIXED BIN(31);
/*            FIXED BIN(31);
/*            FLOAT DEC(6);
/*            FLOAT DEC(6);
/*            FLOAT DEC(6);
/*            FLOAT DEC(6);
/*            FLOAT DEC(6);
/*            (*) FLOAT DEC(6)) OPTIONS(FORTRAN INTER);
/*  A(*,*,*)
/*  Y(8192) DEF A
/*            FLOAT BIN(21) CONTROLLED,
/*            FLOAT BIN(21);
00000170
00000180
00000190
00000200
00000210
00000220
00000230
00000240
00000250
00000260
00000270
00000280
00000290
00000300
00000310
00000320
00000330
00000340
00000350
00000360
00000370
00000380
00000390
00000400
00000410
00000420
00000430
00000440
00000450
00000460
00000470
00000480
00000490
00000500
00000510
00000520
00000530
00000540
00000550
00000560
00000570
00000580
00000590
00000600
00000610
00000620
00000630
00000640
00000650
00000660
00000670

```

STMT LEV NT

			M(2)	FIXED BIN(15) INIT(6,6),	00000680
			ERROR	CHAR(1),	00000690
			NDIM	FIXED BIN(15) INIT(2),	00000700
			TITLE	CHAR(80),	00000710
			T(20) DEF TITLE	FLOAT DEC(6),	00000720
			(COS,FLOAT,COSD,SIND,CHAR)	BUILTIN,	00000730
			(X,YB(4),YE(4))	FIXED BIN(15),	00000740
			WTOP	LABEL(TOPR,TOPL),	00000750
			WBOT	LABEL(BOTR,BOTL),	00000760
			INC	FIXED BIN(15),	00000770
			(FSTART,FSTOP,WSTART,WSTOP)	FIXED BIN(15),	00000780
			(YSTART,YSTOP)	FIXED BIN(15),	00000790
			I(4)	CHAR(30),	00000800
			(RAD,SIZE,XOFF,YOFF,ANG1,ANG2)	FLOAT BIN(21),	00000810
			NPTS	FIXED BIN(15),	00000820
			(I,J,K,XBOUND,YBOUND)	FIXED BIN(31),	00000830
			SYSPRINT	FILE PRINT;	00000840
3	1	0	OPEN FILE(SYSPRINT) LINESIZE(133);		00000850
4	1	0	XBOUND=64;		00000860
5	1	0	YBOUND=64;		00000870
6	1	0	ALLOCATE A(XBOUND,YBOUND,2);		00000880
			/* 4 BOXES SIZE=8 SEPARATION=5 */		00000900
7	1	0	YB(1)=10;		00000910
8	1	0	YE(1)=17;		00000920
9	1	0	YB(2)=23;		00000930
10	1	0	YE(2)=30;		00000940
11	1	0	YB(3)=36;		00000950
12	1	0	YE(3)=43;		00000960
13	1	0	YB(4)=49;		00000970
14	1	0	YE(4)=56;		00000980
15	1	0	A=0;		00000990
16	1	0	DO I=1 TO 4;		00001000
17	1	1	DO J=29 TO 36;		00001010
18	1	2	DO K=YB(I) TO YE(I);		00001020
19	1	3	A(J,K,I)=1;		00001030
20	1	3	END;		00001040
21	1	2	END;		00001050
22	1	1	END;		00001060
23	1	0	TITLE='23 4 BOXES SIZE=8 SEPARATION=5';		00001070
24	1	0	CALL PLTHID(A,XBOUND,YBOUND,8.,4.,1.,64.,-1.,TI);		00001080
			/* DOTS */		00001090
25	1	0	YB(1)=2;		00001100
26	1	0	YB(2)=4;		00001110
27	1	0	YB(3)=24;		00001120
28	1	0	YB(4)=30;		00001130
29	1	0	XOFF=32;		00001140
30	1	0	T(1)=24 DOT RADIUS=2 INC=3;		00001150
31	1	0	T(2)=25 DOT RADIUS=4 INC=3;		00001160
32	1	0	T(3)=26 DOT RADIUS=24 INC=1;		00001170
33	1	0	T(4)=27 DOT RADIUS=10 INC=1;		00001180
34	1	0	DO K=1 TO 4;		00001190
35	1	1	A=0;		00001200
36	1	1	DO I=0 TO 360 BY 1;		00001210
37	1	2	X=YB(K)*COSD(I)*XOFF;		00001220

OPTIMIZING COMPILER

FF1: PROC OPTIONS(MAIN) REORDER;

STMT LEV NT

38	1	2	DO J=32-YB(K)*SIND(I) TO 32+YB(K)*SIND(I);	00001230
39	1	3	A(X,J,1)=1;	00001240
40	1	3	END;	00001250
41	1	2	END;	00001260
42	1	1	TITLE=T(K);	00001270
43	1	1	CALL PLTHID(A,XBOUND,YBOUND,8.,4.,1.,64.,-1.,TI);	00001280
44	1	1	END;	00001290
			/* CIRCLE */	00001300
45	1	0	A=0;	00001310
46	1	0	TITLE='28 CIRCLE RADIUS=2 INC=3';	00001320
47	1	0	DO I=0 TO 360 BY 3;	00001330
48	1	1	A(2*COSD(I)+32,2*SIND(I)+32,1)=1;	00001340
49	1	1	END;	00001350
50	1	0	CALL PLTHID(A,XBOUND,YBOUND,8.,4.,1.,64.,-1.,TI);	00001360
			/* SQUARE */	00001370
51	1	0	A=0;	00001380
52	1	0	TITLE='29 BOX SIZE=2';	00001390
53	1	0	DO J=31,32;	00001400
54	1	1	DO I=31 TO 32;	00001410
55	1	2	A(J,I,1)=1;	00001420
56	1	2	A(I,J,1)=1;	00001430
57	1	2	END;	00001440
58	1	1	END;	00001450
59	1	0	CALL PLTHID(A,XBOUND,YBOUND,8.,4.,1.,64.,-1.,TI);	00001460
			/* SQUARE */	00001470
60	1	0	A=0;	00001480
61	1	0	TITLE='30 SQUARE SIZE=3';	00001490
62	1	0	DO J=31,33;	00001500
63	1	1	DO I=31 TO 33;	00001510
64	1	2	A(J,I,1)=1;	00001520
65	1	2	A(I,J,1)=1;	00001530
66	1	2	END;	00001540
67	1	1	END;	00001550
68	1	0	CALL PLTHID(A,XBOUND,YBOUND,8.,4.,1.,64.,-1.,TI);	00001560
			/* UOTS */	00001570
69	1	0	YB(1)=12;	00001580
70	1	0	YB(2)=16;	00001590
71	1	0	YB(3)=24;	00001600
72	1	0	YB(4)=30;	00001610
73	1	0	XOFF=32;	00001620
74	1	0	T(1)=18 DOT RADIUS=12 INC=3';	00001630
75	1	0	T(2)=19 DOT RADIUS=16 INC=3';	00001640
76	1	0	T(3)=20 DOT RADIUS=24 INC=3';	00001650
77	1	0	T(4)=21 DOT RADIUS=30 INC=3';	00001660
78	1	0	DO K=1 TO 4;	00001670
79	1	1	A=0;	00001680
80	1	1	DO I=0 TO 360 BY 3;	00001690
81	1	2	A=YB(K)*COSD(I)+XOFF;	00001700
82	1	2	DO J=32-YB(K)*SIND(I) TO 32+YB(K)*SIND(I);	00001710
83	1	3	A(X,J,1)=1;	00001720
84	1	3	END;	00001730
85	1	2	END;	00001740
86	1	1	TITLE=T(K);	00001750
87	1	1	CALL PLTHID(A,XBOUND,YBOUND,8.,4.,1.,64.,-1.,TI);	00001760

STMT LEV NT

```

86      1 1      END;
89      1 0      /* 2 DOTS */
90      1 0      TITLE='17 2 DOTS RADIUS 2 SEPARATION 8 INC=3';
91      1 0      YB(1)=26;
92      1 0      YB(2)=38;
93      1 0      RAD=2;
94      1 0      A=0;
95      1 1      DO I=1 TO 2;
96      1 1      DO J=0 TO 360 BY 3;
97      1 2      X=RAD*COS(J)+YB(I);
98      1 2      DO K=32-RAD*SIND(J) TO 32+RAD*SIND(J);
99      1 3      A(X,K,1)=1;
100     1 3      END;
101     1 2      END;
102     1 0      CALL PLTHID(A,XBOUND,YBOUND,8.,4.,1.,64.,-1.,TI);
103     1 0      /* CIRCLE */
104     1 0      A=0;
105     1 0      TITLE='12 CIRCLE - 16 INC=3';
106     1 1      DO I=0 TO 360 BY 3;
107     1 1      A(8*COS(I)+24.8*SIND(I)+24,1)=1;
108     1 0      END;
109     1 0      CALL PLTHID(A,XBOUND,YBOUND,8.,4.,1.,64.,-1.,TI);
110     1 0      /* BOX */
111     1 0      YB(1)=24;
112     1 0      YB(2)=20;
113     1 0      YE(1)=39;
114     1 0      YE(2)=43;
115     1 0      T(1)='1 BOX -16';
116     1 0      T(2)='2 BOX -24';
117     1 1      DO I=1 TO 2;
118     1 1      A=0;
119     1 1      DO J=YB(I) TO YE(I);
120     1 2      DO K=YB(I) TO YE(I);
121     1 3      A(J,K,1)=1;
122     1 3      END;
123     1 2      END;
124     1 1      TITLE=T(1);
125     1 0      CALL PLTHID(A,XBOUND,YBOUND,8.,4.,1.,64.,-1.,TI);
126     1 0      END;
127     1 0      /* RECTANGLE */
128     1 0      T(1)='3 RECTANGLE - 8 X 16';
129     1 0      T(2)='4 RECTANGLE - 8 X 24';
130     1 1      DO I=1 TO 2;
131     1 1      A=0;
132     1 1      DO J=28 TO 35;
133     1 2      DO K=YB(I) TO YE(I);
134     1 3      A(J,K,1)=1;
135     1 3      END;
136     1 2      END;
137     1 1      TITLE=T(1);
138     1 0      CALL PLTHID(A,XBOUND,YBOUND,8.,4.,1.,64.,-1.,TI);
139     1 0      END;
140     1 0      /* SQUARE */

```

```

00001770
00001780
00001790
00001800
00001810
00001820
00001830
00001840
00001850
00001860
00001870
00001880
00001890
00001900
00001910
00001920
00001930
00001940
00001950
00001960
00001970
00001980
00001990
00002000
00002010
00002020
00002030
00002040
00002050
00002060
00002070
00002080
00002090
00002100
00002110
00002120
00002130
00002140
00002150
00002160
00002170
00002180
00002190
00002200
00002210
00002220
00002230
00002240
00002250
00002260
00002270
00002280
00002290
00002300

```

OPTIMIZING COMPILER

FFT: PROC OPTIONS(MAIN) REORDER;

STMT LEV NT

137	1	0	A=0;	00002310
138	1	0	TITLE='8 SQUARE -16';	00002320
139	1	0	DO J=24,39;	00002330
140	1	1	DO I=24 TO 39;	00002340
141	1	2	A(J,I)=1;	00002350
142	1	2	A(I,J)=1;	00002360
143	1	2	END;	00002370
144	1	1	END;	00002380
145	1	0	CALL PLTHD(A,XBOUND,YBOUND,8.,4.,1.,64.,-1.,TI);	00002390

```
FFT: PROC OPTIONS(MAIN) REORDER;
```

146	1	0	SHIFT:PROC REORDER;			00002400
147	2	0	DCL (I,J)	FIXED BIN(15);		00002410
			S	FLUAT BIN(21);		00002420
148	NN	0	S=1;			00002430
149	NN	0	DO I=1 TO ABOUND;			00002440
150	NN	1	S=-S;			00002450
151	NN	1	DO J=1 TO YBOUND;			00002460
152	NN	1	A(I,J,1)=A(I,J,1)*S;	/* SHIFT FUNCTION	*/	00002470
153	NN	2	S=-S;	/* SHIFT FUNCTION	*/	00002480
154	NN	2	END;			00002490
155	NN	0	END;			00002500
156	NN	0	END SHIFT;			00002510


```

0001      SUBROUTINE PLTHID(A,XBOUND,YBOUND,XLNTH,YLENTH,XMIN,XMAX,SCALE,TITLE)00002630
0002      XE)00002640
0003      INTEGER*4 XBOUND,YBOUND00002650
0004      REAL*4 SCALE,POINT,YMIN,YMAX,TITLE(20),NOTITLE(20)/'NONE'/00002660
0005      DIMENSION A(XBOUND,YBOUND,2),APLOT(64,64),X(130),00002670
0006      XYP(400),AG(400),G(400),XM(400),H(400),AG1(400),G1(400)00002680
0007      CALL ERKSEL(209,255,0,1,1,1)00002690
0008      YMIN=00002700
0009      YMAX=00002710
0010      ASSIGN 700 TO ISEL00002720
0011      IF(SCALE) 600,400,30000002730
0012      SCALE=XBOUND*YBOUND00002740
0013      GO TO 50000002750
0014      SCALE=100002760
0015      ASSIGN 600 TO ISEL00002770
0016      DO 10 I=1,XBOUND00002780
0017      DO 10 J=1,YBOUND00002790
0018      GO TO ISEL0,(700,800)00002800
0019      POINT=A(I,J,1)00002810
0020      GO TO 90000002820
0021      POINT=SQRT(A(I,J,1)*A(I,J,1)+A(I,J,2)*A(I,J,2))/SCALE00002830
0022      IF(POINT.GT.YMIN) GO TO 90000002840
0023      YMIN=POINT00002850
0024      GO TO 10000002860
0025      IF(POINT.LT.YMAX) GO TO 10000002870
0026      YMAX=POINT00002880
0027      10 APLOT(I,J)=POINT00002890
0028      IF(SCALE.LT.0) WRITE(9) TITLE,YMIN,YMAX,APLOT00002900
0029      WRITE(6,100)((APLOT(I,J),I=1,XBOUND,4),J=1,YBOUND,4)00002910
0030      FORMAT(1X,16F8.3)00002920
0031      N=XBOUND00002930
0032      N1=XBOUND00002940
0033      NG=00002950
0034      NG1=-300002960
0035      NFNS=YBOUND00002970
0036      NFNS1=00002980
0037      MAXDIM=40000002990
0038      DELTAX=(XMAX-XMIN)/XLNTH00003000
0039      DELTAY=(YMAX-YMIN)/YLENTH00003010
0040      SCALE=(XMAX-XMIN)/FLOAT(XBOUND-1)00003020
0041      DO 1 I=1,XBOUND00003030
0042      1 X(I)=XMIN+(I-1)*SCALE00003040
0043      DO 2 I=1,XBOUND00003050
0044      DO 3 J=1,YBOUND00003060
0045      3 YP(J)=APLOT(I,J)00003070
0046      2 CONTINUE00003080
0047      RETURN00003110
0048      END00003120

```

OPTIMIZING COMPILER

FFTM:

/* TO CALCULATE MULTIDIMENSIONAL FFT

*/

SOURCE LISTING

STMT LEV NT

```

1      0  |FFTM:  /* TO CALCULATE MULTIDIMENSIONAL FFT
          |PROC(A,M,NDIM,OPT,ERROR)REORDER;
          |
          |      /******
          |      /* PARAMETERS */
          |      /******
2      1  0  |      DCL A(*)FLOAT BIN(21),
          |              M(*)FIXED BIN(15),
          |              NDIM FIXED BIN(15),
          |              OPT CHAR(1),
          |              ERROR CHAR(1)
          |              ;
          |
          |      /******
          |      /* LOCAL VARIABLES */
          |      /******
3      1  0  |      DCL (PI INIT(3.14159265),
          |              RTH INIT(.7071067811),
          |              RI,
          |              TR,T2R,T2I,T3R,T3I,T4R,T4I,
          |              U1R,U1I,U2R,U2I,U3R,U3I,U4R,U4I,
          |              WR,WI,W2R,W2I,W3R,W3I
          |              )FLOAT BIN(21)STATIC,
          |
          |              (I,IND,J,JM,K,K2,K3,K4,KDIF,KINC,
          |              KM,KMIN,L,LJ,LMAX,MM,MMAX,NA,NAD,NB,
          |              NBH,NIN,NT
          |              )FIXED BIN(15)STATIC,
          |              N(NDIM)FIXED BIN(15)
          |              ;
          |
4      1  0  |      ERROR='P';
          |
5      1  0  |      IF NDIM<1
          |      THEN GOTO RETURN;
          |
6      1  0  |      NT=2;
          |
7      1  0  |      DO I=1 TO NDIM;
8      1  1  |              N(I),K=108**M(I);
9      1  1  |              IF K<1
          |              THEN GOTO RETURN;
10     1  1  |              NT=NT*K;
11     1  1  |      END;

```

OPTIMIZING COMPILER

FFTM:

/* TO CALCULATE MULTIDIMENSIONAL FFT

*/

STMT LEV NT

12	1	0		NA=2;
13	1	0		DO IND=NDIM TO 1 BY -1;
14	1	1		NIN=N(IND);
15	1	1		NB=NA*NIN;
16	1	1		IF NIN=1
17	1	1		THEN GOTO MULTI;
18	1	1		NBH=NB/10B;
				J=1;
19	1	1		DO I=1 TO NB BY NA;
20	1	2		IF J<=I
21	1	2		THEN GOTO MOD1;
22	1	2		KM=I+NA-2;
				JM=J-I;
23	1	2		DO K=1 TO KM BY 2;
24	1	3		DO L=K TO NT BY NB;
25	1	4		LJ=L+JM;
26	1	4		WR=A(L);
27	1	4		WI=A(L+1);
28	1	4		A(L)=A(LJ);
29	1	4		A(L+1)=A(LJ+1);
30	1	4		A(LJ)=WR;
31	1	4		A(LJ+1)=WI;
32	1	4		END;
33	1	3		END;
34	1	2		MOD1: K=NBH;
35	1	2		DO WHILE(J>K);
36	1	3		J=J-K;
37	1	3		K=K/10B;
38	1	3		END;
39	1	2		J=J+K;
40	1	2		END;
41	1	1		NAD=NA+NA;
42	1	1		ODD: IF NIN<2
43	1	1		THEN GOTO LEN4;
				IF NIN=2
44	1	1		THEN GOTO LEN2;
45	1	1		NIN=NIN/100B;
				GOTO ODD;
46	1	1		LEN2: DO I=1 TO NA BY 2;
47	1	2		DO K=I TO NT BY NAD;
48	1	3		L=K+NA;
49	1	3		WR=A(L);
50	1	3		WI=A(L+1);
51	1	3		A(L)=A(K)-WR;

OPTIMIZING COMPILER

FFTM:

/* TO CALCULATE MULTIDIMENSIONAL FFT

*/

STMT LEV NT

52	1	3		A(L+1)=A(K+1)-WI;
53	1	3		A(K)=A(K)+WR;
54	1	3		A(K+1)=A(K+1)+WI;
55	1	3		END;
56	1	2		END;
57	1	1		ILEN4: MMAX=NA;
58	1	1		MAIN: IF MMAX>=NBH
59	1	1		THEN GOTO MULTI;
60	1	1		MM=MMAX+MMAX;
				LMAX=MAX(NAD,MMAX/10B);
61	1	1		DO I=NA TO LMAX BY NAD;
62	1	2		J=I;
63	1	2		IF MMAX<=NA
				THEN GOTO INITL;
64	1	2		R1=-PI*J/MM;
65	1	2		IF OPT='1'
				THEN R1=-R1;
66	1	2		WR=COS(R1);
67	1	2		WI=SIN(R1);
68	1	2		DOUBLE: W2R=WR*WR-WI*WI;
69	1	2		W2I=WR*WI*000010E+00B;
70	1	2		W3R=W2R*WR-W2I*WI;
71	1	2		W3I=W2R*WI+W2I*WR;
72	1	2		INITL: L=1;
73	1	2		STRT: IF MMAX=NA
				THEN KMIN=L;
74	1	2		ELSE KMIN=L+NIN*J;
75	1	2		KDIF=NIN*MMAX;
76	1	2		INCR: KINC=KDIF*100B;
77	1	2		DO K=KMIN TO NT BY KINC;
78	1	3		K2=K+KDIF;
79	1	3		K3=K2+KDIF;
80	1	3		K4=K3+KDIF;
81	1	3		IF MMAX=NA
				THEN DO;
82	1	4		U1R=A(K)+A(K2);
83	1	4		U1I=A(K+1)+A(K2+1);
84	1	4		U2R=A(K3)+A(K4);
85	1	4		U2I=A(K3+1)+A(K4+1);
86	1	4		U3R=A(K)-A(K2);
87	1	4		U3I=A(K+1)-A(K2+1);
88	1	4		U4R=A(K3+1)-A(K4+1);
89	1	4		U4I=A(K4)-A(K3);
90	1	4		END;
91	1	3		ELSE DO;

STMT LEV NT

92	1	4	T2R=W2R*A(K2)-W2I*A(K2+1);
93	1	4	T2I=W2R*A(K2+1)+W2I*A(K2);
94	1	4	T3R=WR*A(K3)-WI*A(K3+1);
95	1	4	T3I=WR*A(K3+1)+WI*A(K3);
96	1	4	T4R=W3R*A(K4)-W3I*A(K4+1);
97	1	4	T4I=W3R*A(K4+1)+W3I*A(K4);
98	1	4	U1R=A(K)+T2R;
99	1	4	U1I=A(K+1)+T2I;
100	1	4	U2R=T3R+T4R;
101	1	4	U2I=T3I+T4I;
102	1	4	U3R=A(K)-T2R;
103	1	4	U3I=A(K+1)-T2I;
104	1	4	U4R=T3I-T4I;
105	1	4	U4I=T4R-T3R;
106	1	4	END;
107	1	3	IF OPT='1'
			THEN DO;
108	1	4	U4R=-U4R;
109	1	4	U4I=-U4I;
110	1	4	END;
111	1	3	A(K)=U1R+U2R;
112	1	3	A(K+1)=U1I+U2I;
113	1	3	A(K2)=U3R+U4R;
114	1	3	A(K2+1)=U3I+U4I;
115	1	3	A(K3)=U1R-U2R;
116	1	3	A(K3+1)=U1I-U2I;
117	1	3	A(K4)=U3R-U4R;
118	1	3	A(K4+1)=U3I-U4I;
119	1	3	END;
120	1	2	KMIN=L+(KMIN-L)*100B;
121	1	2	KDIF=KINC;
122	1	2	IF KDIF<=NBH
			THEN GOTO INCR;
123	1	2	L=L+2;
124	1	2	IF L<NA
			THEN GOTO STRT;
125	1	2	J=J+LMAX;
126	1	2	IF J<=MMAX
			THEN DO;
127	1	3	TR=WR;
128	1	3	WR=(TR+WI)*RTH;
129	1	3	WI=(WI-TR)*RTH;
130	1	3	IF OPT='1'
			THEN DO;
131	1	4	TR=WR;
132	1	4	WR=-WI;
133	1	4	WI=TR;
134	1	4	END;
135	1	3	GOTO DOUBLE;

OPTIMIZING COMPILER

FFTM;

/* TO CALCULATE MULTIDIMENSIONAL FFT

*/

STMT LEV NT

136	1	3		END;
137	1	2		END;
138	1	1		NIN=3-NIN;
139	1	1		MMAX=MM;
140	1	1		GOTO MAIN;
141	1	1		MULTI; NA=NB;
142	1	1		END;
143	1	0		ERROR='0';
144	1	0		RETURN; END FFTM;

0001

SUBROUTINE HIDE

1 (X,Y,XG,G,XH,H,NG,MAXDIM,N1,NFNS,TITLE,
2 XLNTH,YLNTH,XMIN,DELTAX,YMIN,DELTAY)

THIS SUBROUTINE PRODUCES A 2-DIMENSIONAL REPRESENTATION OF A
3-DIMENSIONAL FIGURE OR SURFACE. THE FIRST CALL TO HIDE
IS FOR INITIALIZATION AND PLOTTING THE CURVE NEAREST TO THE
FOREGROUND. ON EACH SUBSEQUENT CALL, A CURVE FURTHER FROM
THE VIEWER IS PLOTTED.

.....X IS THE ABSCISSA ARRAY FOR THE CURVE TO BE PLOTTED BY HIDE
ON THIS CALL. THE X VALUES MUST BE INCREASING. IF
X(I) >= X(I+1) FOR SOME I, MAXDIM WILL BE SET TO ZERO, AND A
RETURN WILL BE EXECUTED.

.....Y IS THE ORDINATE ARRAY.

.....G VS. XG IS THE CURRENT VISUAL MAXIMUM FUNCTION ON EACH
RETURN FROM HIDE.

.....XH AND H ARE WORKING ARRAYS.

.....ON EACH RETURN FROM HIDE, NG IS THE NUMBER OF POINTS IN THE
CURRENT MAXIMUM FUNCTION. ON THE FIRST CALL, NG IS A
NONPOSITIVE INTEGER WHICH SPECIFIES CERTAIN OPTIONS:

-1: DO NOT DRAW AN 8 1/2 BY 11 BORDER

-2: PLOT UNHIDDEN MINIMUM RATHER THAN MAXIMUM. IN THIS
CASE G VS. XG WILL BE THE NEGATIVE OF THE VISUAL
MINIMUM FUNCTION.

-3: DO NOT PLOT BORDER. PLOT MINIMUM RATHER THAN MAXIMUM.
0: PLOT BORDER, PLOT MAXIMUM.

IF THE BORDER IS DRAWN, ITS LEFT, BOTTOM CORNER WILL BE
WHERE THE PLOTTING REFERENCE POINT WAS JUST BEFORE THE
FIRST CALL TO HIDE, AND THE REFERENCE POINT WILL BE
MOVED 1 INCH RIGHT AND 2 INCHES UP.

IF THE BORDER IS NOT DRAWN, THE REFERENCE POINT WILL NOT
BE MOVED BY HIDE.

.....MAXDIM IS THE DIMENSION IN THE CALLING PROGRAM OF THE

*****01) IEY0331 COMMENTS DELETED *****

DIMENSION X(N1),Y(N1),G(MAXDIM),H(MAXDIM)

DIMENSION XG(MAXDIM),XH(MAXDIM),TITLE(20)

INTEGER TITLE

DATA EPS1/0.00001/,NONE/4HNONE/

-F(A,B,C,D,E)=C+(A-B)*(E-C)/(D-B)

IF (MAXDIM .LE. 0) RETURN

IFPLOT = 1

IF (N1 .GT. 0) GO TO 100

N1 = -N1

IFPLOT = 0

100 DO 105 I = 2,N1

IF (X(I-1) .LT. X(I)) GO TO 105

MAXDIM = 0

GO TO 110

105 CONTINUE

IF (NG .GT. 0) GO TO 155

IF (N1+4 .LE. MAXDIM) GO TO 120

MAXDIM = -MAXDIM

RETURN

110 SIGN = 1.0

IF (NG .LT. -1) SIGN = -1.0

FNSM1 = 0.0

IF (NFNS .EQ. 1) NFNS = -1

IF (NFNS .LE. 0) GO TO 125

00000010

00000020

00000030

00000040

00000050

00000060

00000070

00000080

00000090

00000100

00000110

00000120

00000130

00000140

00000150

00000160

00000170

00000180

00000190

00000200

00000210

00000220

00000230

00000240

00000250

00000260

00000270

00000280

00000290

00000300

00000310

00000320

00000330

00000510

00000520

00000530

00000540

00000550

00000560

00000570

00000580

00000590

00000600

00000610

00000620

00000630

00000640

00000650

00000660

00000670

00000680

00000690

00000700

00000710

00000720

00000730

00000740

```

0026      FNSM1 = NFNS - 1                                00000750
0027      DXIN = (9.0 - ABS(XLNTH)) * DELTAX / FNSM1      00000760
0028      DYIN = (6.0 - ABS(YLNTH)) * DELTAY / FNSM1      00000770
0029      IF (NG .EQ. -1 .OR. NG .EQ. -3) GO TO 130        00000780
0030      CALL PLOT(11.0, 0.0, 2)                          00000790
0031      CALL PLOT(11.0, 8.5, 2)                          00000800
0032      CALL PLOT(0.0, 8.5, 2)                          00000810
0033      CALL PLOT(0.0, 0.0, 2)                          00000820
0034      CALL PLOT(1.0, 2.0, -3)                         00000830
0035      IF (TITLE(1) .NE. NONE) CALL SYMBOL(-.28,-1.0,   00000840
130      1 0.14,TITLE,0.0,72)
0036      IF (XLNTH .LT. 0) GO TO 139                     00000850
C      CALL ROUTINE TO DRAW THE HORIZONTAL AXIS. THE     00000870
C      LEFT END IS SPECIFIED IN INCHES RELATIVE TO THE  00000880
C      POINT BY THE FIRST TWO ARGUMENTS                 00000890
C      00000900
0037      CALL AXIS(9.0 - XLNTH, 0.0, 1H, -1, XLNTH, 0.0, 00000910
1  XMIN, DELTAX)
0038      IF (YLNTH .LT. 0.0) GO TO 140                   00000920
C      DEPTH AXIS                                         00000930
C      00000940
C      00000950
0039      CALL PLOT(9.0-XLNTH,0.0,3)                      00000960
0040      CALL PLOT(0.0,6.0-YLNTH,2)                      00000970
0041      IF (YLNTH .LT. 0.0) GO TO 140                   00000980
C      VERTICAL AXIS                                     00000990
C      00001000
C      00001010
0042      CALL AXIS(0.0,6.0-YLNTH,1H, 1,YLNTH,90.0,YMIN,DELTAY) 00001020
0043      INDEXT = 3                                       00001030
0044      DO 145 J = 1,N1                                  00001040
0045      XG(INDEXT) = X(J)                                00001050
0046      G(INDEXT) = SIGN * Y(J)                         00001060
0047      INDEXT = INDEXT + 1                             00001070
0048      CONTINUE                                         00001080
0049      EPS = EPS1 * (ABS(XMIN)+ABS(DELTAX))              00001090
0050      NG = N1 + 4                                       00001100
0051      XG(1) = -FNSM1 * DXIN + XMIN - ABS(XMIN) - ABS(XG(3)) - 1.0 00001110
0052      XG(2) = XG(3) - EPS                             00001120
0053      XG(N1+3) = XG(N1+2) + EPS                       00001130
0054      ZZ = YMIN                                         00001140
0055      IF (SIGN .LT. 0.0) ZZ = -YMIN-50.0*DELTAY       00001150
0056      G(1) = ZZ                                         00001160
0057      G(2) = ZZ                                         00001170
0058      G(N1+3) = ZZ                                       00001180
0059      G(NG) = ZZ                                        00001190
0060      XSTART = XMIN - (9.0 - ABS(XLNTH)) * DELTAX     00001200
0061      IF (IFPLOT .NE. 1) GO TO 154                   00001210
0062      X(N1+1) = XSTART                                  00001220
0063      X(N1+2) = DELTAX                                  00001230
0064      Y(N1+1) = YMIN                                    00001240
0065      Y(N1+2) = DELTAY                                  00001250
0066      CALL LINE(X,Y,N1,1,0,0)                         00001260
0067      CONTINUE                                         00001270
0068      DXKK = 0.0                                        00001280
0069      DYKK = 0.0                                        00001290
0070      RELINC = DELTAX / DELTAY                       00001300
0071      00001310
0072      00001320

```



```

0071      XG(NG) = SIGN
0072      RETURN
C
C      FOLLOWING STATEMENT IS REACHED IF ANY EXCEPT THE
C      CURVE NEAREST TO THE VIEWER IS TO BE PLOTTED
C
0073      155      SIGN = XG(NG)
0074      XG(NG) = X(N1)
C
C      TRANSLATE AXES TO SIMULATE STEPPING IN DEPTH DIMENSION
C
0075      IF (NFNS) 175,165,160
0076      160      DXKK = DXKK + DXIN
0077      DYKK = DYKK + DYIN
0078      165      DO 170 J = 1,N1
0079          Y(J) = SIGN * (Y(J) + DYKK)
0080          X(J) = X(J) - DXKK
0081      170      CONTINUE
0082      175      CALL LOOKUP(X(1),XG(1),JJ)
0083      IF (JJ .GE. MAXDIM) GO TO 300
0084      DO 180 J = 1,JJ
0085          XH(J) = XG(J)
0086          H(J) = G(J)
0087      180      CONTINUE
0088      IG = JJ + 1
0089      XH(IG) = X(1)
0090      H(IG) = F(X(1),XG(JJ),G(JJ),XG(IG),G(IG))
0091      INDEXG = JJ
0092      INDEXT = 1
0093      Z1 = X(1)
0094      F1 = H(IG) - Y(1)
0095      IT = 2
0096      JJ = IG
0097      IF (H(IG) .GE. Y(1)) GO TO 190
0098      IF (JJ .GE. MAXDIM) GO TO 300
0099      JJ = IG + 1
0100      H(JJ) = Y(1)
0101      XH(JJ) = Z1 + EPS
0102      190      LAST = 0
0103      X1 = Z1
0104      200      IF (XG(IG) .LT. X(IT)) GO TO 205
0105      IWHICH = 0
0106      X2 = X(IT)
0107      F2 = F(X2,XG(IG-1),G(IG-1),XG(IG),G(IG)) - Y(IT)
0108      IT = IT + 1
0109      GO TO 210
0110      205      X2 = XG(IG)
0111      IWHICH = 1
0112      F2 = G(IG) - F(X2,X(IT-1),Y(IT-1),X(IT),Y(IT))
0113      IG = IG + 1
0114      210      IF (F1*F2 .GT. 0.0) GO TO 220
0115      IF (F1 .EQ. F2 .OR. X1 .EQ. X2) GO TO 220
0116      SLOPE = (F2-F1)/(X2-X1)
0117      IGG = IG - 1 - IWHICH
0118      ITT = IT - 2 + IWHICH
0119      IF (ABS(SLOPE*RELINC) .GT. 1.0E-6) GO TO 215
0120      Z2 = X2
0121      GO TO 230

```

```

00001330
00001340
00001350
00001360
00001370
00001380
00001390
00001400
00001410
00001420
00001430
00001440
00001450
00001460
00001470
00001480
00001490
00001500
00001510
00001520
00001530
00001540
00001550
00001560
00001570
00001580
00001590
00001600
00001610
00001620
00001630
00001640
00001650
00001660
00001670
00001680
00001690
00001700
00001710
00001720
00001730
00001740
00001750
00001760
00001770
00001780
00001790
00001800
00001810
00001820
00001830
00001840
00001850
00001860
00001870
00001880
00001890
00001900

```

```

0122      215  Z2 = X1 - F1/SLOPE
0123      GO TO 230
0124      220  X1 = X2
0125      F1 = F2
0126      IF (IT .LE. N1) GO TO 200
0127      225  LAST = 1
0128      Z2 = X(N1)
0129      CALL LOOKUP(Z2, XG(INDEXG), IGG)
0130      IGG = INDEXG + IGG - 1
0131      ITT = N1 - 1
0132      230  Z2 = 0.99*Z1 + 0.01*Z2
0133      CALL LOOKUP(Z2, X(INDEXT), K1)
0134      CALL LOOKUP(Z2, XG(INDEXG), K2)
0135      K1 = K1 + INDEXT - 1
0136      K2 = K2 + INDEXG - 1
0137      IF ( F(ZZ, X(K1), Y(K1), X(K1+1), Y(K1+1)) .GT.
1      F(ZZ, XG(K2), G(K2), XG(K2+1), G(K2+1)) )
2      GO TO 245
0138      IF (JJ+IGG-INDEXG .GE. MAXDIM) GO TO 300
0139      IF (INDEXG .EQ. IGG) GO TO 240
0140      J1 = INDEXG + 1
0141      DO 235 I = J1, IGG
0142      JJ = JJ + 1
0143      XH(JJ) = XG(I)
0144      H(JJ) = G(I)
0145      235  CONTINUE
0146      240  JJ = JJ + 1
0147      XH(JJ) = Z2
0148      H(JJ) = F(Z2, XG(IGG), G(IGG), XG(IGG+1), G(IGG+1))
0149      INDEXG = IGG
0150      INDEXT = ITT
0151      GO TO 260
0152      245  NGRAPH = ITT - INDEXT + 2
0153      IF (JJ+NGRAPH-1 .GT. MAXDIM) GO TO 300
0154      N2 = JJ
0155      IF (NGRAPH .EQ. 2) GO TO 255
0156      J1 = INDEXT + 1
0157      DO 250 I = J1, ITT
0158      JJ = JJ + 1
0159      XH(JJ) = X(I)
0160      H(JJ) = Y(I)
0161      250  CONTINUE
0162      255  JJ = JJ + 1
0163      XH(JJ) = Z2
0164      H(JJ) = F(Z2, X(ITT), Y(ITT), X(ITT+1), Y(ITT+1))
0165      IF (IFPLOT .NE. 1) GO TO 257
0166      XH(N2+NGRAPH) = XSTART
0167      XH(N2+NGRAPH+1) = DELTAX
0168      H(N2+NGRAPH) = SIGN * YMIN
0169      H(N2+NGRAPH+1) = SIGN * DELTAY
0170      CALL LINE(XH(N2), H(N2), NGRAPH, 1, 0, 0)
0171      257  CONTINUE
0172      INDEXT = ITT
0173      INDEXG = IGG
0174      260  IF (LAST .EQ. 1) GO TO 265
0175      X1 = X2
0176      F1 = F2
0177      Z1 = Z2

```

```

00001910
00001920
00001930
00001940
00001950
00001960
00001970
00001980
00001990
00002000
00002010
00002020
00002030
00002040
00002050
00002060
00002070
00002080
00002090
00002100
00002110
00002120
00002130
00002140
00002150
00002160
00002170
00002180
00002190
00002200
00002210
00002220
00002230
00002240
00002250
00002260
00002270
00002280
00002290
00002300
00002310
00002320
00002330
00002340
00002350
00002360
00002370
00002380
00002390
00002400
00002410
00002420
00002430
00002440
00002450
00002460
00002470
00002480

```

```

0178      IF (IT .LE. N1) GO TO 200
0179      GO TO 225
0180      265  IF (XG(NG) .LF. XG(NG-1)) NG = NG - 1
0181      IF (XG(NG) .LF. X(N1)) GO TO 275
0182      IF (JJ+3+NG-IGG .GT. MAXDIM) GO TO 300
0183      XH(JJ+1) = XH(JJ) + EPS
0184      JJ = JJ + 1
0185      H(JJ) = F(X(N1), XG(IGG), G(IGG), XG(IGG+1), G(IGG+1))
0186      IGGP1 = IGG + 1
0187      DO 270 J = IGGP1, NG
0188          JJ = JJ + 1
0189          XH(JJ) = XG(J)
0190          H(JJ) = G(J)
0191      275  NG = JJ + 2
0192      IF (NG .GT. MAXDIM) GO TO 300
0193      DO 280 I = 1, JJ
0194          G(I) = H(I)
0195          XG(I) = XH(I)
0196      280  CONTINUE
0197      XG(JJ+1) = XG(JJ) + EPS
0198      G(JJ+1) = YMIN + DYKK
0199      IF (SIGN .LT. 0.0) G(JJ+1) = -YMIN - 50.0 * DELTAY + DYKK
0200      G(NG) = G(JJ+1)
0201      285  IF (NFNS .LT. 0) GO TO 295
0202      DO 290 I = 1, N1
0203          X(I) = X(I) + DXKK
0204          Y(I) = SIGN * Y(I) - DYKK
0205      290  CONTINUE
0206      295  XG(NG) = SIGN
0207      RETURN
0208      300  MAXDIM = -MAXDIM
0209      GO TO 285
0210      END

```

```

00002490
00002500
00002510
00002520
00002530
00002540
00002550
00002560
00002570
00002580
00002590
00002600
00002610
00002620
00002630
00002640
00002650
00002660
00002670
00002680
00002690
00002700
00002710
00002720
00002730
00002740
00002750
00002760
00002770
00002780
00002790
00002800
00002810

```

0001		SUBROUTINE LOOKUP (X, XTBL, J)	00002820
	C	THIS SUBROUTINE IS CALLED BY HIDE TO PERFORM A TABLE	00002830
	C	LOOKUP. BECAUSE OF PRECAUTIONS TAKEN IN HIDE, A TEST	00002840
	C	TO SEE IF X IS OUTSIDE THE TABLE IS UNNECESSARY.	00002850
0002		DIMENSION XTBL()	00002860
0003		J = 2	00002870
0004	100	IF (XTBL(J) - X) 200,300,400	00002880
0005	200	J = J + 1	00002890
0006		GO TO 100	00002900
0007	300	RETURN	00002910
0008	400	J = J - 1	00002920
0009		RETURN	00002930
0010		END	00002940

Appendix C

SOURCE LISTING

STMT LEV NT

```

1      0  .SIM:PROC OPTIONS(MAIN) REORDER;                      .00000040
          ./******                                .00000050
          ./* MASK TABLE                                .00000060
          ./* 1. BOX - 16                                .00000070
          ./* 2. BOX - 24                                .00000080
          ./* 3. RECTANGLE - 16                          .00000090
          ./* 4. RECTANGLE - 24                          .00000100
          ./* 5. DOT - 32                                .00000110
          ./* 6. DOT - 48                                .00000120
          ./* 7. CIRCLE - 16                              .00000130
          ./* 8. SQUARE - 16                             .00000140
          ./* 9. 2 DOTS - WIDTH 16 SEPARATION 16        .00000150
          ./* 10. DOT - 16 INC=3                         .00000160
          ./* 11. DOT - 24 INC=3                         .00000170
          ./* 12. CIRCLE - 16 INC=3                     .00000180
          ./* 13. 2 DOTS SIZE 16 SEPARATION 16 INC=3    .00000190
          ./* 14. 2 DOTS SIZE 16 SEPARATION 16 INC 3    .00000200
          ./* CONTEXTS */
          ./* 1. FLANKS 8 TARGET 8 SEPARATION 5 */      .00000210
          ./******                                .00000220
2      1  0  .DCL (XBOUND,YBOUND) FIXED BIN(15),          .00000230
          ./* (EUC,EUM) CHAR(3),                        .00000240
          ./* (DIFLI,DIFGE,DIFTOI,DIFRT) FLOAT BIN(21), .00000250
          ./* (I,J,K) FIXED BIN(15),                    .00000260
          ./* UFLOW LABEL(M,C),                        .00000270
          ./* (MH,CH) FLOAT DEC(6),                     .00000280
          ./* 1 MASK,                                    .00000290
          ./* 2 MTAG CHAR(80),                          .00000300
          ./* 2 MMIN FLOAT(6),                          .00000310
          ./* 2 MMAX FLOAT DEC(6),                      .00000320
          ./* 2 MDATA(64,64) FLOAT DEC(6),              .00000330
          ./* 1 CONTEX1,                                .00000340
          ./* 2 CTAG CHAR(80),                          .00000350
          ./* 2 CMIN FLOAT(6),                          .00000360
          ./* 2 CHAX FLOAT DEC(6),                      .00000370
          ./* 2 CDATA(64,64) FLOAT DEC(6),              .00000380
          ./* SUBSTR BUILTIN,                          .00000390
          ./* (MASKFIM,CONFIM) FILE RECORD SEQL BUFFERED ENV(VBS TRKOFL), .00000400
          ./* SYSPRINT FILE PRINT;                      .00000410
          ./* ON UNDERFLOW GO TO UFLOW;                .00000420
          ./* ON ENDFILE(MASKFIM) EOM='EOM';            .00000430
          ./* ON ENDFILE(CONFIM) EOC='EOC';             .00000440
          ./* OPEN ENDFILE(SYSPRINT) LINESIZE(133),FILE(MASKFIM)INPUT,FILE(CONFIM) .00000450
          ./* INPUT;                                     .00000460
          ./* XBOUND,YBOUND=64;                         .00000470
          ./* EUM='GO';                                  .00000480
          ./* READ FILE(MASKFIM) INTO(MASK);             .00000490
          ./* DO UNTIL(EOM='EOM');                      .00000500
          ./* EUC='GO';                                  .00000510
          ./* READ FILE(CONFIM) INTO(CONTEXT);          .00000520
          ./* DO UNTIL(EOC='EOC');                      .00000530
          ./*                                           .00000540

```

STMT LEV NT

14	1	2	.	DIFGE,DIFLT,DIFTOT,DIFRT=0;	.00000550
15	1	2	.	DO J=1 TO ABOUND;	.00000560
16	1	3	.	DO K=1 TO YBOUND;	.00000570
17	1	4	.	UFLOW=M;	.00000580
18	1	4	.	MH=MDATA(J,K)/MMAX;	.00000590
19	1	4	.	GO TO CONT;	.00000600
20	1	4	.	M: MH=0;	.00000610
21	1	4	.	CONT: UFLOW=C;	.00000620
22	1	4	.	CH=CDATA(J,K)/CMAX;	.00000630
23	1	4	.	GO TO DTOT;	.00000640
24	1	4	.	C: CH=0;	.00000650
25	1	4	.	DTOT: IF MH>CH THEN DIFGE=DIFGE+1;	.00000660
26	1	4	.	ELSE IF MH<CH THEN DIFLT=DIFLT+1;	.00000670
27	1	4	.	ELSE DIFTOT=DIFTOT+1;	.00000680
28	1	4	.	IF CH>0 THEN DIFRT=DIFRT+MH/CH;	.00000690
29	1	4	.	END;	.00000700
30	1	3	.	END;	.00000710
31	1	2	.	.PUT SKIP(2) EDIT('DIFRT=',DIFRT,'DIFLT=',DIFLT,'DIFGE=',DIFGE,'DIFTOT=',	.00000720
			.	'DIFTOT,MTAG,CTAG)(COL(1),(4)(A,F(10,1),X(5)),(2)(COL(80),A));	.00000730
32	1	2	.	READ FILE(CONTFIM) INTO (CONTEXT);	.00000740
33	1	2	.	END;	.00000750
34	1	1	.	CLOSE FILE(CONTFIM);	.00000760
35	1	1	.	OPEN FILE(CONTFIM) INPUT;	.00000770
36	1	1	.	READ FILE(MASKFIM) INTO (MASK);	.00000780
37	1	1	.	END;	.00000790
38	1	0	.	END SIM;	.00000800

APPROVAL SHEET

The dissertation submitted by Gregory John Ozog
has been read and approved by the following committee;

Dr. Mark M. Mayzner, Director
Professor, Psychology, Loyola

Dr. Richard Bowen
Assistant Professor, Loyola

Dr. William Yost
Director, Parmlly Hearing Institute, Loyola

The final copies have been examined by the director of the
dissertation and the signature which appears below verifies
the fact that any necessary changes have been incorporated
and that the dissertation is now given final approval by
the Committee with reference to content and form.

The dissertation is therefore accepted in partial fulfill-
ment of the requirements for the degree of Doctor of
Philosophy.

July 9, 1979
Date

Mark M. Mayzner
Director's Signature